KAUNAS UNIVERSITY OF TECHNOLOGY

BASANT KUMAR BAJPAI

ROLE OF SLOW ARTERIAL BLOOD PRESSURE WAVES IN CEREBRAL AUTOREGULATION MONITORING

Doctoral dissertation
Technological Sciences, Measurement Engineering (T 010)

2021, Kaunas

This doctoral dissertation was prepared at Kaunas University of Technology, Health Telematics Science Institute during the period of 2016–2020.

Scientific Supervisor
Prof. Dr. Arminas RAGAUSKAS, (Kaunas University of Technology, Technological Sciences, Measurement Engineering – T 010)

Doctoral dissertation has been published in:
http://ktu.edu

Editor:

Armandas Rumšas (Publishing House “Technologija”)

KAUNO TECHNOLOGIJOS UNIVERSITETAS

BASANT KUMAR BAJPAI

LĖTŲJŲ ARTERINIO KRAUJOSPŪDŽIO BANGŲ VAIDMUO SMEGENŲ AUTOREGULIACIJOS STEBĖSENOJE

Daktaro disertacija
Technologijos mokslai, Matavimų inžinerija (T010)

2021, Kaunas

Disertacija rengta 2016-2020 metais Kauno technologijos universiteto Sveikatos telematikos mokslo institute.

Mokslinis vadovas:

Prof. dr. Arminas RAGAUSKAS (Kauno technologijos universitetas, technologijos mokslai, matavimų inžinerija – T 010)

Interneto svetainės, kurioje skelbiama disertacija, adresas:
http://ktu.edu

Redagavo:

Armandas Rumšas (Leidykla “Technologija”)

ACKNOWLEDGMENTS

First and foremost, I thank my supervisor Prof. DSc Ph.D. Arminas Ragauskas. It was an honor to be his international Ph.D. student. I appreciate all his input of time, suggestions, and cooperation to make my Ph.D. experience effective and appealing. The delight and devotion he has for his research are contagious and inspiring. I cannot forget his quick responses via e-mails even at late nights, which is why I have been able to publish articles with impact factors in 2019–2020. I am also grateful to all reviewers for their valuable comments and suggestions for improving my dissertation.

The members of the Health Telematics Science Institute of Kaunas University of Technology have contributed immensely to my personal and professional time in Kaunas. Without their contribution and support, this thesis would not be as innovative and heavy as it is. They helped beyond their limits in the experiments and data collections during my Ph.D. I would also like to thank Mr. Aidanas Preiksaitis, MD, and Mr. Saulius Rocka, MD, Prof., from Vilnius University generously provided the patients' data from traumatic brain injury patients that were important in this thesis.

Moreover, I would like to express my gratitude towards Vytautas Petkus, DSc, for his help to provide the TBI patient data and help in understanding the complexity of filtering the raw data during the initial days of my doctoral studies.

I want to thank Rolandas Zakelis for helping me by providing the technical descriptions of the noninvasive time of flight measurement technology. I am also grateful to the senior administrator of Health Telematics Science Institute, Vilma Putnynaite, for her help and support in the documentation and departmental works. My time at KTU was also enriched by the help and support provided by the KTU doctoral office as well as international office. I want to especially acknowledge Reda Zilenaite, Jolita Steponkeviciute, Vita Daudaraviciene, and Audrone Rackauskiene. I do not want to forget Vice-Rector for Research and Innovations, Leonas Balasevicius, for his administrative and leadership efforts to create a positive research environment at University for the researchers and scientists. I gratefully acknowledge the funding received towards my Ph.D. study from the Research Council of Lithuania. I highly appreciate the support received through the Lithuanian academy of sciences and KTU to participate in various international conferences to present the research works.

My time in Kaunas was made enjoyable in large part due to the friends who became part of my life. My enormous gratitude goes to the people in my personal life. I am very grateful to my parents, especially my father, Nandkishor Bajpai, for his support throughout my life and for showing his tremendous faith in me. And most of all, for my loving, supportive, encouraging, and patient fiancée Evelina Seduikyte whose faithful support during all stages of this Ph.D. was beyond appreciation.

I hope this thesis will contribute to improving the traumatic brain injured patient's life and save suffering patient lives.

Table of Contents

ABBREVIATIONS

ABP – Arterial Blood pressure

ABPopt – Optimal Arterial Blood Pressure

ARI – Autoregulation Index

AUC – Area Under the Curve

BP – Blood Pressure

BF – Blood Flow

CA – Cerebrovascular Autoregulation

CBF –Cerebral Blood Flow

CaBV – Cerebral Arterial Blood Volume

CBF – Cerebral Blood Flow

CBFV/FV – Cerebral Blood Flow Volume Velocity

CBV – Cerebral Blood Volume

CFF – Continuous Flow Forward

COx – Cerebral Oximetry Index

CSF – Cerebrospinal Fluid

CPC – Cerebral Performance Category

CPP – Cerebral Perfusion Pressure

CBP – Cardiopulmonary Bypass

CPPOPT – Optimal Cerebral Perfusion Pressure

CVR – Cerebrovascular Resistance

CT– Computer Tomography

CNN – Convolution Neural Network

DCA – Dynamic Cerebral Autoregulation

ECG – Electrocardiogram

EEG –Electroencephalography

EMD – Empirical Mode Decomposition

FV –Flow Velocity

FIR – Finite Impulse Response

FFT – Frequency Spectra

GCS – Glasgow Coma Scale

GOS – Glasgow Output Scale

GOSHD – GOS after Hospital Discharge

HR – Heart Rate

IBV – Intracranial Blood Volume

ICP – Intracranial Pressure

In Situ – In the normal location

In Vivo – In a living organism

IIR – Infinite Impulse Response

IH – Intracranial Hypertension

ICH – Intracerebral Hemorrhage

ICU – Intensive Care Unit

IMF – Intrinsic Mode Functions

LLA – Lower Limit of Autoregulation

MAP – Mean Arterial Blood Pressure

MAP – Mean Arterial Pressure

MCA – Middle Cerebral Artery

MRI –Magnetic Resonance Imaging

Mx – Pearson's correlation coefficient between cerebral blood flow and arterial blood pressure

NIR – Near-infrared

NIRS – Near-infrared Spectroscopy

NICU – Neuro Intensive Care Unit

OA – Ophthalmic Artery

optCPP – Optimal CPP

PI – Pulsatility Index

PET – Positron Emission Tomography

PCT – Perfusion Computed Tomography

POCD – Postoperative Cognitive Dysfunction

PRx – Pressure Reactivity Index

Pbo2 – Continuous brain tissue oxygen

ROC – Receiver Operating Characteristics

SD – Standard Deviation

SPECT – Single-photon Emission Computed Tomography

SAH – Subarachnoid hemorrhage

SCAE – Stacked Convolutional Autoencoder

TBI –Traumatic Brain Injury

TCD – Transcranial Doppler

TOF – Time-Of-Flight

TBI – Traumatic Brain Injury

TF – Transfer Function Analysis

VRx1 – Volumetric Reactivity Index based on ultrasonic time of flight

VRx2 – Volumetric Reactivity Index based on ultrasonic attenuation

wPRx – Wavelet Pressure Reactivity Index

1. INTRODUCTION

Relevance of the research

Traumatic Brain Injury (TBI) is a prominent reason for mortality across the globe, causing suffering to patients and relatives as considerable costs to society. Around 2.5 million people in the European Union suffer from TBI. Out of these people, 1.5 million have been admitted to hospital, and 57,000 have lost their lives. Globally, it impacts 50 million people and costs the global economy US$400 billion annually. An estimate study states that every year in the USA $1 in every $200 is spent on TBI [2]. American innovation strategy [3] spends over 300 million US dollars for the *BRAIN Initiative* project which aims to help researchers better understand brain disorders, post-traumatic stress disorder (PTSD), and TBI for managing and analyzing large data sets involved in the severity. TBI is a complicated and severe condition; however, the evidence for treatment recommendations is lacking, and approaches are seldom adequately targeted. Generally, clinical TBI research is reduced to the attempts to isolate single factors for treatment. These single factors for the treatment approach do not account for the complexity of TBI and lack generalizability. Modern computational techniques and the availability of robust risk adjustment models facilitate more holistic approaches [2,3].

In the process of combatting this burden, we will entirely depend on improving understanding of TBI pathophysiology. After the primary injury, a pathophysiological implication is set, and, if it is not investigated, it could cause everlasting disability or mortality. Effective monitoring of the condition is essential to manage severe TBI based on immediate detection, and alteration of abnormal physiology could yield better results. Because keeping up the distribution of oxygen and nutrients to the brain via cerebral blood flow (CBF) is required for the brain to function, where intracranial hemodynamic monitoring is a fundamental element of neuromonitoring after severe TBI [4].

CBF is maintained by the cerebral autoregulation process, where CBF is proportional to the pressure gradient across the cerebral vascular bed monitoring after severe TBI, which includes monitoring of the difference between the arterial pressure (ABP) and the intracranial pressure (ICP). The difference between ABP and ICP has been denoted as the cerebral perfusion pressure and is used clinically to guide treatment along with the ICP value. This process is known as cerebral autoregulation (CA) [4].

It is an intrinsic ability of the brain to maintain stable CBF, while mean arterial blood pressure (MAP) and cerebral perfusion pressure (CPP) are changing [1,4]. The regulatory mechanism provides metabolic substrates under physiological and pathological conditions, for instance, after neuro-trauma or spontaneous intracranial hemorrhage. Constant CBF is regulated by altering the arteriolar diameter, which will change the cerebral blood volume (CBV) and, hence, ICP, while ICP is the sum of the partial pressures of the brain tissue, cerebrospinal fluid (CSF), and CBV [4,5]. CPP is defined as:

$$CPP = MAP - ICP \quad (1)$$

Autoregulation has been explained as a balancing act between vasoconstriction and vasodilation as the cerebrovascular bed's resistance accepts slow variations in CPP. CA's impairment influences the outcomes most of all, which means that it is essential to explore CA continuously in real-time [5,6]. This is essential to have a useful method or tool for the estimation and monitoring of CA. The relationship between ABP, ICP, and cerebral arterial blood flow velocity (CABFV) produces information on CA's operating behavior [4–6]. The development of the pressure reactivity index (PRx), calculated as a moving correlation coefficient between the slow-wave of ABP and ICP, has allowed for continuous CA monitoring over time. Since ICP and ABP are frequently employed measurement methods in TBI patients in the intensive care unit (ICU), and since no external ABP handlings are essential, PRx became a universally acknowledged CA condition marker. However, PRx, being a simple correlation coefficient, is noisy due to its non-discriminant nature; it is also inherent, incoherent, and physiologic [7].

The slow pressure waves in the cranial enclosure and the slow waves from blood vessels were first explained by Janny and Lundberg [8,9]. The ABP is obtained from the peripheral ABP signal, such as the radial artery. Pulse and respiratory waves, respectively, derived from cardiac and breathing events, are excluded. The ICP slow waves originate from the intracranial blood volume, termed as the *plateau wave* [8–10]. The relationships between ICP and ABP waves, CPP, and autoregulation, are still debatable.

Increased ICP has been related to low CA reactivity [11,12,13,14] and has emerged as an essential physiological driver of continuous deterioration. CPP values with the uppermost and lower limits are linked to poor CA reactivity and construct the base for individualized CPP target spectrum in adult TBI care, summarized as the 'optimal' CPP(CPPopt) theory.

The CPPopt theory has become popular during the last decade with the observation that PRx and CPP reflect a U-shaped relation over time with the least PRx occurring at a CPP, for which, CA reactivity is excellently secured; [13,14] reflects the parabolic relationship between PRx and CPP in adult TBI. Deviations in the achieved CPP from the CPPopt value have been associated with worse outcomes [15–16].

The only productive idea is to identify in real-time optimal cerebral perfusion pressure, which is identified using PRx. However, the most significant disadvantage of this method is the long delay in identifying the first conclusion for the individual patient, which requires waiting for hours. Impairment of the autoregulation for more than 5 minutes can kill the patient because the patient will lose the neuron cells. Physicians have as little as 5 minutes for the treatment decision making in order to save the patient. There are several questions but not enough answers in the field. Many scientists are working in this field by using different approaches; some are working on creating a new technology; some are working on automatic decision making (Artificial Intelligence, deep learning), while others are enhancing the currently available technology. Yet, there are not many novel ideas for such complicated problems. Neither the modern medicine nor the modern pharma industry can help with the treatment decision making of severe traumatic patients.

This thesis is a focused and vital study to enhance the existing technology to estimate correct cerebral autoregulation and prevent neuron (brain cell) damage by analyzing ABP and ICP signal. This further improves the signal quality for the estimation of the reactivity indexes (i.e., PRx, volumetric reactivity index (VRx)) that could also be used for identifying patient-specific optCPP (Optimal perfusion pressure).

Scientific-technological questions

The scientific-technological questions that are being resolved in this thesis are as follows:

How can the quality of the slow wave from the arterial pressure reference signal recorded from the human body be improved to get a reliable, sensitive, and specific estimation of autoregulation?

How can cerebral autoregulation be measured and controlled non-invasively with sensitivity and specificity as needed for the clinical practice? Is there any better alternative to the currently available methods?

Hypothesis

It is possible to improve the reliability, sensitivity, and specificity of cerebrovascular autoregulation outcomes by automatic elimination of artifacts in the arterial line and by the higher quality (increased signal to noise ratio) filtering of slow arterial blood pressure waves.

It is possible to measure and monitor CA non-invasively and continuously by ultrasound attenuation dynamic measurement in the human brain.

Aim of the thesis

This research aims to develop a method for the extraction of a higher quality slow wave as a reference signal from the arterial line and to identify a slow wave of higher and acceptable quality for reliable, sensitive, and specific cerebral autoregulation monitoring by filtering the unwanted signals (any signal which has no relation to physiology) in both invasive and non-invasive autoregulation by their reactivity index assessment in a cost-effective way (without artificial intelligence or supercomputers).

Objectives of the research

The primary objectives of the research are listed below:

1. To examine and select the best possible method of artifact removal in the invasive, non-invasive arterial and intracranial line.
2. To assess the clinical association between the CA index, PRx, and the quality of ABP and ICP signals.
3. To perform a comparative study between two novel non-invasive methods based on the volumetric reactivity index.
4. To propose a novel cost-effective, non-invasive CA monitoring technology: *Ultrasonic attenuation in the brain*.

These objectives of this thesis provide the basis for each of the result chapters (4,5,6,7). In the subsequent chapters of the thesis, the literature review study was covered in Chapter 2, methods used in the thesis are outlined in Chapter 3, and detailed each of the studies in Chapters 4,5 and 6, while Chapter 1 consists of an introduction and working hypotheses. In the final Chapter, 7, conclusions are summarized.

Scientific novelty of the work

The raw signal from the arterial blood pressure (ABP) line and intracranial line (ICP) contains a higher number of artifacts in the recorded data, which adversely impacts the monitoring effectiveness. Such signals full of artifacts are being evaluated, improved, and enhanced by filtering process which provides improved CA value that helps physicians make patient treatment decisions efficiently. The collected raw data has been processed and filtered with various filters, and, among those, the FIR (Parks–McClellan) filter was found to be efficient, which provides filtered data that offers significantly better PRx outcomes than any other tested filters.

Slow wave analysis for the cerebral autoregulation index by using the FIR (Parks–McClellan) filtration method in traumatic brain-injured patients and a healthy volunteer was novel and value-adding for cerebral-autoregulation index (PRx, VRx) estimation.

Also, proposing a novel noninvasive volumetric reactivity index (VRx2- based on ultrasonic attenuation) is cost-effective approach than any other noninvasive CA monitoring methods including the transcranial doppler, which makes it advantageous in the developing countries.

Research methods and tools

The retrospectively collected data that was utilized in two of the studies comprising this thesis was harvested in TBI patients admitted to the Republican Vilnius University Hospital (Lithuania). Each patient exhibited a clinical need for ICP monitoring; ICP and additional computerized bedside signal recordings are within the database.

The study of healthy volunteers was performed at the Health Telematics Science Institute of Kaunas University of Technology, where IBV recording was done by a noninvasive ultrasonic monitor developed by the Health Telematics Science Institute of Kaunas University of Technology (Kaunas, Lithuania).

MATLAB software and ICM+ were used to process the data recorded during the studies.

SPSS statistical software package was used to implement a statistical analysis of the data.

Practical importance of the work

The yearly incidence of TBI is approx. 500 out of 100,000 in the US and Europe. TBI ranges from 100–330 new cases of 100,000 population every year. It is one of the significant causes of death and disability, particularly among young individuals, leading to suffering in victims and relatives, and substantial direct and indirect costs to the society. In the USA, a yearly burden of around $ 60 billion is observed. In

patients with severe TBI, the lifetime cost per case is estimated at $ 396,000 with patient damage and medical rehabilitation costs by a factor of 4. A recent study shows that TBI's total costs in Europe, excluding non-hospitalized patients, produced a figure of € 33 billion. Up to 1/3 of TBI patients who were not admitted to hospital could also develop a lifelong disability [3].

TBI is known for the heterogeneity, including etiology, mechanisms, pathology, severity, and treatment, with widely varying outcomes. Traffic incidents cause various types of injuries across the globe. TBI can be diffuse damage, contusion brain damage, and intracerebral hematoma. Structural damages may or may not be visible on imaging. The clinical severity ranges from a minor injury to survivable damage. Center TBI found significant differences in outcomes between centers with a higher risk of 'poorer' vs. 'better' centers after adjustment. They also recognize that TBI is not merely an acute event, but it can trigger a chronic process, with a progressive injury over hours, days, weeks, months, and even years [3].

As mentioned above, European (Center TBI) and American (Track TBI) institutions have been working with the traumatic brain-injured patients to achieve better treatment by transferring all the current research efforts to treat better into the modern concept of precise medicine, individual-tailored medicine. Nevertheless, no precise ideas have been developed yet to resolve the above-mentioned problems. The only way to resolve these are higher-quality signals, improved monitoring, better individual patient treatment decision-making, and a better prognosis.

Description of analysis on ABP, ICP, and cerebral autoregulation monitoring

It is already known that the continuous assessment of ICP, ABP, and cerebral autoregulation has been available during the last two decades. However, the quality of the collected neurophysiological (ICP, ABP) signal is unknown, and the impact of the signal quality on CA monitoring variables has not been described.

Association and impact of invasive ICP and ABP slow-wave for CA monitoring in TBI patients

Mean ABP(t) and ICP(t) is essential for a shorter period to calculate the pressure reactivity index (PRx), and the most common approach being used is the moving average. The main aim of this study is to bring attention to the need for ABP and ICP signal analysis in TBI patients as cerebral autoregulation (CA) index PRx(t) shows the importance of quality of ABP(t) and ICP(t) signals for the diagnostic value of CA monitoring.

Novel Non-invasive method of cerebral autoregulation monitoring

The novel non-invasive ultrasound attenuation volumetric reactivity index (VRx2) is similar to the time-of-flight volumetric reactivity index (VRx1) which is used these days for scientific research and studies. The ultrasonic attenuation volumetric reactivity index (VRx2) is an appealing, economic surrogate to the time-of-flight reactivity index (VRx1) and potentially easy for hardware miniaturization.

Statements for defense

For the best possible filter selection, in the filtration of neurophysiological signals to avoid the intensive care unit's false alarm, the finite impulse response (FIR) filtering approach is adopted. Among the five filters, the FIR (PM) filtering approach offers higher quality of the filtered slow wave. It is better than the Kalman filter, the Butterworth low pass filter, the Chebyshev filter, and slightly better than the moving average.

The PRx, TBI patient's clinical outcome, and the quality of ABP and ICP signal indicated that the FIR (Parks–McClellan) filtered data was more sensitive for discriminating between intact and impaired cerebral autoregulation for TBI treatment decision making.

The comparative study of the noninvasive ultrasonic volumetric reactivity indexes VRx1 (time-of-flight) and VRx2 (attenuation) monitoring showed a significant correlation. The attenuation based volumetric reactivity index (VRx2) can be used as a noninvasive alternative autoregulation index similar to the ultrasonic time of flight based VRx1 and could be used to reflect essential information related to the CA status.

Dissemination of findings

• Two publications related to the doctoral thesis were published in the scientific journals with IF (see Publications on page 99).

• The concept presented at five international conferences in 5 countries: Glasgow (Scotland, UK), Madrid (Spain), Cardiff (Wales, UK), Copenhagen (Denmark), and at a University conference in Kaunas (Lithuania).

Structure of the dissertation

The dissertation consists of seven chapters excluding the list of references:

Chapter One of the dissertation discusses the problem and hypothesis, including the relevance of the research.

Chapter Two covers the literature review study, where the currently existing solution technologies and their limitations are discussed.

Chapter Three explains the methodologies used in the thesis.

Chapter Four presents the study conducted to select the best filter for filtering the ABP/ICP signal slow wave.

Chapter Five presents the results of the association of sensitivity and specificity of ABP/ICP quality with clinical outcomes.

Chapter Six presents the findings of the association between the novel volumetric reactivity index (VRx2) compared to the Ultrasonic time of flight reactivity index (VRx1).

Chapter Seven contains the overall conclusion and limitations of the research.

The total volume of the thesis is 98 pages. There are 34 figures, 11 tables and 227 references in the text.

2. LITERATURE REVIEW – CEREBRAL AUTOREGULATION MONITORING

A hemodynamic model for the CBF has been described to allow investigating CBF regulation [17, 18]. This model relies on the pressure applied to the ABP, the backpressure in the cranial enclosure (ICP), and the resistance of the diameter of the small cerebral vessels (cerebrovascular resistance (CVR), see Fig. 2.1). This relationship can be simplified as:

$$CBF = \frac{ABP - ICP}{CVR} \quad (2)$$

Hence, cardiovascular, ICP, and cerebrovascular elements are essential factors of CBF or circulation. This model specifies understanding of the physiological determinant that manages brain perfusion in normal conditions and explains that CBF regulation is generally impaired [4,17,18].

The main objective of a clinical study of TBI is to improve the management of severe TBI; the main factors influencing the treatment outcomes are CA [6,11]. Autoregulation is explained as a balancing act between vasoconstriction and vasodilation as the cerebrovascular bed's resistance accepts slow variations in CPP. Where cerebral autoregulation impairment influences the outcomes the most, it is essential to continuously explore cerebral autoregulation over time (real-time) [13–16]. Czosnyka *et al*. exposes the relationship between slow changes in mean ABP and ICP, leading to the relationship between CPP and the cerebral blood flow (CA) by developing PRx. PRx is most commonly obtained by the calculation of pressure reactivity index (PRx), as the Pearson correlation between ABP and the intracranial pressure (ICP) slow waves [15,16]. The rise in luminal ABP will lead to passive cerebrovascular dilation, increasing cerebral blood volume, and ICP. In that case, the correlation coefficient (PRx) between ABP and ICP will be positive.

2.1 Regulation of Cerebral and Arterial Circulation

The brain requires nutrients and oxygen to function adequately. Hence, a circulatory structure is essential to keep up the stable CBF for the brain's various requirements. Oxygen and supplement distribution are based on the pumping to the heart–brain system to make sure the accurate regulation of its perfusion. The cerebral vessels have the excellent capability to adjust quickly and respond to the brain's pressure in the cerebral vessels. Cardiovascular, intracranial pressure, and cerebrovascular components are all essential regulators of the cerebral circulation.

2.1.1 Cardiovascular element/component study

The brain vessels' pressure is based on key factors outside of the brain: the heart provides the cardiac output, whereas the peripheral vessels provide the resistance. Both contribute to the ABP supply to the cerebral structure. The balance between the brain cerebrovascular resistance and the total resistance determines the proportion of the cardiac output supplied to the brain. Hence, any pathophysiological event that impacts the heart can change cerebral circulation. Hence, circumstances, for example,

cardiogenic shock and arrhythmia, damage CBF [19, 20]. We must consider that pathologies influencing ABP can impact CBF [21,22]. Vasopressors operate to buffer ABP by shrinking peripheral vessels, and inotropes and cardiopulmonary bypass mechanisms operate to modulate cardiac results (Fig.2.1). An essential consideration to these ABP enhancement-based methods is that the connection among ABP and CBF variations is usually nonlinear because functional alterations in the vascular tone occur at the cerebral arterioles because of CA [23–26]. Additionally, regulating ABP as a remedy will raise the blood flow to the brain and raise the blood flow to any vascular beds with small vascular resistance.

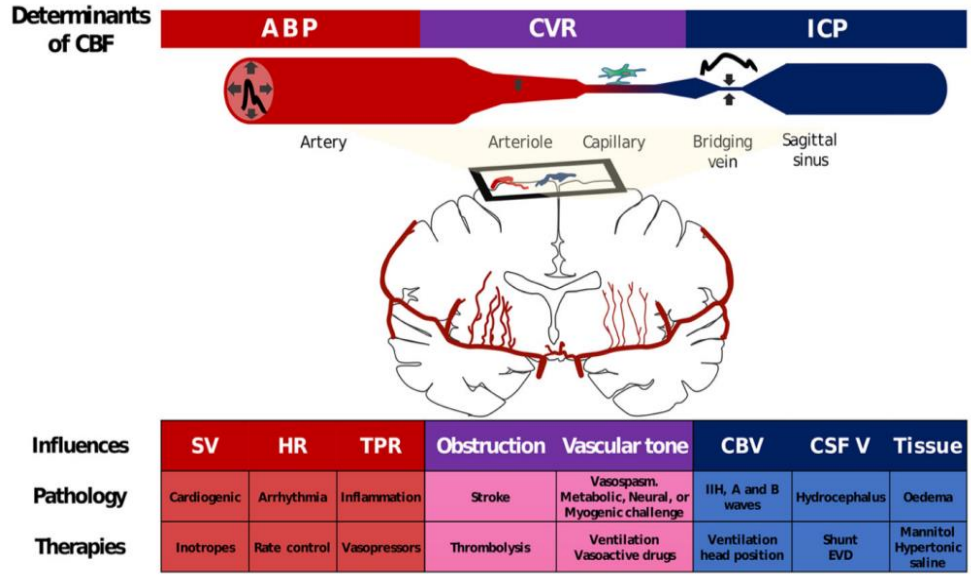

Fig. 2.1. Regulation of the cerebral blood flow (circulation). The microvasculature is directly proportional to perfusion pressure and inversely proportional to vascular resistance. ICP places its effect on CBF through changes in perfusion pressures [4]

2.1.2 Intracranial element

The venous pressure is related to larger cerebral veins and the intracranial pressure. If the ICP pressure is higher in the lateral lacunae that feed into the large venous sinuses, then these compressed vessels go to a post-capillary venous pressure above ICP [27,28]. Thus, an increase in ICP leads to the decreased longitudinal pressure gradient across the vascular bed – the cerebral perfusion pressure, and, if there are no compensatory changes in CVR, CBF decreases [29]. A rise in the volume of the intravascular compartment, the CSF compartment, or the brain parenchymal compartment, can increase ICP and therefore have the potential to decrease CBF [30].

2.1.3 Cerebrovascular element

CBF can be handled by dynamic changes in the |regulating vessels' diameter, thus influencing the cerebral vascular resistance (CVR). The main site of active

regulation of the cerebral circulation occurs at the arterioles [17,18]. Nevertheless, larger conduit arteries, capillaries, and venous shapes are valuable in certain conditions [31,32], such as neuronal awakening, relaxation of pericytes neighboring capillaries are considered responsible for a significant portion of the flow gain [32–34].

Such cerebral vascular resistance changes are predictable while brain activation, an increase in the neuronal activity elicits a significant increase in the blood flow [35] mediated via vessel dilation. While the vasospasm is linked to subarachnoid hemorrhage, large cerebral arteries compress, and repeatedly develop a higher local CVR and lower CBF [36].

Alteration in the cerebral vessels' vascular environment is created by constriction and dilating materials, such as vasoactive materials, possibly provided to the vessels by the bloodstream (e.g., pCO2) created locally. This heterogeneity in the identified sites of vasoactive material production can cause difficulty in physiological mechanisms [37].

The autonomous nervous system could impact the vascular tone of cerebral vessels. Except for animal studies, a rich innervation of the dilating parasympathetic and constricting sympathetic fibers, CBF's autonomous control in humans remains questionable [38, 39].

Moreover, cerebrovascular resistance, mean arterial pressure, and intracranial pressure, the heart's outcome, is an autonomous regulator of CBF [40,41,42]. Such an opinion was made from studies that have demonstrated CBF change after interventions that change the cardiac output but have no impact on the MAP [43,44].

As per the traditional model (Fig.2.1), for a rise in cardiac outcome to produce a raised CBF without alteration in ABP, absolute peripheral resistance and cerebrovascular resistance must be reduced [42]. The ABP measured in the studies (vascular regulation researches) is not the ABP in the large cerebral arteries, but rather the pressure in a narrow peripheral vessel, or measured at the finger or arm non-invasively. A rise in the cardiac outcome causes a rise in CBF, ICP and unchanged ABP.

The simple schema provided in Fig.2.1 must be interpreted with the knowledge of the variables' interdependence. The cerebral circulation has multiple brain-protective mechanisms, such as if ABP falls, aortic and carotid baroreceptors will change automatically to increase HR, and, hence, buffer ABP and CBF [44]. In the same way, according to Lassen *et al*., on reacting to a fall in ABP, vessels will widen to buffer CBF [23]. These essential Cerebro protective techniques are termed cerebral autoregulation (CA); in the later sections, it will be explained in detail because of the CA's critical role.

2.2 Methods of Intracranial and Arterial Hemodynamic Monitoring

Considering the multiple post physiologic conditions to TBI that could badly damage the cerebral circulation, correct and realistic intracranial hemodynamic monitoring technologies are essential. Sometimes, choosing a suitable monitoring technique is an efficient requirement that depends on the clinical sequence of events. Non-invasive monitoring techniques, such as transcranial Doppler (TCD) and near-

infrared spectroscopy (NIRS) [45,46], both are portable and possible to assess in the medical ICU room or the operation theatre. Besides, they have also collected high frequency and repeated data over time, which could be linked with other techniques, such as ABP, to provide CA and CO2 reactivity information.

Non-invasive cerebral perfusion methods including brain tissue oxygen oximetry, laser Doppler flowmeter, and thermal diffusion [47,48], applicable for severe patients because of its noninvasive character, these techniques benefit from a bit more prosperous durable monitoring of the cerebral circulation. On the other hand, brain imaging techniques (computer tomography (CT), positron emission tomography (PET), and magnetic resonance imaging (MRI)) are advantageous to offer an excellent spatial resolution of CBF data and the capability to evaluate certain CBF. However, they do not apply to bedside measurement because of its size, temporal resolution, and radiation exposure [49,50]. A list of CBF monitoring approaches is explained in Table 2.1.

Table 2.1. Methods for assessing cerebral blood flow

Technique	**Principle**	**Bedside and Continuous**	**Type of CBF assessment**	**Robustness**	**Invasive/ Non-Invasive**
PET	Radioactive tracers emit positrons dependent on perfusion	No	Global and local	Excellent	Minimal
CT	Attenuation of Iodine contrast (perfusion CT)	No	Global and local	Excellent	Minimal
TCD	Doppler	Yes	Global	Fair	Non-Invasive
NIRS	Absorbance of O2Hb and HHb	Yes	Local	Good	Non-Invasive
MRI	Perfusion dependent T2 signal changes with gadolinium	No	Global and local	Excellent	Minimal
PBTO2	Clark electrode	Yes	Local	Excellent	Invasive

LDF	Doppler	Yes	Local	Excellent	Invasive
Thermal diffusion	Thermal diffusion	Yes	Local	Excellent	Invasive

2.2.1 Intracranial Pressure (ICP) and Cerebral Perfusion Pressure (CPP) monitoring

ICP monitoring turns into a standard of care in serious post-TBI; however, it is further used for some cases of subarachnoid hemorrhage (SAH) or broad ischemic strokes. Because the brain sits inside the stiff cranium, rises in the volume of all three crucial sections (tissue, blood, CSF) cause a rise in ICP. Thus, monitoring ICP can alert the clinician of a critical physiological condition, such as developing edema, extending injuries, or developing hydrocephalus. Any cause rises in ICP can reduce global perfusion by a reduction in CPP, as explained in Fig.2.1, or cause an impressive reduction in the local perfusion in the areas of herniation. In herniation syndromes, because of the pressure gradients inside the brain, fragments of the skull tissue are pressed with force opposite to the stiff frame, such as the *foramen magnum*, the *tentorium cerebelli*, or the *falx cerebri*, and the resultant local compression activates impressive reduction in CBF.

The assessment of ICP needs access to the cranium, usually accomplished with a frontal burr hole. Even though the best location for assessing ICP is from the parenchyma, pressure can be transduced from various positions inside the skull, i.e., the subdural, epidural, or intraventricular locations [51]. Intraventricular transducing is specifically advantageous in some circumstances due to a fluid-filled intraventricular catheter that can admit ICP assessment and drainage of CSF as a measure to reduce a raised ICP. Intraventricular drains, yet, need a fluid-filled transducing line and thus carry extra chances of infection. As ICP influences cerebral venous pressure, it is regularly monitored together with ABP to give CPP. Same as monitoring ICP, monitoring CPP is suggested after severe TBI. CPP presents the clinicians with some warning of whether the brain will be hypo or hyper perfused and permit careful titration of the potential technique to adjust CBF clinically [52].

2.3 Cerebrovascular Autoregulation (CA)

CA is the homeostatic system by which the brain keeps up almost continuous CBF regardless of alteration in systemic BP and CPP [53, 54]. A temporary variation in CPP offers efficient adjustments in cerebrovascular resistance by complex neurogenic, myogenic, and metabolic mechanisms to protect constant CBF. Such a process is termed as DCA (dynamic cerebral autoregulation). DCA maintains enough supply of glucose and oxygen to the brain to meet its high metabolic needs. Impaired

autoregulation has been explained after TBI [55–58], ischemic stroke [59–61], and intracerebral hemorrhage (ICH) [62,63], and has been related to poor outcomes [62].

2.3.1 Static and dynamic autoregulation monitoring

Static autoregulation monitoring indicates the relation between ABP and CBF alterations at a steady-state, which is the durable CBF response to a maintained variation in ABP. On the contrary, dynamic measurement of autoregulation indicated CBF changes in response to temporary alterations in ABP. Dynamic CA measurement needs constant ABP (e.g., fluid-filled pressure transducer, or from a non-invasive photoplethysmogram) and an alternate CBV or CBF, NIRS, brain oxygenation, ICP, see Table 2.1. DCA is frequently tested with persuaded transient alterations in ABP. Techniques to alter ABP for DCA measurement consist of contraction of supra-systolic thigh cuffs [64,65], postural maneuvers [66], and the lower body negative pressure [67].

The static autoregulation was explained by Lassen *et al*. by the CA curve. For plotting equilibrium state assessment, two of ABP and CBF from 11 research articles, explaining an autoregulatory plateau and lower limit of autoregulation (LLA) are used [23]. The authors concluded that the LLA for the brain is at a mean ABP of 50 mm Hg. This principle had been carrying through in medical exercise just before the recent recognition that the LLA is variable throughout pathological settings [68,69]. Irrespective of the procedures employed to evaluate dynamic or static autoregulation, some appearance of a static *Lassen's curve* has to be produced if the aim is to recognize an LLA and allocate ABP and CPP objectives.

Besides specifying the lower boundary of autoregulation from demographic data, equilibrium state assessment of CBF and CPP can be evaluated with an individual, linear measure, the static rate of autoregulation. An individual change in CVR (CVR= CPP/CBF) is evaluated in reaction to an individual alteration in CPP [70]. Usually, ABP rises by the slow perfusion of a vasopressor to gradually raise the ABP by approximately 20 mm Hg. In different situations, ABP or CPP is extremely changeable; the CA curve can be estimated by plotting CBF at an average in ABP or CPP (Fig. 2.2).

Dynamic autoregulation, an alternative approach to static autoregulation assessment, continuously monitors the CBF response to natural slow variations ABP [71]. This kind of approach has essential warnings, the inherent ABP changes cannot be hard enough to resist CBF, and alterations in CBF can happen by all elements except for ABP. Nevertheless, the benefits are that the monitoring has no hazard to the patients, and, because the monitors can be continuously used, someone may evaluate trends over time CA in a patient. The study of slow ABP trends and CBF for CA measurement can be split into the time domain (the correlation approach) or in the frequency domain (transfer function or wavelet transform analysis). The most widely used CA indexes are enlisted in Table 2.1.

The frequency-domain approach considers that CA serves as a high pass filter. Into the model, rapid, higher frequency variations above 0.3 Hz in ABP (such as pulse wave) directly transmit to the cerebral circulation. Meanwhile, slow, low-frequency variations below <0.15 Hz in ABP are filtered out and incompletely transmitted to

CBF. The transfer function exploits the ABP and CBF waves' FFT to measure three variables, phase, gain, and coherence in the chosen frequency range (0.02–0.07 Hz and 0.07–0.15 Hz) [72]. The phase is the angle of counterbalance between the CBF and the ABP wave and, in the core, presents the physiological timing by which CBF varies in response to a slow variation in ABP. An improved phase change reflects the initial counter regulative alterations in CBF and perfect autoregulation, while a phase change near 0 reflects simultaneous timing of variations in the wave, and, hence, impaired autoregulation. The attainment shows the volume of transfer of slow waves in ABP to slow waves in CBF.

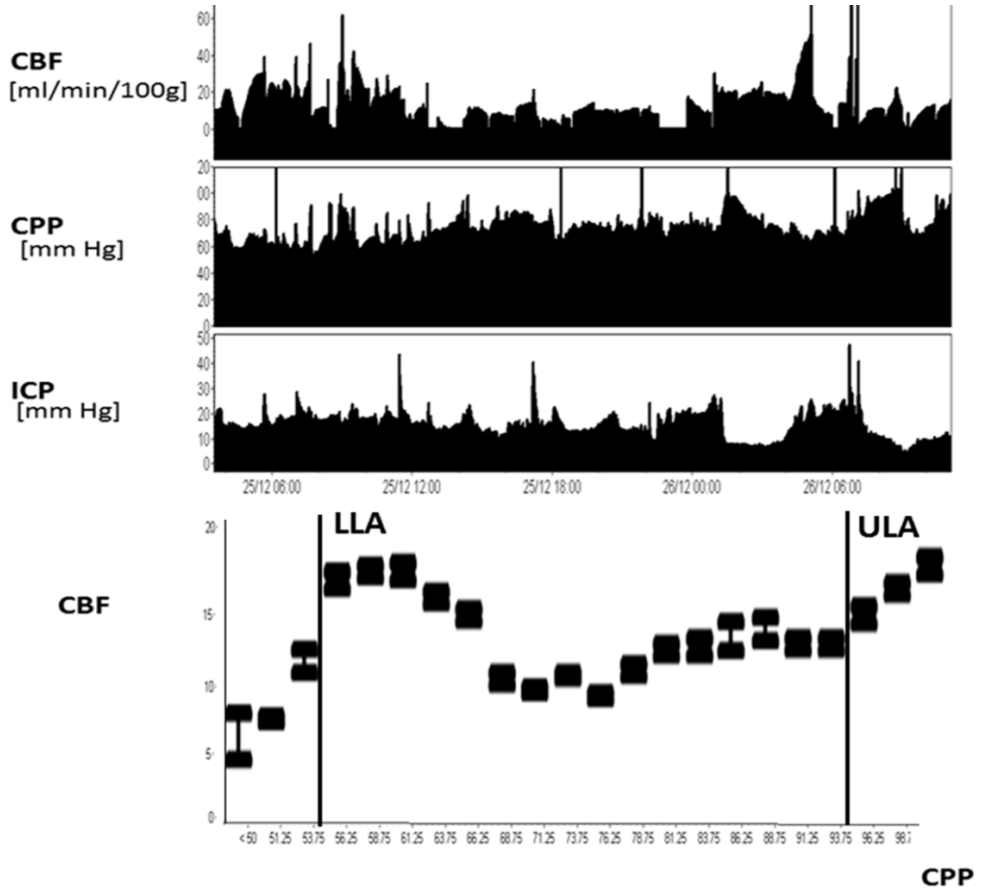

Fig. 2.2. Example of the invasive CBF and CPP monitoring, representing the Lassen's curve reflecting CA. The curve also shows the lower and upper limits of CA [4]

At last, coherence represents the statistical association between the two signals. High coherence between ABP and CBF describes a linear system and is an essential condition for reliable phase and gain calculation [71–73]. ABP and CBF, when time-averaged (10s), minimize the influence of the cardiac pulse and respiration, and 30 such samples are usually used for a single Pearson correlation coefficient [74,75]. A positive correlation among ABP and CBF reflects damaged autoregulation, while 0 or

a negative correlation represents intact autoregulation. These outcomes could be by using different elements of the ABP signal, such as the mean values represented by Mx, diastolic values Dx, and systolic values Sx. The benefit of correlation dependent ARIs in monitoring the moving trends in autoregulation can be observed in a TBI patient while observing the plateau waves in ICP (Fig. 2.3). The rise in ICP and a further reduction in CPP generates a reduction in the CBF pace and disturbance in the correlation index (Mx). After three waves of ICP and CA derangement, ICP and Mx get back to the baseline values. NIRS can also be used for estimating the CA in the time and frequency domain and is easily applicable in many situations (compared to TCD). NIRS based CA indexes estimates the relationship between CPP/ABP and cerebral oxygenation [76].

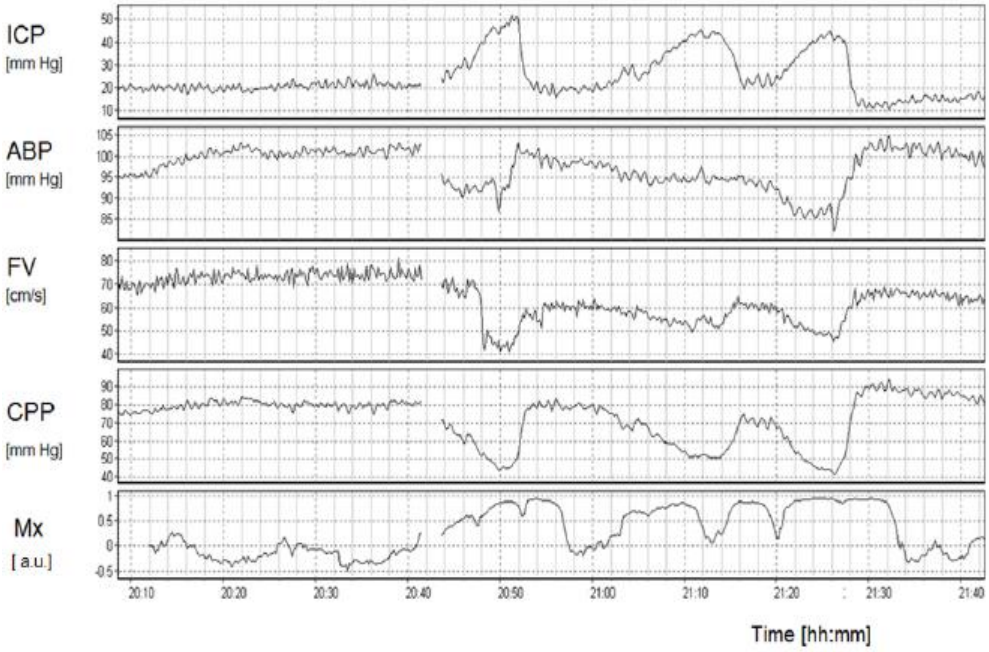

Fig. 2.3. Time-correlation CA during repeated ICP plateau waves in a TBI patient. The Mx index was calculated continuously along with other brain modalities (ICP, ABP, FV, CPP) [76]

2.3.2 Cerebral autoregulation assessment

The concept of CA has proven to be useful in neurosurgical populations by cerebrovascular pressure reactivity. The CA pressure response evaluates the relation between ABP and ICP by taking variations in ICP to reflect variations in the cerebral blood volume (CBV). The essential physiology of CA pressure reactivity in vigorously autoregulating vessels is a reduction in cerebral ABP will induce intracranial vessels to enlarge [25], which raises CBV. A rise in CBV will induce whether an increase in ICP or no variations in ICP shall be observed. On the other hand, with impaired autoregulation, a decrease in ABP will cause a passive reduction in the vessel diameter and decrease CBV and ICP.

The relation among ABP, vessel, CBV, and ICP construct the base for the PRx. PRx is comparable to most of the time domain ARIs and is estimated as the continuous correlation among thirty sequential time-averaged (mean) ABP and ICP values [77]. A positive index (positive correlation) implies impaired cerebral autoregulation, while a negative (or zero) index implies intact autoregulation.

We already know that PRx is a naturally noisy (polluted by artifacts and other sources) index. This pollution or noise can be reduced/removed by averaging the duration or timing. One more essential characteristic of the PRx is the constant measurements which reflect the patterns online or in real-time. In that case, a patient admitted with TBI is monitored with continuous ABP, ICP, CPP, and PRx for days.

The PRx method establishes a causal relationship between ABP, cerebral blood volume, and ICP; however, the PRx approach does not estimate CBF or the cerebral blood volume, nor does it assess time-delays. Keeping in mind these factors, PRx provides a continuous, computationally parsimonious, physiologically based assessment of autoregulation that has prognostic relevance [77]. Thus, PRx is possibly the optimal way to constantly monitor CA reactivity for the long term in anesthetized or coma patients with ICP monitoring [78]. Significantly, as a concept validation, Brady *et al*. explained in a pig imitation that PRx varied from -ve to +ve values when the LLA attains hemorrhage [79].

In medical practice, PRx greater than 0 does not always indicate a CPP under the LLA, even with the averaging of time, though, frequently, a U-shaped curve of PRx can be viewed [15,80,81], with the CPP at the minimal value of PRx comparable to the section of the greater stability of the blood flow. Whenever CPP versus PRx is plotted, a U-shaped curve can be seen with the higher -ve values of PRx corresponding to the center of the autoregulatory region as reflected by the CPP-CBF relation. Therefore, experimental data, clinical examination of large groups [79–81], and specific clinical monitoring shows that PRx is a useful indicator of autoregulation.

2.3.3 Arterial Blood pressure for CA assessment (Invasive and non-Invasive)

As we already know, unregulated cerebral blood flow may require active blood pressure management in the Neurointensive care unit (NICU) setting in monitoring autoregulation to shape clinical settings although the gold standard does not exist for estimating or monitoring autoregulation. Among different approaches, TCD, combined with *Finapres*, has become apparent as a non-invasive method of evaluating DCA. This method has a wonderful temporal resolution by estimating the blood flow velocity response to the BP variation [82,83].

The usual approach to estimate DCA is the correlation of the time period approach and the transfer function study. The correlation approach evaluates CBFV and systemic BP for an interval of time and obtains the correlation coefficient among time-averaged (mean) CBFV and MAP velocity index [4]. Optionally, DCA can be estimated from automatic fluctuations in BP and middle cerebral artery FV at specific frequencies by a transfer function study [84,85].

Both approaches have been cross-verified non-invasively by employing *Finapres* [86]. *Finapres* is used in the NICU, though, because of peripheral vasoconstriction [87]. In such cases, BP is usually estimated invasively via the intra-

arterial catheter. However, non-invasive measurement of ABP with the *Finapres* verified with intravascular ABP for sleep monitoring [87], it is not much known whether they are equivalent in assessing DCA. Therefore, Petersen *et al*. [88] tested the hypothesis that *Finapres* can achieve comparable results to assessment with invasive blood pressure monitoring while using an arterial catheter.

There is considerable methodological diversity among studies measuring DCA, such as TCD, combined with *Finapres*, which has been the method of choice for DCA's non-invasive assessment. Hence, this is essential that arterial methods should be available to estimate CA [57]. Comparison of the fidelity and correctness (accuracy and precision) of *Finapres* to invasive arterial estimation has been explained in measuring BP [89]; Nevertheless, less confidence has been expressed if various approaches are utilized interchangeably to measure CA. Lavinio compared the ARI estimated as the correlation coefficient among variations of CPP and CBFV with an entirely non-invasive technique using *Finapres* as an alternative of CPP. For the estimation of CPP, they evaluated intravascular radial artery BP and ICP [89]. This is the case where two assumptions apply: the negligibility of ICP fluctuation on DCA estimation, and secondly, the accuracy of *Finapres* BP slow-wave evaluation. It is unclear either this was because of the dissimilarity in the BP measurement or the result of the ICP fluctuation. In the above investigation, excellent correlation (and agreement) between both approaches as BP sources was observed. Mean ABP evaluation does not differ by *Finapres* and arterial catheters.

A good correlation was observed between the DCA estimates obtained with *Finapres* and arterial catheters [90,91]. However, a significant difference in the absolute values for the mean phase shift and Mx was observed. It was stated that it might be likely that a small amount of noise rises in the *Finapres* signal driven to the low correlation coefficient. It is challenging to clarify the dissimilarity in a phase shift which was reduced with an arterial catheter compared with *Finapres*.

Their study agreed with the study examining the impact of invasive ABP measurement on the variables of DCA. Sammons *et al*. examined the phase change by *Finapres* and an intra-aortic catheter in patients experiencing coronary catheterization. He found a comparable bias, and all the evaluation was taken from the radial artery so that to make less probable that the expansion of the pulse pressure waveform from the aorta to the peripheral circulation is an essential element. It could be possible that the distant position of the *Finapres* could have caused the variation in a phase shift/change [91]. Sammons *et al*. further hypothesized that a medication effect might have played a role, as 76% of their patients took beta-adrenergic antagonists.

Hence, it could be stated that *Finapres* cannot reproduce the dynamic changes in the low-frequency range and invasive monitoring. Omboni and colleagues [90] found that *Finapres* systolic BP fluctuates within a very low-frequency range, thus increasing the phase shift. However, absolute variations in estimating autoregulation are probably not a major concern in patients monitored with one approach or the other.

The different mode among the techniques becomes essential if different approaches regarding carrying out patients' linear measurements at different timings. This can introduce a strong bias, and the figures should perhaps be adjusted when an

arterial line approach is substituted with the *Finapres* or the opposite. Such as, if an arterial catheter obtains measurements in traumatic patients only with *Finapres*, it may seem as though DCA has improved when it is, in fact, only due to the inter-method bias. Additionally, they found that the greater cohesion among CBF velocities and ABP was adapted from the arterial catheter in contrast to *Finapres*. Consequently, the least measurements had be to rule out from the evaluation to fulfill the inclusion's cohesion limit [90, 91].

2.3.4 Comparison of the wavelet and correlation method for CA assessment

Cerebrovascular autoregulation was mediated by vasoreactivity with the changes in cerebrovascular resistance. Autoregulation could be a dysfunctional post-cardiac arrest, a traumatic brain injury, and raised intracranial pressure (ICP) [92–97] with changes in the ABP autoregulation limits.

The mean optimal arterial blood pressure (ABPopt) is determined where autoregulatory reactivity is the most intact after a pediatric hypoxic brain injury [95,98,99]. Aiming the CPPopt might enhance the neurological outcomes after an adult traumatic brain injury [96,101]. However, the ABPopt should be used after a pediatric cardiac arrest because invasive ICP monitoring will not be estimated regularly. A constant blood pressure close to ABPopt depends upon a less neurologic injury in kids who are at risk of a hypoxic brain injury, including a cardiac arrest [95,100] and those with hypoxic-ischemic encephalopathy [98–100].

Near-infrared spectroscopy (NIRS) helps in continuous autoregulation monitoring in the frontal cortex via a widely used method that uses low pass filters and correlation coefficients between the perfusion pressure and the surrogate of ICP or the cerebral blood volume (IBV) [96,105]. The correlation method is commonly used in TBI and the cardiopulmonary bypass [106] research even though they found that the correlation between a NIRS-based cerebral blood volume measure and ABP was associated with the outcome after pediatric cardiac arrest.

Liu X. *et al*. [7] sought a new metric for autoregulation and vasoreactivity monitoring in pediatric hypoxic brain injury. They validated a wavelet-based method between ABP and ICP [7] that was excellent in identifying the ABP lower limit of autoregulation (LLA) in pigs with IH than the widely used, ICP-based, correlation matrix known as the pressure reactivity index (PRx) [77]. Moreover, the wavelet technique served better for identifying CPPopt and better-predicted outcomes in adult TBI [101]. The enhanced ability to identify CPPopt by the wavelet method may be related to the lower index time-variability with less signal noise. They compared the wavelet and the correlation matrix in pigs. Many autoregulation assessment indexes were estimated by the correlation and wavelet methods, such as the PRx and wavelet PRx (wPRx), COx, and wavelet Cox (wCOx). They also stated that the wavelet approach would minimize the autoregulation index variability compared to the correlation methods and that wavelet indexes can differentiate functional from dysfunctional autoregulation in the developing brain after cardiac arrest.

Doppler flowmetry enables a standard measure of the autoregulatory function to identify the individual LLA in each piglet. Wavelet and correlation indexes are differentiated by functional or dysfunctional autoregulation. The wavelet method

minimizes the index variability with a slight decrease in the standard deviation for wHVx, wCOx, wPRx relative to their correlation indexes. The pooled wavelet index had better U-shapes with ABPopt than the correlation index curves. Hence, wavelet NIRS indexes may be used to monitor autoregulation with a lower signal variation than the commonly used correlation indexes [93–95]. The more impaired autoregulatory function is associated with a more significant risk of death and severe disability. However, the ability to distinguish fine neurologic deficits remains limited with these methods. Liu X. *et al*. [106] provided preclinical validation of wavelet-based NIRS autoregulation monitoring against a laser Doppler flow measure of the cerebral blood flow in the brain. Efficient monitoring methods should be denoted by greater signal-to-noise ratios. Many widely employed NIRS autoregulation approaches, comprising the correlation indexes such as HVx and COx, produced greater signal variation that might not depict physiologic procedures. This has a small transformation of the correlation indexes into medical practice.

Liu X. *et al*. [106] also demonstrated that wavelet indexes had lesser variation than their equivalent correlation indexes. The wavelet approach reduces the signal to noise (SNR) through a coherence boundary to eliminate lower cohesive signals. This increases the possibility of analyzing the physiologic appropriate phase change among ABP and CBV instead of the signal noise.

They produced separate time intervals with many hours of intact or impaired autoregulation, side-by-side continuous normocapnia, continuous oxygen delivery, the small difference in the hemoglobin level, and a anesthetized regimen. These test settings improve the autoregulation measurement. On the contrary, TBI patients are denoted by more significant clinical and physiological variation, which increases the signal noise (SNR) in the correlation indexes. The least variations in the waveform in the wavelet approach could enhance the clinical performance [101].

The wavelet indexes create clearer U-shaped curves with ABPopt at the vertex. This variation was particularly evident when ABP rose over the optimal (ABPopt) value (Fig. 2.4). ABPopt could be recognized by various approaches, such as the methods that need neuromonitoring software or a visual check of the curves because researchers and physicians are often unable to access the multiwindow technique.

They [106] calculated the wavelet and correlation indexes in the same piglets during identical physiologic changes from induced hypotension. Clinical neonatal wavelet NIRS methods studied hypoxic-ischemic encephalopathy [107,108] and prematurity [109]. wPRx and PRx, along with wCOx and Cox, had a similar capacity to recognize dysfunctional autoregulation.

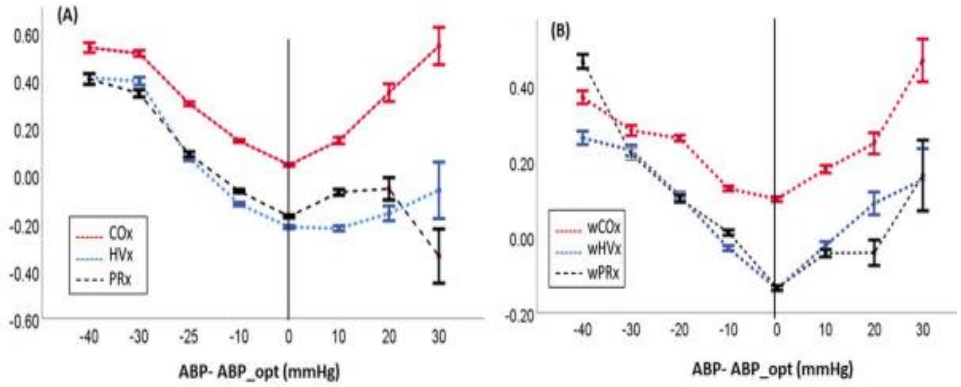

Fig. 2.4. Example of ABPopt at the index. (A) The correlation indexes turn positive as the blood pressure decreases below ABPopt. (B) The wavelet indexes depict a U-shape with higher values as ABP deviates lower/ higher than ABPopt [106]

In the study by Liu X. *et al*. [106], the pigs developed whole-body hypothermia. Although the clinical study of therapeutic hypothermia post-cardiac arrest shows uncertain advantages from hypothermia, the delay in inducing hypothermia could minimize the study's therapeutic potential. There was not a sufficient size of the sample to stratify the population of pigs according to the temperature treatment. However, this specific study aimed to determine the agreement between the wavelet and correlation indexes in paired analyses. Moreover, it was suggested that wavelet NIRS could be tested during hypothermic cardiopulmonary bypass or adult cardiac arrest. The limitation of the study was the test in a unisex (male) population. It is required to test the accuracy of wavelet NIRS methodology in both males and females, and post-recovery from cardiac arrest as secondary brain injury evolves with and without vasopressor treatment [104,105].

2.3.5 Assessment of CA Indexes (Autoregulation Indexes)

Cerebral autoregulation refers to cerebral resistant arterioles responding to the rise or reduction of CPP or ABP. It is an essential equilibrium-based technique that saves the brain from damage because of insufficient or excessive CBF [72,83,110–113]. In the last two decades, many methodologies have been introduced and used in CA assessment, i.e., the autoregulation index (ARI), the transfer function analysis (TF), and the mean flow index (Mx), [70,101, 114–120]. With the improved CA assessment [79,99], there is still a reported confusion whichever method should be considered as the 'gold standard' [114,121,122]. Although some comparisons between various CA parameters have been published [123–129] based on ABP and cerebral CBFV measurements, CA's reliability remains a significant issue [114].

Liu X. *et al*. [130] aimed to assess the relationship among three widely used CA indexes in a controlled environment and assess the influence of noise on CA assessment [131], where they estimated Mx and TF parameters compared with ARI values based on controlled situations, undisturbed by unknown factors. Panerai *et al*. incorporated variable noise artifact pollution on the artificial data in order to evaluate

artifact influence on these relations. According to the white paper [133], the study concentrated on two frequency spectra: 0.02~0.07Hz, and 0.07~0.2Hz.

Liu X. *et al*. [130] also explored the relationship between three widely used CA metrics: 1. transfer function analysis, 2. a second-order linear model, and 3. time-based correlation (Mx). Their study also showed that the intensity of the noise had a more significant impact on all the CA parameters. They simulated the autoregulation index for reference for comparison with the other means. The relation between Mx and the autoregulation index agreed with the metric convergence and common interchangeability of the indexes from a scientific grade. Nevertheless, in practice, as shown by noise simulations, this range is shorter and shifted down towards the lower values of Mx (Fig.2.5A).

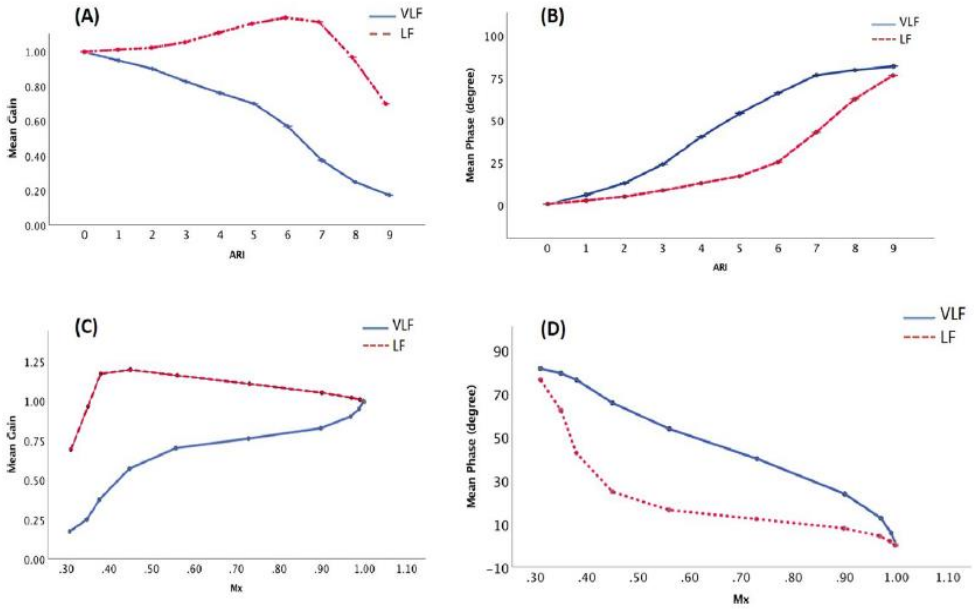

Fig. 2.5. Example of the relationship between ARI and the estimated transfer function parameters (A, B) and Mx with transfer function under the no-noise condition (C, D) [129]

A linear system is ideal while using TF for CA assessment. This cohort of simulated data met the criteria, and the continuous relationships between the TF phase with ARI or Mx agreed with the theoretical interchangeability of metrics. If we look at the grading outcome from the study of different autoregulation levels, an almost 'S'-shaped relationship between the phase and the indexes shows a noise-free situation, thus a phase from 0 to 70 degrees can go for grading CA (Fig.2.5).

The ABP and CBFV normalized into Z scores before TF analysis. As per the white paper [133], they removed mean values before TF analysis, thus minimizing spectral leakage. However, normalizing ABP/CBFV rather than in absolute units has been raised. The normalization is expected to reduce the intrasubject variations of the CBFV amplitude and impact the gain estimates, thus influencing the shape of the relationship between Gain and ARI [133]. This could be one of the reasons why the

LF gain comes out so poorly in the analysis. Therefore, an in-depth analysis to investigate the effect of normalization is needed.

This study shows that various approaches can lead to a weak correlation among autoregulation parameters, even in well-controlled simulated data – this explains why clinical measurements are weakly correlated. By generating artificial CBFV data, the real estimation will remove all external noise from the CA estimates.

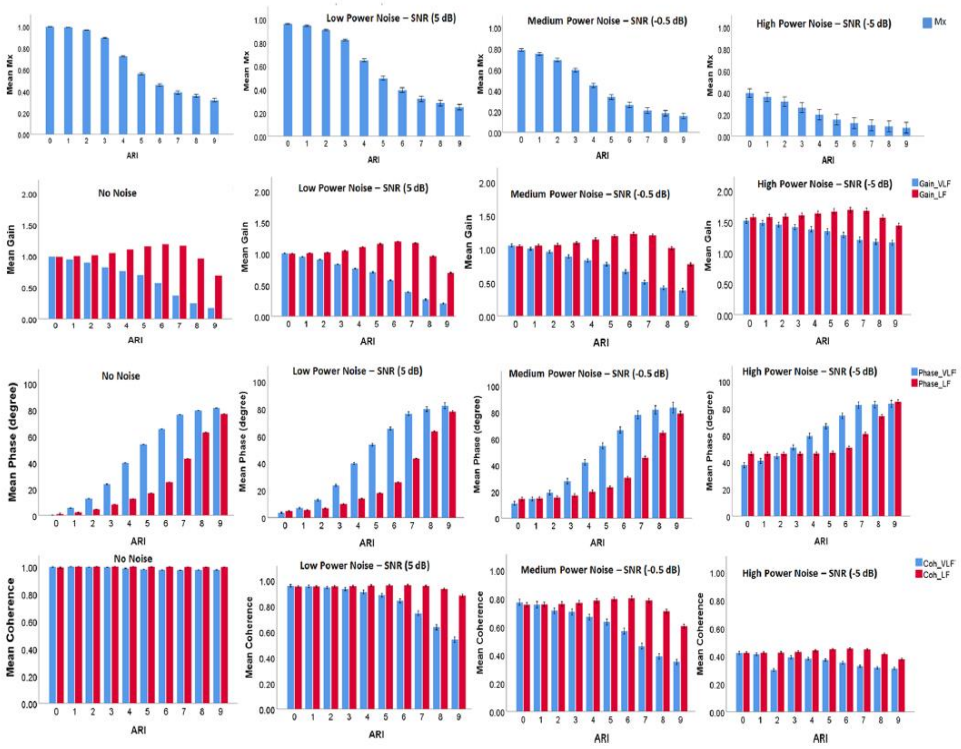

Fig 2.6. Example of relationships between Mx, TF parameters, and ARI with noise artifact [130]

The relationship between ARI and Mx by artificial data is noisy qualitatively, which indicates that a simple method could offer an acceptable approximation to the existing noise observed in real data. The intensity of noise influences all CA parameters, mainly regarding the relationship between coherence and ARI. The linear model is used in the absence of noise, but, with various noise intensities, the coherence-ARI relationship's character varies (see Fig.2.6). Mean value normalization would reduce the variability of the CBFV amplitude and impact the gain estimates. Hence, the shape of the relationship between Gain and ARI was affected. That could have been a significant cause of the low gain of LF (correlation with ARI). Moreover, in this research, they unwrapped the phase to degrees, and the negative values were removed, whereas studies using real data showed a varying outcome on the relationships between CA parameters. This varying outcome can be observed because of various reasons, e.g., different analytic constructions; hence, they may not reflect the same aspect of the physiological response. Unrelated, unknown noise in the real

data impacts the outcome and the low reproducibility of CA parameters that might differ in different subjects [130].

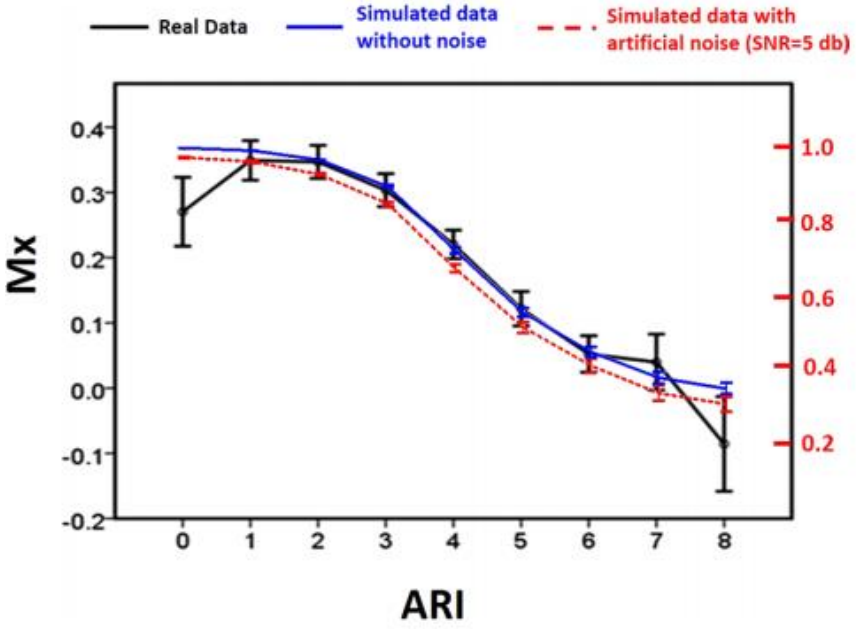

Fig. 2.7. Example of Mx-ARI relationship comparison between real data and modeled data [130]

In this study, various methods were explained, which could lead to the weak correlation between autoregulation parameters, such as well-controlled simulated data with a simple linear model, which also provides an additional explanation as for why clinical measures are weakly correlated. To mimic a similar scenario and investigate the impact of the noise on the CA assessment, they use three simulated noise levels of 5 dB, −0.5 dB, −5 dB. According to Katsogridakis *et al*., the distribution of the signal to noise ratio of the actual CBFV measurement was in the range of 4–6 dB in a study of 60 volunteers. Hence, they select the simulated noise of 5dB to mimic the real scenario of clinical CA assessment. The relationship between ARI and Mx by simulated data with the real data qualitatively similarly derived from Liu X. *et al*.'s study using the real data of 288 TBI patients (Fig. 2.7) [130]. The study outcome reflects the intensity of noise has a significant impact on all CA parameters, especially on (TF) coherence and ARI. Moreover, with various noise intensities, the coherence-ARI relationship varies. Coherence is essential for detecting strongly non-linear relationships as expected when autoregulation is strong. The different TF variables, such as the phase and attain or gain, along with Mx and its connection with ARI, were impacted by the disturbance at different levels. However, the form of the association curve among the variables and ARI stays mostly static. The grading was majorly impacted in terms of rising noise artifacts, Mx decreases because of unrelated components inserted by noise. As we know, a low Mx is considered as good autoregulation; with a higher noise, Mx would overestimate autoregulation.

Therefore, in different 'noise' conditions, the same TF parameter value or Mx value will correspond to different CA stages. This could describe the weak repeatability of CA variables among various patient groups. Re-calibration of the CA indexes as per the background noise for a specific patient may be needed for stable CA scaling. It might certainly be not exactly a feasible solution, as the extent of the background noise will be unidentified, probably changeable, and usually unmeasurable [130].

This study's limitation was that the connection among the CA variables is mostly kept for simulated data, and it is derived from the numerical perspective. The outcome might not show the real connection of the actual recordings, as confirmed by Panerai and colleagues. The impact of noise on these CA parameters could be helpful, but the relationship between the parameters using artificial data with no noise could be beyond real. Moreover, the data used for modeling was taken from TBI patients; other patients' cohorts need to be tested. Furthermore, the SNR was measured throughout the entire frequency, then again, the noise was filtered out, thus eliminating lots of its power, and the relevant (applicable) SNR for the signal of interest is much larger [130].

CBF measurement methods and the adaptability of signal processing approaches offer various autoregulation indexes. Table 2.2 emphasizes the reasoning of these indexes and provides an impression as to their relevance.

Table 2.2. Synopsis of autoregulation indexes [4]

Autoregulation measure	**Signals required**	**Computation**	**Explanation**	**Remarks**
Autoregulation index (ARI)	ABP and Fv	By comparing the CBF to alter in the ABP	When ARI is 0, it means absent autoregulation, ARI 9 means perfect autoregulation	Moderately complex signal processing required
Flow index (Mx, Sx, Dx)	ABP (CPP), Fv	Pearson correlation between CPP and mean Fv	When the autoregulation is impaired, the Mx, Dx, and Sx are higher	Simplistic yet prognostically relevant
The transfer function	ABP, Fv	From the transfer function of FFT of ABP and Fv signals	When the autoregulation is impaired, it represents the lower phase, greater attain, and greater cohesion	Reasonably complicated signal processing. prognostically relevant

TOx, COx, THx, HVx	ABP (CPP), NIRS oxygenation	Pearson correlation among consecutive short means of ABP and tissue oxygenation	When the autoregulation is impaired, the indexes are higher	Related to the TCD approach, however, permits for longer monitoring
TOIHRx	HR, NIRS oxygenation	Pearson correlation among consecutive short means of HR and NIRS oxygenation	When TOIHRx is higher, the autoregulation is impaired	comparisons with standard autoregulation indexes required
Transfer function	NIRS, ABP oxygenation	The transfer function of FFT of ABP and oxygenation signals. Phase shift is essential to align oxygenation and ABP signals	When the autoregulation is impaired, it represents the low phase, high gain, and high coherence	Moderately complex signal processing
PRx	Mean ICP ABP	Pearson correlation among consecutive short means of ABP and ICP	Higher PRx represents impaired autoregulation	Robust measure for long monitoring periods
PAx	The amplitude of ICP and ABP	Pearson correlation among consecutive short means of ABP and ICP	Higher PAx represents impaired autoregulation	Same as PRx
ORx	PBTO2, ABP	Pearson correlation among consecutive short means of ABP and PBTO2	High ORx represents impaired autoregulation	Validation required
VRx	ABP, IBV	Pearson correlation among consecutive short means of ABP and IBV	Higher VRx represents impaired autoregulation	Similar to PRx, IBV was used as a surrogate instead of an ICP.

2.4 Slow-wave Signal Artifact in Cerebral Autoregulation Monitoring

Artifacts are termed as unwanted variations in the signal due to external sources to the parameter of interest [134].

Beate [135] and Qiao *et al*. [136] classified some most common types of ABP signal artifacts based on the phenomena of the origin of the artifact. They are described as a) Maximum ABP saturation (5 to 20 seconds); they are originated because of the flushing of the arterial line, blood clot, or thrombosis of the arterial line.

b) Minimum ABP saturation; Transient constriction in the ABP, for example, pinching from an arm movement causes such artifacts.

c) Pulse pressure artifact; Such artifacts are the same as systolic and diastolic ABP saturation artifacts slowly reducing the pulse pressure. The origin of such an artifact can be because of damping in the arterial line.

d) Square wave artifact; The origin of such artifacts comes as square waves with fluctuating cycles.

e) High-frequency artifacts; They are originated by the movement or disturbance of the transducer (such as covering the patient with a cloth over the arterial line).

f) Impulse-like artifacts; They are motion or sharp mechanical artifacts, such as crimping of the tubing.

On the other hand, Kevin *et al*. [134] highlighted three different artifacts that impact all physiological recordings: a) Environmental artifacts; They originate from the mains power leads that surround the body, which can be seen in the form of 50/60 Hz.

b) Experimental errors; They are unwanted variations in the experimental setup.

c) Physiological artifacts; They are variations in the desired signal due to other physiological processes in the body.

2.4.1 Problem background

Care of severe patients in the ICU, who may experience life-threatening deterioration sometimes over minutes or even seconds, is highly dependent on the quality of the data [137]. Continuous monitoring of signals, like invasive arterial blood pressure (ABP), and different other cranial or intracranial pressure, are an extreme example providing a wealth of complex, heterogeneous yet highly structured data at optimal sampling frequencies. Signal artifacts often impact reliability in estimating their derived parameters, analysis, and causing uncertainty in individual patient decision making. The prominent reason could be handling the missing data, often considering simple techniques that are biased, and the underestimation of variability, for example, linear interpolation of the observed data.

In the ICU, various key factors could create/cause the noise and artifacts in the monitoring signals, e.g., catheter flush, patient movement, pressure transducer blockage, power-line interference, signal amplification, quantization, and device saturation, which results in clipping the signal. Hence, inadequate handling of noise and artifacts causes an extremely large number of false alarms in the ICU, leading to the disruption and decreased quality of care [134,138–141], desensitization of the clinical staff to warnings, and slowing down of the response times [142]. The presence of noise and artifacts can also challenge different algorithms' performance designed for the detailed analysis of the morphology of pulsatile physiological signals [143]. As a result, noise handling has to be an intrinsic component of such algorithms to ensure their high performance. An indicator, because of artifacts in the monitoring wave, reduces the healthcare settings' efficacy, prominently in intensive and critical care units. Hence, it is essential to develop a technique for identifying these false alarms (artifacts) versus actual alarms (the real changes in a patient's physiologic state) [143,144].

ABP monitoring is usually exposed to noise pollutants and moving artifacts. However, ABP monitored via non-invasive sensors can be impacted by repeated signal adjustment phrases that disturb the physiologic signal. This temporary loss of waveform or corruption is a significant issue in clinical settings. Though, various methods to advance ABP signal evaluation, such as cardiac output [139] or ICP measurement, are based on a greater quality ABP signal to be inserted into the evaluation algorithm. If the acquired ABP signal's quality is insufficient, the quality of the resulting estimates cannot be reliable [139].

For patients in Neuro Intensive Care Units (NICUs), mainly for TBI patients, continuous ICP monitoring is exceptionally vital to save the brain from secondary damages caused by IH. ICP monitoring these days depends entirely on visual inspections by neuro-clinicians and nurses, and ICP controlling interventions are treated on severe patients only after longer observed ICP elevations in NICUs. The current methods are prone to errors, reactive, and inefficient. Automatic alarms in the clinical setting of IH and effective prediction models to pre-alarm the impending episodes of IH are highly required [145,146].

The continuous ICP slow wave recordings overtimes, in NICU settings, are mostly polluted by noise and artifacts. The artifacts could be due to several reasons, for example, due to the motion of patients, a faulty contact, an error in the measuring method, and the operator's fault. For example, motion artifacts and polluted signals lead to a higher wrong alarm ratio in automated IH alarm systems. Artifacts and noise pollute the data's essential properties, which drives the precise prediction of upcoming IH impossible [145,146]. ICP levels are invasively measured with a fiber-optic intraparenchymal gauge (*Codman and Shurtleff*, Taynham, MA, USA) by placing it under the skull. A significant amount of artifacts often pollutes the collected ICP waves. According to one of the studies, an average of 5% of data points in the collected ICP signals are polluted by artifacts, and, in the worst case, more than 20% of signals can be contaminated. Fig.2.8 shows examples of ABP and ICP monitoring signals with artifact peaks.

Artifacts can be recognized as high and sharp 'spikes'. These spikes are called artifacts because they show quick and dramatic variations in their ICP levels' oscillations which are not impossible clinically as stated by the neuroscientist or neurologists. Moreover, as highlighted in Fig. 2.8, an artifact consists of a cluster of data points, not merely one or two data points. A cluster of artifacts is called an 'artifact episode'. An artifact episode can be demonstrated by its location and morphology, i.e., width [145,146], See Fig. 2.9.

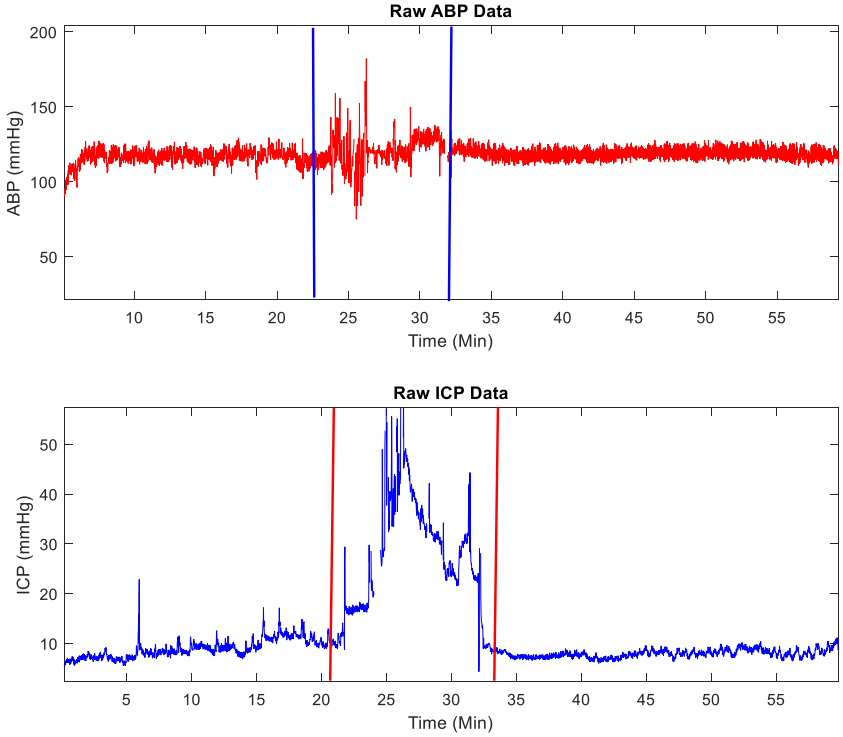

Fig. 2.8. An example of an artifact in ABP and ICP monitoring signal

Artifact identification has been a complicated and costly task requiring time, human annotation, or thresholding depending on wave-specific feature engineering [138], particularly as artifacts arise from a variety of internal and external noise sources, sensor noise, patient movement, and clinical interventions. There are three major sources of artifacts that influence physiological recordings: environmental artifacts, experimental errors, and systemic physiological artifacts [134].

2.4.2 ABP and ICP data Artifacts

The ABP/ICP slow-wave measurement is often subject to noise and artifacts. Moreover, ABP measured through noninvasive sensors can be affected by recurrent signal calibration phrases that interrupt the physiologic waveform.

Physiological monitoring is essential in the acute stage of severe TBI. At this stage, the patient's neurological status rapidly deteriorates because of increased ICP, followed by a decrease in CPP [91]. ICP monitoring also allows indirect, continuous monitoring of cerebral autoregulation (pressure reactivity index, PRx) when correlated with arterial blood pressure (ABP) monitoring. [147]. However, continuously measured physiological signals are often contaminated by signal artifacts which significantly reduce the derived parameters' reliability and may even lead to erroneous clinical decisions [148,149].

Care of severe patients in the ICU, who may experience life-threatening deterioration sometimes over minutes or even seconds, is highly dependent on the quality of the data [138]. Continuous monitoring of signals, like invasive arterial

blood pressure (ABP), and different other cranial or intracranial pressure, are extreme examples providing a wealth of complex, heterogeneous yet highly structured data at optimal sampling frequencies. Signal artifacts often impact the reliability in estimating their derived parameters, analysis, and causing uncertainty in individual patient decision making. One of the prominent reasons could be handling the missing data, often considering simple techniques that are biased and underestimating variability, for example, the linear interpolation of the observed data.

Yet, various techniques to advance the ABP signal study, for example, cardiac output [138,139] or ICP evaluation, depend on a superior quality ABP signal to be inserted into the evaluation algorithm. If the grade (quality) of the obtained ABP waveform is inadequate, the outcome's quality could not be reliable. Similarly, if the obtained ABP waveform is damaged from frequent, small irregular signal loss, a substantial quantity of the obtained waveform may be required to be rejected. The evaluation of the waveform quality and the possible imputation of the realistic waveform signals over short periods of data loss becomes an essential preprocessing step [139].

2.4.3 State of the art

As we have observed in the above sections, Intracranial pressure (ICP) monitoring has an important place in managing neurological and neurosurgical disorders in patients, including the traumatic brain-injured patients.

Lundberg explained the wave patterns as A, B, and C in the 1960s [150]. B waves were characterized as the small repetition of peaks of ICP in the range of 10–20 mmHg of the frequency between 0.5–2 waves per minute. These B waves have been observed in ICP measurement in the ICU for TBI patients. However, ICP is also measured in various brain diseases covering a broad spectrum from acute and subacute critical care settings to elective follow-up on the critically ill patients.

2.4.4 Problem with the terminology

In recent times, a vast number of patient populations go for ICP monitoring for any severe sickness where medical signal patterns are unclear. In such cases, signal patterns are termed B waves; however, differences in the magnitude and visual aspects are determined according to Lundberg. These kinds of B waves (slow-wave) have a lower magnitude or amplitude and have abnormal patterns, but they were still not classified. The Source of B waves is unknown, and they are often related to cerebral dysfunction. Their clinical significance is complicated, as they may also appear as normal physiological phenomena [151,152]. Their source is related to vasogenic activity [153]. This imposes a challenge to their description and quantification, hindering their identification in diagnosis and treatment. Because of these difficulties, the clinical practice focuses on ICP-related research and is currently primarily restricted to readings of the mean ICP. The identification of signal abnormality by visual appearance is a common clinical approach – this is based on personal empiric experience, which pushes the researcher to think about interobserver reproducibility. Automatic detection of B waves became a necessity and is evidently highly useful in both clinical and research settings. This automatic finding is possible if the signal

shape and size are clearly defined, preferably by consensus in the scientific community. A quantitative detection system may permit identifying B wave variations and other 'non-Lundberg' patterns, which may replace regular visual inspection.

B waves are recognized by two main factors: frequency and amplitude. The frequency of waves that fit a fixed time period is usually estimated as waves per minute and a frequency range of 0.5–2 waves/min, as Lundberg originally defined [150]. B waves of a lower frequency were termed 'slow waves' [154, 155]. The 'slow waves' were used to define waves in a frequency range of 0.33 to 3 waves/min [156]. Their amplitude can also define B waves. Lundberg stated a maximum amplitude of 50 mmHg in 1960. In pathology, this level of elevation is less often seen to this extent these days, and B waves with low amplitudes are more commonly observed. Lower amplitude B waves are present in the normal pressure in hydrocephalus, where B waves are not related to high ICP [156]. Martinez-Tejada *et al*. [155] classified the overall terms used for B waves based on the frequency of terminology in their review study, where the term *B waves* was found to be used in most articles, followed by *slow waves* and *ICP slow waves*, see Fig. 2.9.

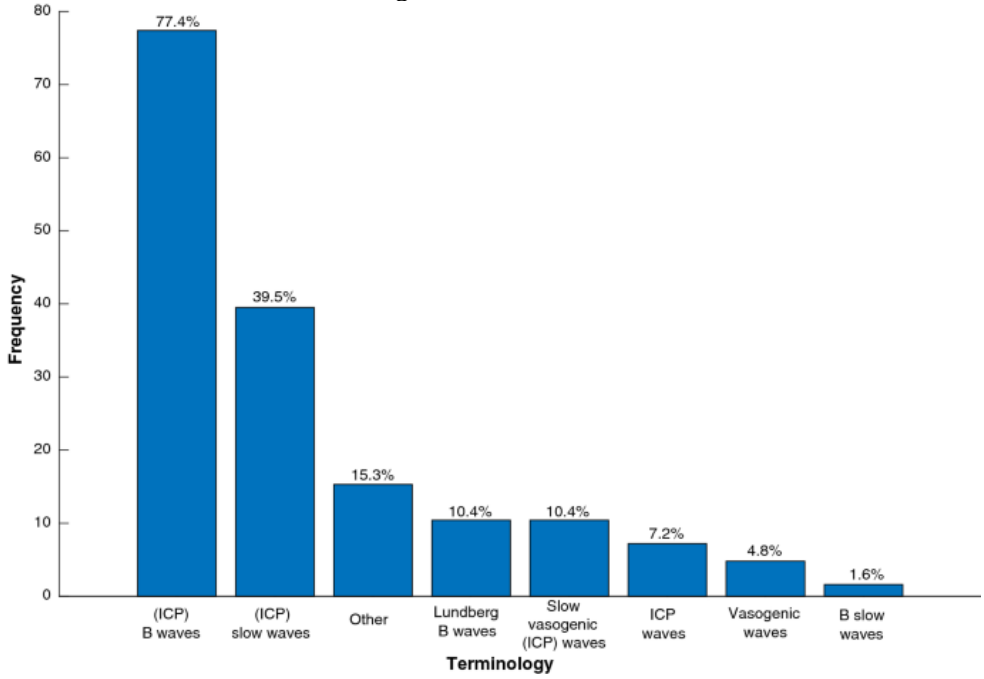

Fig. 2.9. Classification of the overall terms used for B waves based on the frequency of terminology [154]

Moreover, apart from frequency and amplitude, two other parameters are generally defined to understand B waves. Their shape can also define B waves and whether a plateau phase is present or not. The shape seems symmetrical if the time taken for the incline and decline phases is the same. If the incline phase is longer, the shape is considered asymmetrical. These parameters are divided into subclasses within B waves. All subclasses recognize B waves with an extended frequency spectrum but mainly differ in their morphology, see Fig. 2.10.

The ICP wave is used to define B waves. They classify three morphology-based subclasses: (a) short symmetrical waves with an amplitude below 10 mmHg, (b) symmetrical waves with an amplitude above 10 mmHg, and (c) intermediate waves, which have the same frequency as symmetrical waves, but the amplitude is the same as in plateau waves [157–159]. A recent study [154] shows that B waves are categorized into different subclasses according to shapes and amplitudes. These classifications may be used as supplementary evidence that the traditional waveform categories do not address waveforms identified in the clinical practice today. The B waves' amplitude and the frequency and pulse wave parameters help to categorize them. They are based on the three subpeaks: P1, P2, P3 systolic peak, tidal peak, and dicrotic peak [160].

Martinez-Tejada *et al*. [154] explain the disagreement with the nomenclature and definitions chosen to describe B waves. Various titles were utilized to define a similar fact and to demonstrate the features and structural differences of the wave or the cause of their appearance. This enhances the chance of confusion around the mathematical modeling of B waves and makes the model more complicated. The nature of complex terminologies made the selection or development of an analysis tool that can be used to define them. B wave identification may be a path that enables enhanced understanding of ICP variations from the normal to the severe condition state. However, the concentration of the existing estimation resources on determining B waves imposes a restraint of losing the data linked to other essential waveform variations. Hence, the occurrence of ICP that may include essential data on the physiological method influencing the brain is possibly ignored. However, the terminology selected for this thesis uses the *slow wave* term as we are using a frequency range of 0.33 to 3 waves/min of slow-wave extraction from ABP and ICP waves.

Two main applications from the data given by the slow pressure waves are assessing intracranial volume-pressure relationships, which has been proposed since 1989 [161], and the quantification of vasoreactivity, the CA. The understanding of autoregulation may be essential mostly in the management of ICH after TBI. ICH and damage to CA are prominent reasons for cerebral ischemia [161]. However, losing specific or overtime autoregulation value [162,163] under severe or moderate TBI is unclear [164,165], and the functionality of slow ICP waves is not sufficiently determined. The greater amplitude and longer duration waves may reduce the CBF, maybe at a specific location or in the entire brain by decreasing the CPP or decreasing microcirculation because of a greater intraparenchymal pressure.

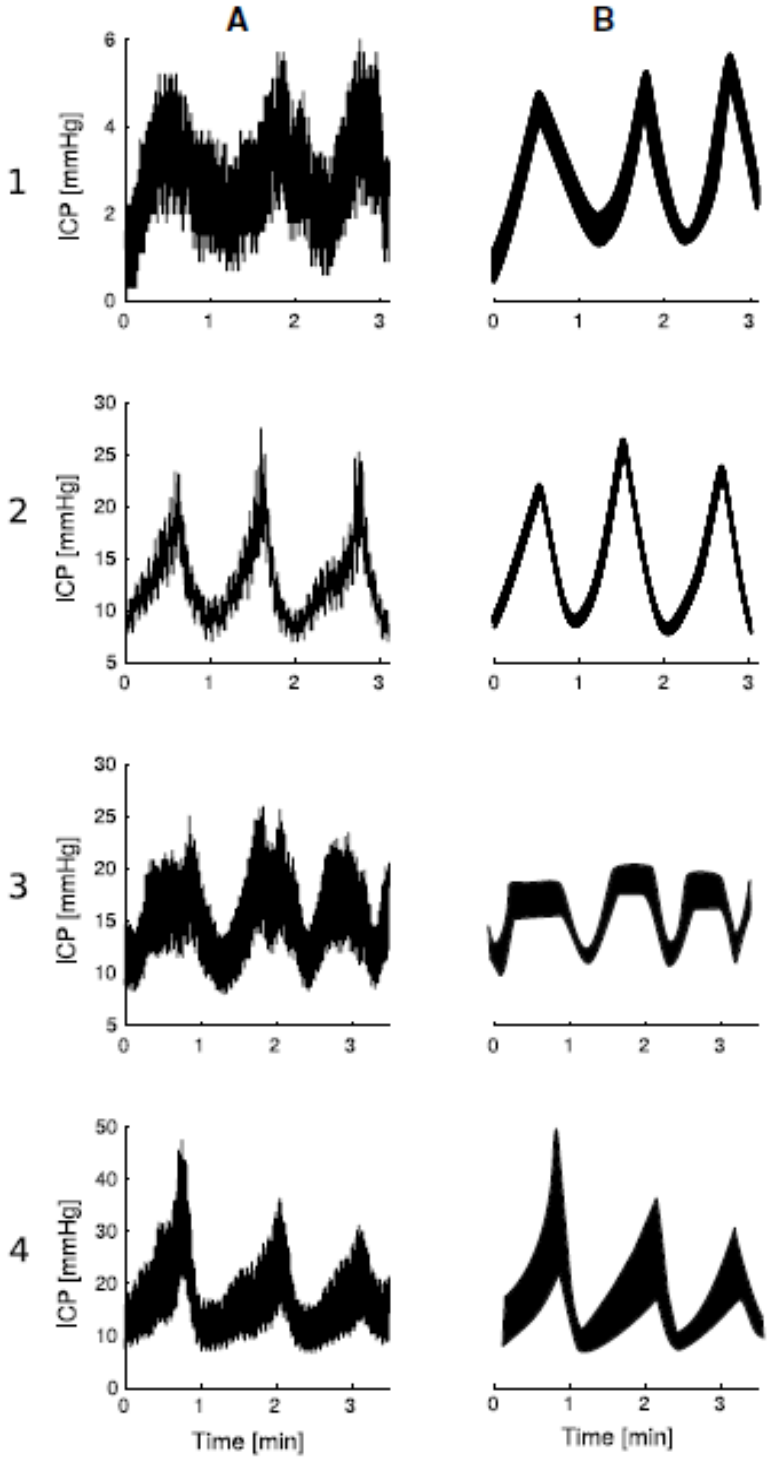

Fig. 2.10. Presentation of different B waves sub-classification patterns. Line 1 and 2 shows B waves with an amplitude lower and higher than 10 mmHg, respectively. Line 3

depicts the B waves with plateau waves. Line 4 shows examples of asymmetrical B waves [154]

Measuring the waves to identify and to address these events seems to be indicated; however, the threshold, the time period, before the medical care remains to be detected even though the time of 5 or 15 min [166,167] was proposed. These days, ICP and ABP estimation are utilized for measuring the CPP.

As shown in the literature, the quantification of the slow pressure waves also seems useful in treating hydrocephalus for determining the excellent patient outcome. A reduction in B waves was proposed as a goal in the treatment of hydrocephalus [168]; however, the waves' pathological character is yet to be demonstrated.

Above all, the problems such as the methodology, terminology, problem definition, moving artifact and sensor touching the arterial wall (create much noise), and, hence, artifacts, in obtaining the arterial and cranial signal (slow-wave), all of these require serious attention, as not much of the research is being conducted on these aspects. This thesis work shall bring all these to the attention, especially the quality of the signal.

The detailed analysis will be described in Chapter 4, and the experimental analysis and application is outlined in Chapters 5 and 6.

3. METHODOLOGY

There is a significant resemblance within the methodologies in the three studies provided in this thesis. Two of the three methods retrospectively studied an already collected TBI patient database to produce unique understanding associated with: 1) selection of the best possible filter for artifact rejection; 2) Applied FIR (Parks–McClellan) filtering to estimate the pressure reactivity index of intensive care patients and the final study where applied ultrasonic attenuation to measure the blood volume, considered as a surrogate of ICP to estimate the volumetric reactivity index (VRx2) and to compare that with the already existing ultrasonic time of flight method (VRx1), in a healthy volunteer.

All the studies detailed in this thesis are described within their corresponding chapter. There are significant overlaps in many of the methodological aspects across the studies. Mathematical tools, such as MATLAB for signal processing and SPSS for statistical analysis, have been used to prepare the methodologies of this thesis. The methods are listed in Table 3.1.

3.1 Patients and Volunteers

3.1.1 Retrospective patient data

The retrospectively gathered data that was used in two of the methods included in this dissertation were collected from 60 adult TBI patients admitted to the Republican Vilnius University Hospital (Lithuania) between 2016 and 2019. ICP was recorded by Codman CP, and ABP was measured in the artery by ABP monitor *Baxter Healthcare*, CA, USA. Each patient exhibited a clinical need for ICP monitoring; ICP and additional computerized bedside signal recordings are within this database. The computerized data storage protocol was reviewed and approved by Vilnius Regional

Ethics Committee of Biomedical Studies (Vilnius, Lithuania) with Approval No. 158200-15-801-323.

The benchmarks to include the patient data for the studies were at least 2–3 hours of invasive ICP and ABP measurement, the presence of the Glasgow Coma Scale (GCS) score with the outcome data where *1* corresponds to death, *2* corresponds to a vegetative state, *3* corresponds to severe disability, *4* corresponds to moderate disability, and *5* corresponds to a good recovery.

All the patients were anesthetized during this timeframe; patients were treated per protocol aiming to maintain ICP below 20 mm Hg and CPP above 70 mm Hg. In particular, ICP was controlled by using stepwise positioning, sedation, ventriculostomy drainage, and hypothermia.

3.1.2 Healthy volunteer data

The collected data from healthy volunteers utilized and presented in this thesis is part of a new database of 43 healthy volunteers (volunteers with healthy or intact autoregulation) data collected at the Health and Telematics Science Institute, Kaunas University of Technology. The computerized data storage protocol was reviewed and approved by Kaunas Regional Ethics Committee which approved the study with Approval No. BE-2-49 (16 November 2017), Kaunas, Lithuania. The ABP data from 43 healthy volunteers was collected continuously with an ABP monitor (*Finapres Nova*) that displayed the ABP signal. Out of 43 healthy volunteers, 33 were male, and 10 were female in the age range from 18 to 36 years of age[1].

For intracranial blood volume (IBV) recording, a noninvasive ultrasonic monitor developed by the Health Telematics Science Institute of Kaunas University of Technology (Kaunas, Lithuania) was used. Moreover, data recording and processing were accomplished by using ICM+ software (*Cambridge Enterprises Ltd*., Cambridge, UK). The real-time estimation of the noninvasive CA indexes from ABP and IBV was achieved. All the recorded data was analyzed in real-time/overtime[1].

Volunteers were ruled out of the study if they were minor, missing prior mental ability to give consent, or were not able to securely undergo transcutaneous measuring because of a skin disease, known or unknown medical conditions, or allergies. Before the study, written informed consent was filled following a discussion with the patients' family member or representative or a professional clinical consultant. See Table 3.1 details of the methods used in the thesis and the study subjects' condition when participating in the study.

[1] This paragraph may contain some similar information as publication "Comparative Study of Novel Noninvasive Cerebral Autoregulation Volumetric Reactivity Indexes Reflected by Ultrasonic Speed and Attenuation as Dynamic Measurements in the Human Brain." *Brain Sci.* **2020**, *10*, 205

Table. 3.1. List of the methods presented in the thesis and the clinical condition of the study subjects

Chapter	Study Title	Patient/ Volunteer Demographics	Condition Studied	Retrospective or Prospective
4	Methods of Artefact removal: Multiple filter comparison for selection of best artifact rejection filter (Analysis)	Two patients (Age range: 18–45 years, admission GOS: 1–4) and two healthy volunteers (Age range: 18–36)	TBI/Healthy	Retrospective
5	Association Between Patient's Clinical Outcome, and Quality of ABP(t) and ICP(t) Signals for CA Monitoring	60 patients (Age range: 18–45 years, admission GOS: 1–5)	TBI	Retrospective
6	Applicability of Novel Noninvasive Cerebral Autoregulation Volumetric Reactivity Indexes by Ultrasonic Attenuation as Dynamic Measurements in the Human Brain	60 patients (Age range: 18–36 years)	Healthy	Prospective

3.2 Data Acquisition and processing

3.2.1 TBI patient data processing

ICP was measured with an invasive intraparenchymal microsensor inserted and/or fixated under the frontal cortex (Codman CP), and ABP was measured in the artery with an ABP monitor (*Baxter Healthcare*, CA, USA). The data was collected with software (ICM+, *Cambridge Enterprise*, Cambridge, UK), and one-minute trends were stored. Further data processing was done in the MATLAB software.

The recorded raw data was 50 Hz taken from the ABP and ICP wave to extract slow-wave components in between 0.0083–0.033 Hz range. The recorded signal was first decimated to a 1 Hz sampling frequency, considering the frequency ranges

associated with the cerebral vasogenic activity [169,170,171] and then filtered with a moving average filter and a FIR (PM) filter.

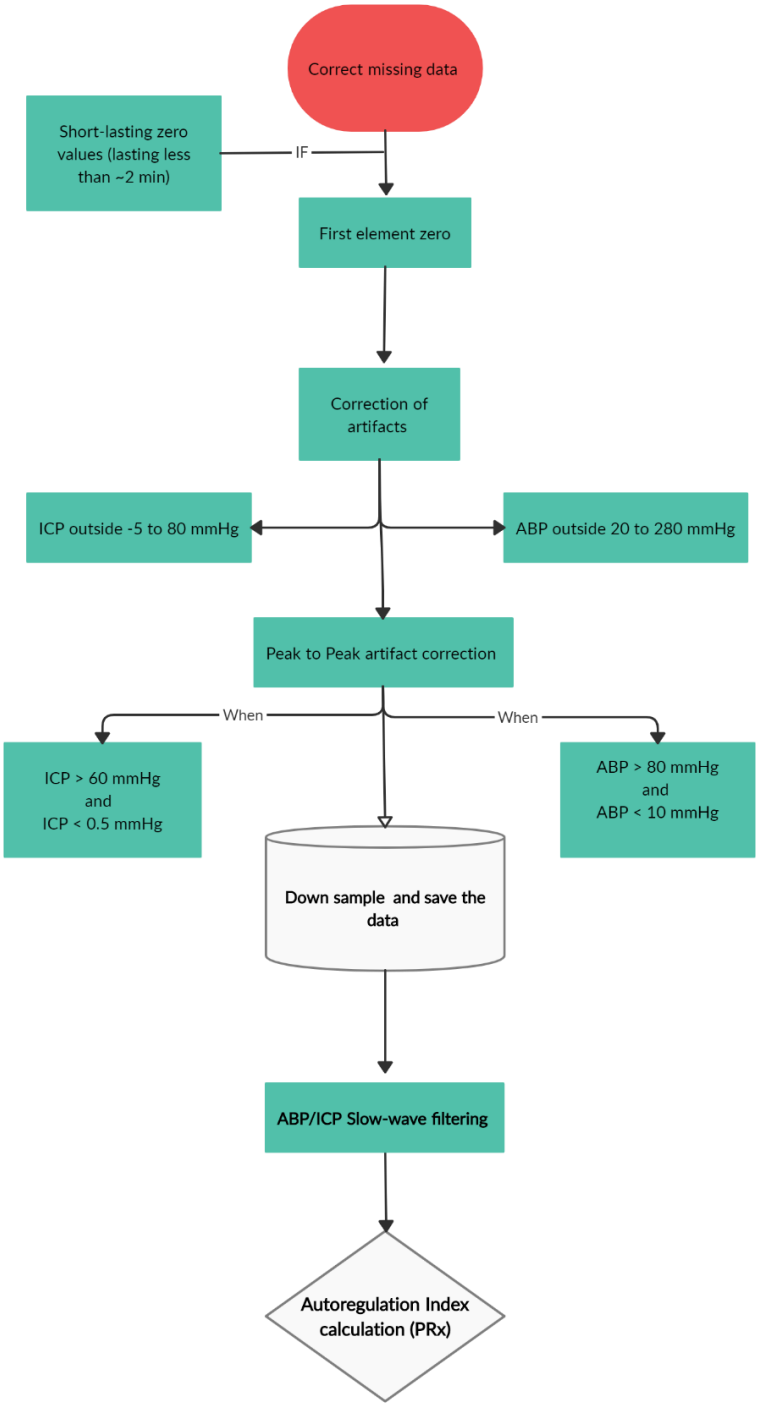

Fig. 3.1. Block diagram of TBI patient's data processing

The filters were designed with similar essential parameters (the sampling frequency, cut off frequency, etc.), where -3 dB cut off frequency (0.5 Hz) was used because most of the (slow-wave oscillation) energy associated with the spectral representation within the wave with a period from 30 s up to 120 s [8,172], a bandwidth range of 0.0083–0.033 Hz (slow-wave frequency range), filter length (N) was 7, and the 6th order filter was used because it provides narrower transition zones with greater attenuation and a sharper (steeper) cutoff, which is highly useful when the artifact frequency is close to the ABP/ICP/IBV signal frequency, the stepwise data processing is illustrated in Fig.3.1.

After the slow waves from ABP and ICP waves had been filtered, the autoregulation index (PRx) was calculated as the Pearson correlation of 30 consecutive 10-second average values of slow ABP and ICP, as shown in Equation 3.

$$PRx = Pearson\ Correlation = Slow\ ABP + Slow\ ICP \quad (3)$$

3.2.2 Noninvasive healthy volunteer data processing

The data from 43 healthy volunteers was collected continuously with an ABP monitor (*Finapres Nova*) that displayed the ABP signal, where 33 were male, and 10 were female out of 43 in the age range from 18 to 36 years.

IBV was monitored with an ultrasonic monitor developed by the Health Telematics Science Institute at Kaunas University of Technology (Lithuania). Data recording was done by using ICM+ software (*Cambridge Enterprises Ltd*., Cambridge, UK) [1]. Further data processing was done with MATLAB software.

The recorded raw data was 50 Hz taken from ABP and ICP waves. To extract or isolate slow-wave components in between 0.0083–0.033 Hz range, the recorded signal was first decimated to a 1 Hz sampling frequency, considering the frequency ranges associated with cerebral vasogenic activity [169,170,171] and then filtered with the Bandpass and FIR (Parks–McClellan) filtering with a bandwidth of 0.0083–0.033 Hz to extract ABP's slow waves and IBV*(t)*. The correlation coefficient was obtained from the bandpass filtered spectra of both channels' slow waves[1]. Afterword's volumetric reactivity index was calculated by moving Pearson correlation between slow ABP and the IBV (ICP surrogate) wave, as shown in Equations 4 and 5:

$$VRx1 = Pearson\ Correlation = Slow\ ABP + Slow\ IBV\ (TOF\ channel) \quad (4)$$

$$VRx2 = = Pearson\ Correlation = Slow\ ABP + Slow\ IBV\ (Attenuation\ channel) \quad (5)$$

[1]This paragraph may contain some similar information as publication "Comparative Study of Novel Noninvasive Cerebral Autoregulation Volumetric Reactivity Indexes Reflected by Ultrasonic Speed and Attenuation as Dynamic Measurements in the Human Brain." *Brain Sci.* **2020**, *10*, 205

Table 3.2. Neuromonitoring Modalities Utilized for Data Capture and Analysis.

Modality	Measuring method	Transducer	Software	Secondary Parameter
Intracranial Pressure	Invasive	Codman microsensor ICP transducer (Codman & Shurtleff, M.A., U.S.A.)	ICM+	Mean ICP PRx
Intracranial blood volume (IBV)	Noninvasive	Novel noninvasive ultrasonic monitor by the Health Telematics Science Institute at Kaunas University of Technology (Lithuania)	ICM+	IBV (Intracranial blood volume)
Arterial Blood Pressure	Invasive	Datex-Ohmeda (GmbH, Duisburg, Germany) and Finapres Nova	ICM+	Mean ABP

4. METHODS OF ARTIFACT REMOVAL: SELECTION OF BEST FILTER FOR CA MONITORING

4.1 Existing Methods of Artifact Removal

Low-pass filtering is one of the known techniques for artifact removal. The low-pass filter is mostly used for stationary signals which have a frequency spectrum over time consistently. On the contrary, Adaptive filtering [145] is one of the known filtering approaches currently being used. The adaptive filters need a reference signal, but this reference signal is not an ICP monitoring option. This technique, applicable to ECG, does not apply to ICP signals. Wavelet transformation is also known for effective artifact removal in biomedical signals [145]. However, the best performance can only be obtained with an optimal basis function.

On the other hand, the use of ICP waveform analysis to translate technologies into the clinical setting includes acquiring the data from the invasive intracranial sensor and obtaining non-artifact ICP waveforms and the translation of ICP waveform analysis into a clinical environment. These contaminants can be categorized as high-frequency or low-frequency noise, high-frequency noise inserted by amplifiers, whereas the patient environment inserts low-frequency noise [146].

Several existing solutions to artifact detection and removal from neuro and cardiovascular based physiological signals (ABP and ICP) exist, such as threshold-based, stability-based, or template matching, and filtering-based artifact rejection also by generative deep learning mathematical neural network model and reconstruction and quantification technique. However, the accuracy and precision of these filtering approaches are still uncertain.

In the past decade, there have been several developments by using different models to detect and remove the artifact(s) from the physiological signals, such as Decomposing the ICP monitoring signal with Empirical Mode Decomposition (EMD) [145]. Due to its high efficiency, EMD is commonly being used for non-stationary non-linear signals. An iterative filtering technique was further proposed to filter out artifacts from the decomposed ICP signals. The proposed iterative filter was robust (with robust statistics) [145].

The combined use of an advanced autoencoder (stacked convolutional autoencoder, SCAE) and a CNN method first detects the ABP pulse onset, thereby allowing the detection of the ICP pulse onset and the segmentation of each pulse waveform [137]. Moreover, a self-maintained artifact detection system combines a convolutional variational autoencoder deep neural network that avoids costly manual annotation [138].

On the contrary, Prof. Thomas Heldt from Massachusetts Institute of Technology proposed a novel method of automatic artifact rejection by quantification of the signal quality and the reconstruction of the ABP/ICP waveform, which thus was one of the prominent proposed methods. This method presents an algorithm for the quantification of the signal quality, and the reconstruction of the ABP waveform in noise corrupted segments of the measurement. The algorithm was tested on ABP waveform signals containing invasive radial artery ABP and noninvasive ABP waveforms (See Figs. 4.1 and 4.2) [139].

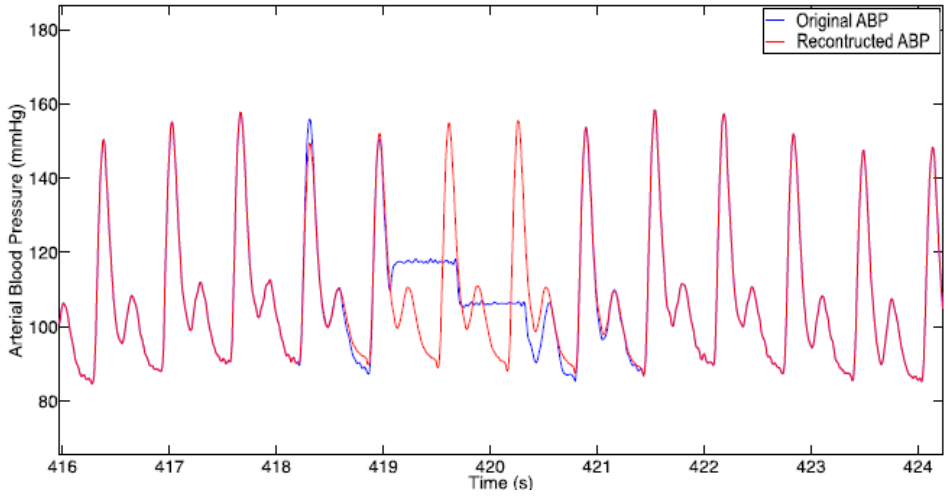

Fig. 4.1. Example of ABP reconstruction in a *Finapres* ABP waveform affected by periodic recalibration [139]

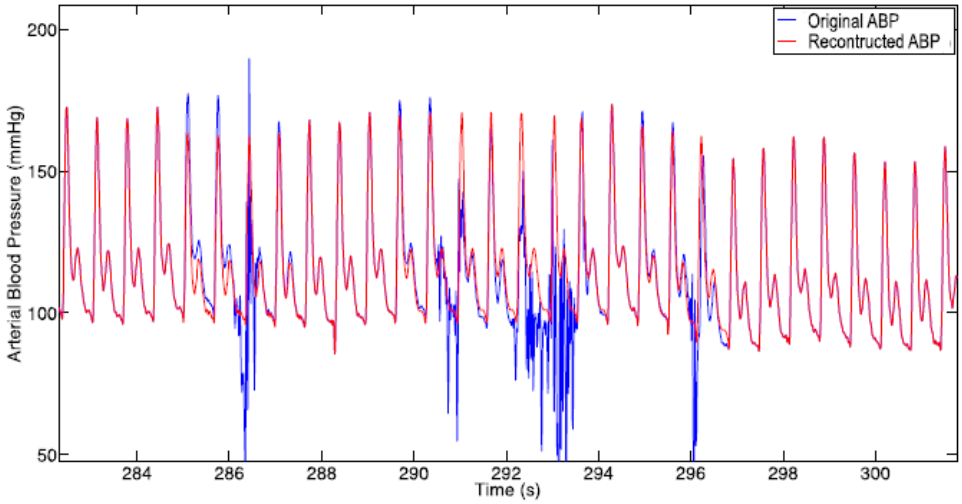

Fig. 4.2. Example of reconstruction of an ABP signal influenced by noise, where the blue waveform represents an authentic ABP waveform, and the red represents the reconstructed signal [139]

A most widely accepted and used filtering technique in biomedical, cardiovascular, and neurophysiological signals is the moving average data filter. It is being used to filter intracranial and arterial pressure waves to avoid the time domain artifacts. The moving average filter is a common filter used for random noise with a sharp step response. This makes it one of the best filters for the time-domain filtering. However, the moving average is an inefficient filter for frequency-domain signals, where it has a poor ability to distinguish frequencies of one band from another [173].

However, where the mean values of every ABP(t) and ICP(t) signal were filtered by using the moving average filter, it has been used widely for pressure reactivity estimation. The most used approaches for artifact rejection/removal are listed in Table 4.1.

Table 4.1. List of existing artifact removal methods [137–146,149]

Methods for artifact removal	**Principle of the method**	**Proposed by**	**Limitation**
Moving average Filtering	Averaging filter	Marek *et al*., Cambridge University.	The window size of the filter must be large. This will induce latency in the signal passing through the filter.

Convolutional variational autoencoder deep neural network	Neural network	Seung-Bo Lee *et al*., Department of Brain and Cognitive Engineering, Korea University, Seoul	Some artifact misclassification of individual pulse waveforms may still occur and could lead to significantly high false-positive rates
Empirical Mode Decomposition (EMD)	After decomposition, the empirical process that decomposes a signal into multiple components, the large-amplitude oscillations in the Intrinsic Mode Functions (IMF) component align perfectly with the artifacts in the original ICP signal	Mengling Feng *et al*., Massachusetts Institute of Technology	It may miss the relatively 'shorter' artifacts
Automatic artifact removal	Convolutional variational autoencoder deep neural network	Tom Edinburgh *et al*., Department of Applied Mathematics and Theoretical Physics, University of Cambridge, United Kingdom	Other signals are not so clear-cut to assign as an artifact categorically
Signal quality quantification and decomposition	Signal decomposition	Thomas *et al*., Massachusetts Institute of Technology	The temporal duration of all the beats of a noisy segment is the same. Second, within the same window, the same template is used to reconstruct all noisy beats
Deep brain recordings	Wave_clus algorithm	Ivan Gligorijevic *et al*, Dept. of Electrical Engineering, Katholieke Universiteit Leuven, Belgium	Random small spikes may be left undetected

Spatial filters	Topographies	Nicole Ille *et al*., Biomagnetism, Department of Neurology, University of Heidelberg	Artifact topographies result in the distortion of spatially correlated signal activity

Among all the existing methods, the standard and widely accepted approach for artifact removal is the moving average proposed by Prof. Marek from Cambridge University.

4.2 Analysis

Considering the problems mentioned above, including false alarming with artifacts in neurophysiological signals and the limitations in the currently existing methods, it is essential to select the best filtering approach to obtain the best possible information from the ABP and ICP waves.

As we know, the short period means of ABP(t) and ICP(t) is needed to calculate the PRx [6,7,11]. The most widely used was the moving average method. It has been argued that FIR (Parks–McClellan) filtering approaches for short-term means of ABP(t) and ICP(t) could be of higher quality than the moving average, whereas the impact of the FIR (Parks–McClellan) filtering approach on PRx/VRx has never been evaluated previously. Hence, we analyzed ABP(t) and ICP(t) signals with different filters and compared the Pressure reactivity index and the volumetric reactivity from outcomes and noninvasive VRx outcomes, to select a higher quality filtering approach based on their pressure reactivity and volumetric reactivity index.

4.2.1 Data processing

Two patient data out of 60 TBI patients and two healthy volunteer data were included for filtration analysis recorded by using an ICP intraparenchymal transducer (Codman microsensor ICP transducer). The ABP was invasively measured by using an ABP monitor (Datex-Ohmeda).

On the other hand, two healthy volunteer data out of 43 were included for filtration analysis, collected continuously by an ABP monitor (*Finapres Nova*) that displayed the ABP signal. IBV monitoring was done by a novel noninvasive ultrasonic monitor from Kaunas University of Technology (Kaunas, Lithuania). Data recording were done by using ICM+ software (*Cambridge Enterprises Ltd*., Cambridge, UK), further data processing was done in MATLAB.

The recorded raw data was 50 Hz taken from ABP and ICP waves. To extract or isolate slow-wave components in between 0.0083–0.033 Hz range, the recorded signal was first decimated to a 1 Hz sampling frequency, considering the frequency ranges associated with cerebral vasogenic activity [169,170,171] and then filtered with five filters including the moving average filter, FIR (PM) filter, Kalman filter, Butterworth low pass filter, and Chebyshev filter. All the filters were designed with similar essential parameters (sampling frequency, cut off frequency, etc.), where -3 dB cut off frequency (0.5 Hz) was used because most of the (slow-wave oscillation) energy associated with the spectral representation within the wave with the period

from 30 s up to 120 s (0.0083 to 0.033 Hz) [8,172], a bandwidth range of 0.0083–0.033 Hz (slow-wave frequency range), filter length (N) was 7, and the 6^{th} order filter was used because it provides narrower transition zones with greater attenuation and a sharper (steeper) cutoff, which is very useful when the artifact frequency is close to the ABP/ICP/IBV signal frequency. These low pass filters were tested for comparison purposes to obtain the best possible filter for slow-wave filtering or extraction.

Furthermore, the moving mean (average) values of ABP and ICP waveform were estimated for 5 s. The estimation was done by employing the moving averaging methodology, and PRx1 was estimated as a linear Pearson correlation for a two-hour period of the mean arterial pressure (MAP) and ICP. Similarly, a non-invasive technology, ICP*(t)*, was replaced with IBV*(t)*.

The moving average filter was used as a reference to the filter comparison. Moreover, TBI patient demographic (Glasgow Output Scale – GOS) reference was used for identifying the specific patient's clinical outcomes.

4.3 Outcomes of the analysis

All the five-filter data from the same patient was used to estimate the Pressure reactivity index (Fig. 4.3. A, B) and volumetric reactivity index (Fig. 4.3. C, D), where the widely used moving average (red color) was considered as reference. The pressure reactivity for Patient 01, in Fig. 4.3.A, shows that the moving average filter and the FIR-Parks–McClellan (blue color) filter has shown almost the same dynamics with clear impaired autoregulation. In contrast, Kalman (green color), Butterworth (magenta color), and Chebyshev filter (black color) showed an intermediate range of autoregulation.

The pressure reactivity index for Patient 11, in Fig.4.3B, shows that the moving average and the FIR (Parks–McClellan) filter range are in the intermediate autoregulation index. In contrast, other filters (Kalman, Butterworth, and Chebyshev filters) showed a range of autoregulation more towards impaired CA, where FIR (Parks–McClellan) seems to be of a slightly higher quality than the moving average in terms of their PRx outcome.

The volumetric reactivity index in non-invasive Volunteer Number 29 in Fig. 4.3.C shows that the moving average (red color) filter and the FIR Parks–McClellan (blue color) filter have almost the same dynamics with clear intact autoregulation. In contrast, other (Kalman (green color), Butterworth (magenta color), and Chebyshev) (black color) filters also showed the intact range of autoregulation, but their VRx ranges were shifted more towards intermediate autoregulation.

The volumetric reactivity index for Volunteer 37, in Fig. 4.3. D shows that the moving average (red color) filter and the FIR Parks–McClellan (blue color) filter have almost the same dynamics with clear intact autoregulation. In contrast, other Kalman (green color), Butterworth (magenta color), and Chebyshev (black color) filters also showed the intact range of autoregulation, but their VRx ranges were more towards intermediate autoregulation, where FIR (Parks–McClellan) seems slightly higher and better than the moving average in their PRx outcome, see Fig.4.3 (C, D).

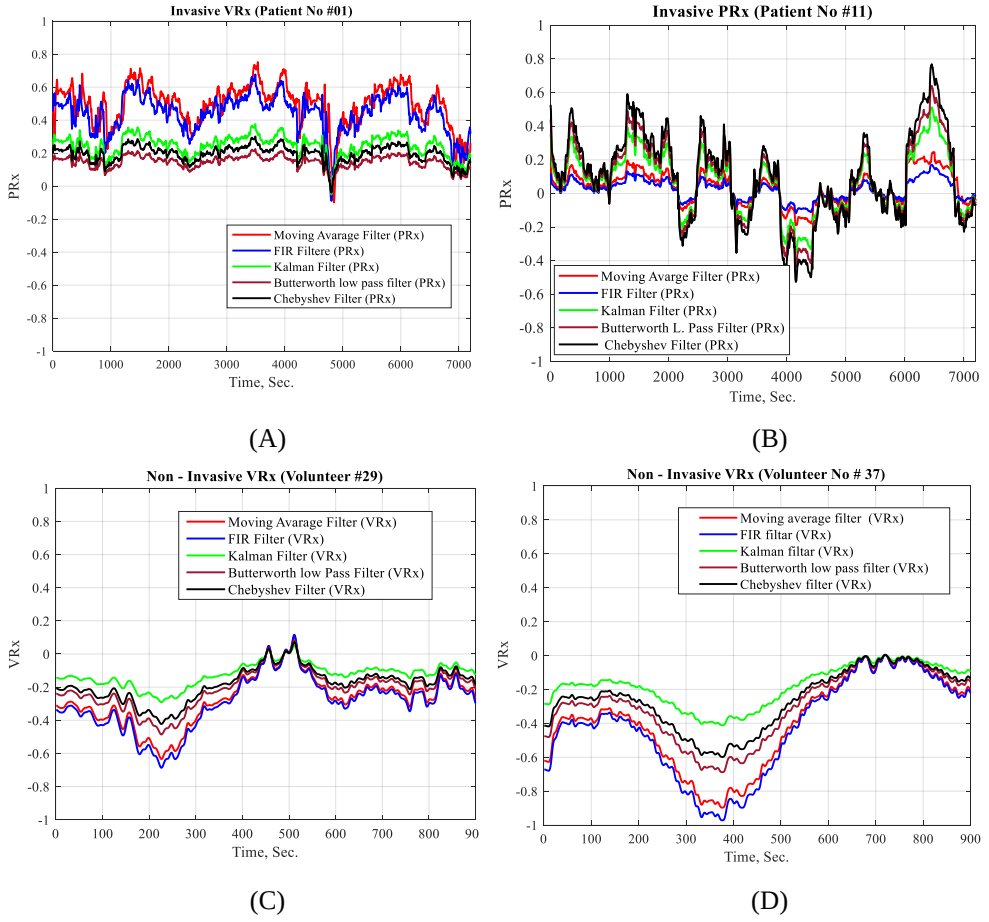

Fig.4.3. Filter comparison in patients with impaired cerebral autoregulation (CA) (A), Intermediate CA (B), Invasive PRx (Traumatic patient) and intact CA (C, D) Noninvasive VRx (Healthy Volunteer)

4.4 Summary of the Chapter

In order to select the best possible filtration of neurophysiological signals to avoid the false alarm in the intensive care unit, five filters were tested. Among the five filters, when compared with the moving average filter, FIR (Parks–McClellan) filter, Kalman filter, Butterworth low pass filter, and Chebyshev filter, the FIR (Parks–McClellan) filter showed the autoregulation correctly and was the most similar to the widely used moving average.

The pressure reactivity (PRx) curves were compared in invasive patient data, where Patient 01 had a clinical outcome as impaired autoregulation (GOS Score 1 = death), and FIR (Parks–McClellan) filter and Moving average showed the impaired outcome clearly; similarly, in Patient 11, the autoregulation was intermediate, and both moving averages and FIR (Parks–McClellan) filter depict that.

On the other hand, volumetric reactivity curves (VRx) were compared in non-invasive volunteer data, where Volunteer 29's FIR (Parks–McClellan) filter and the

Moving average filtering showed the intact outcome clearly; similarly, in Volunteer 37, the autoregulation was intact, and both moving average and FIR (Parks–McClellan) filter depicts that in comparison with the other proposed filtering methods.

The above outcomes reflect that the FIR (Parks–McClellan) filtering approach is of a higher quality (an increased signal to noise ratio) than the Kalman filter, the Butterworth low pass filter, the Chebyshev filter, and a slightly higher quality than the moving average. Hence, the FIR (Parks–McClellan) method would be selected for further autoregulation index estimation studies. Moreover, the detailed comparison of these two filters (moving average and FIR) is performed in Chapter 5 below.

5. PRESSURE REACTIVITY INDEX AND QUALITY OF ABP(t) AND ICP (t) SIGNALS FOR CA MONITORING AFTER TRAUMATIC BRAIN INJURY

This chapter is based on data presented in the publication[2].

5.1 Association between Cerebral Autoregulation Index (Pressure Reactivity), Patient's Clinical Outcome, and Quality of ABP(t) and ICP(t) Signals for CA Monitoring

5.1.1 Background of the study

Severe traumatic brain injury (TBI) is one of the primary causes of traumatic death worldwide. In Europe alone, 2.5 million people suffer TBI every year, with one million being admitted to hospital. Approximately 30–35% of deaths result from such injuries, though it should be noted that some patients suffer from disabilities [174,175]. More attention and research are required to better understand and improve the management of severe TBI.

The main objective of clinical TBI studies is to improve the management of severe TBI, and the main factor that influences treatment outcomes is cerebral autoregulation (CA) [175,176–179]. Autoregulation has been previously described as a balancing act between vasoconstriction and vasodilation, as the cerebrovascular bed's resistance accepts slow dynamic changes in cerebral perfusion pressure. CA impairment is most likely to influence the outcomes, and, thus, it is essential to explore CA over time [4,11] continuously.

Czosnyka *et al*. described the relationship between slow changes in the mean arterial blood pressure (ABP) and intracranial pressure (ICP), which led to a better understanding of the relationship between cerebral perfusion pressure (CPP) and cerebral blood flow (CBF) by using the PRx [109,110]. This index is most commonly obtained by calculating the Pearson correlation between slow-wave ABP and ICP

[2] **Bajpai BK**, Preiksaitis A, Vosylius S, Rocka S. Association Between the Cerebral Autoregulation Index (Pressure Reactivity), Patient's Clinical Outcome, and Quality of ABP(t) and ICP(t) Signals for CA Monitoring. ***Medicina***. 2020;56(3):143. Published **2020 Mar 20**.

[179–181]. With intact CA, slow increases in ABP cause vasoconstriction, which is followed by a decrease in ICP, resulting in a negative PRx; however, while CA is impaired, a rise in luminal ABP leads to passive cerebrovascular dilation and increases in cerebral blood volume and ICP. In such cases, the correlation coefficient (PRx) between ABP and ICP is positive [182,183].

The pressure reactivity index's critical threshold has been suggested and recommended by various researchers (i.e., a PRx above 0.2 or 0.25 is associated with the impaired status, and close to zero or a negative PRx associated with intact autoregulation) [16,96,101,184–188]. Among these PRx thresholds, PRx for survival (0.25) and that for the favorable outcome (0.05) proposed by Sorrentino *et al*. [185] represent the reliable threshold for the estimation of survival and achieving a favorable outcome.

Moreover, a recent study by Akhondi-Asl *et al*. [189] found that PRx can only be evaluated when there are slow but sufficient changes in ABP(t) and ICP(t) waves. The results revealed the sensitivity of the PRx calculation towards small slow wave changes in ABP(t) and ICP(t), and only slight PRx variance was observed [182], which indicated that if ABP(t) and ICP(t) waves changed with the filtering approach, the diagnostic value of the PRx may change as well.

The short period means of ABP(t) and ICP(t) are needed to calculate the PRx [176–188]. The most common approach uses the moving average. It has been argued that another filtering approach (FIR Parks–McClellan filter) for short period means of ABP(t) and ICP(t) is higher in terms of quality than using the moving average to estimate the mean pressure [190]. However, the impact of the FIR filtering approach on PRx has not been evaluated yet. Therefore, we analyzed ABP(t) and ICP(t) signals with an FIR filter and compared the results with the quality of the signal using Czosnyka *et al*.'s moving average. The sensitivity and specificity of the PRx were evaluated, with the quality of the signal based on the clinical outcomes. The Glasgow outcome scale (GOS) score after hospital discharge (GOSHD) was used as the clinical reference (the mortality and survival). GOS outcomes were taken as the reference for the dichotomous outcome for sensitivity, specificity, and ROC curve estimation. The patient's outcome was defined by using the following values: *1* (death), *2* (persistent vegetative state), *3* (severe disability), *4* (moderate disability), and *5* (low disability) [6].

A single CA impairment event lasts for approximately 5 min and is strongly associated with postoperative cognitive dysfunction and cognition deficits [191], which means that a CA monitor must have a time resolution of one minute or less, corresponding to the duration of the output reaction of a filter to an input step function for ABP(t) or ICP(t)). Such a CA monitor would show the start of severe CA impairment with a delay of about 1 min. In this case, a filter with a 1 min time window would be applicable.

5.1.2 Data analysis

The recorded raw data was 50 Hz taken from ABP and ICP waves. To extract or isolate slow-wave components in between 0.0083–0.033 Hz range, the recorded

signal was first decimated to a 1 Hz sampling frequency, considering the frequency ranges associated with cerebral vasogenic activity [169,170,171] and then filtered with the following two filters:

A. Moving average data filter: The mean values of every ABP(t) and ICP(t) signal were calculated for 5 s. The calculation was performed by using the moving average, and PRx1 was calculated as a linear Pearson correlation for a 5 min time window between 60 consecutive values of the mean arterial pressure (MAP) and ICP. The data points included in the analysis were between 50 and 120 mmHg for ABP and ICP values that were greater than zero. The average PRx1 was used for the sensitivity estimation of the ABP(t) and ICP(t) signal quality. This was considered as the first method employed for sensitivity estimation.

B. FIR Parks–McClellan data filter: In FIR (Parks–McClellan) filtering, the mean ABP and ICP were obtained by continuous filtering with a 1 min period of filtering, and PRx2 was calculated as the linear Pearson correlation coefficient with 5 min segments of ICP and ABP signals. The FIR (Parks–McClellan) filter was designed with -3 dB cut off frequency (0.5 Hz) and was used because most of the (slow-wave oscillation) energy associated with the spectral representation within the wave with the period from 30 s up to 120 s [8,172], a bandwidth range of 0.0083–0.033 Hz (slow-wave frequency range), filter length (N) was 7, and the 6^{th} order filter was used because it provides narrower transition zones with greater attenuation and a sharper (steeper) cutoff, which is very useful when the artifact frequency is close to the ABP/ICP/IBV signal frequency. The Parks–McClellan algorithm for designing FIR (Parks–McClellan) filters [192] was used to obtain mean pressure, which had never been used for PRx estimation. There are certain advantages to using the FIR (Parks–McClellan) filter, such as not increasing the computational costs, due to lower sensitivity to artifacts, shorter delays, and higher sensitivity to acute events. With FIR (Parks–McClellan) filters, it is easy to enforce the linear phase constraint if it is stable, and the duration of disruptions is limited to the impulse response duration, which is the filter length [192].

5.1.3 Statistical analysis

Statistical analysis was performed by using the software package *SPSS* (*IBM Inc*., New York, USA), Version 20. Patients included in the study were grouped into those who survived and those who did not. For each group, the average values for PRx1 (from Czosnyka *et al*.'s moving average filtering) and PRx2 (from FIR Parks–McClellan filtering) were created (Table 5.1). An independent *t*-test was used to compare the categorical outcomes (i.e., survivors/non-survivals based on GOS outcomes) and the continuous outcome.

Two additional Tables (Tables 5.2 and 5.3) were created for the sensitivity and specificity calculations with true positive (TP), true negative (TN), false positive (FP), and false-negative (FN) from the PRx outcome of both filtering methods. The GOS scale (i.e., a GOS value of *1* corresponding to death and a GOS value greater than *1* indicative of survival [6]) was considered as the reference clinical outcome. The GOS outcomes were taken as the dichotomous outcomes for true positive (TP), true

negative (TN), false positive (FP), and false-negative (FN) estimation, hence, for sensitivity and specificity.

Two ROC (receiver operating characteristic) curves were constructed in one window for 60 patients for each filtering method to compare the effectiveness of the two filtering methods. The area represented the diagnostic accuracy of the ROC curve under the curve (AUC). AUC values closer to *1* indicated that the screening measures were reliable [193–197].

5.1.4 Outcomes of the analysis

Both PRx values from Czosnyka *et al*.'s moving average filtering (PRx1) and FIR (Parks–McClellan) filtering (PRx2) were estimated for comparative purposes for all 60 TBI patients. The demographic patient data is shown in Table 5.1, where, among 60 patients, 34 male and nine female patients were survivors, while 13 male and four female patients did not survive (fatal outcomes). Moreover, the comparative pressure reactivity index of two hours of PRx1 (Czosnyka *et al*.'s moving average filtering) and PRx2 (FIR-Parks–McClellan filtering) are presented in Fig. 5.1. A–D, including patients with impaired CA (A), intermediate CA (B, C), and intact CA (D).

Table 5.1. Demographic characteristics, clinical findings, and averaged values of data from monitoring TBI patients.

	Survival	**Fatal**	**Total**	***p*-value**
Number of patients	43	17	60	-
Sex (male/female)	34/9	13/4	47/13	-
Age, mean (SD), years	36.84 (16.09)	43.25 (11.64)	38.52 (15.35)	0.028
GCS, median	6 (4-7)	5 (4–6)	5,50 (5-6)	0.015
Average PRx1 (moving average	0.08 (0.31)	0.21 (0.34)	0.11 (0.31)	0.007

filtered), mean (SD)				
Average PRx2 (FIR-Parks–McClellan filtered), mean (SD)	−0.01(0.36)	0.26 (0.22)	0.01(0.37)	0.001

GCS, Glasgow coma scale; PRx, pressure reactivity index; SD, standard deviation; TBI, traumatic brain injury.

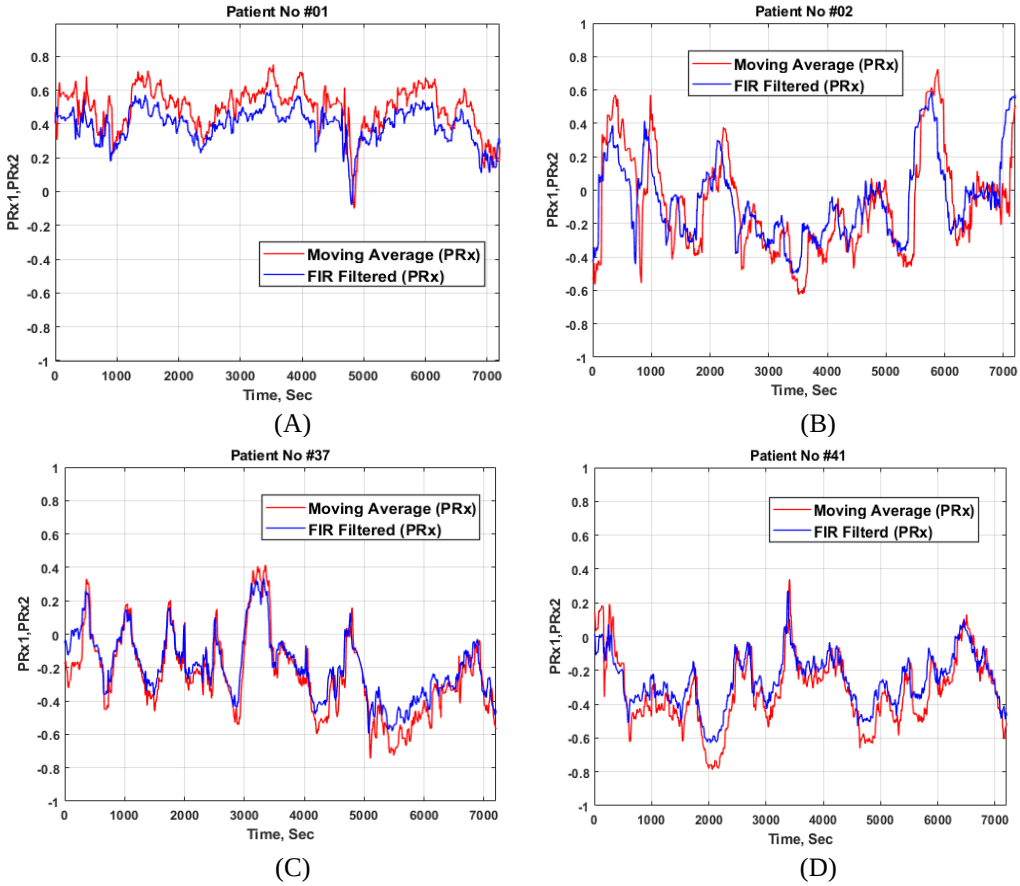

Fig. 5.1. Example of a two-hour period of PRx1 (moving average filtering) and PRx2 (FIR Parks–McClellan filtered data) comparison in patients with impaired cerebral autoregulation (CA) (A), intermediate CA (B, C), and intact CA (D).

5.1.5 Sensitivity and specificity

As shown in Table 5.2, patients were grouped according to PRx outcomes, where the PRx2 from the FIR (Parks–McClellan) filtering approach included 12 patients with true positives, 35 with true negatives, 8 with false positives, and 5 with false negatives, which reflected a sensitivity of 70% and a specificity of 81% (by the FIR Parks–McClellan filtering approach).

Table 5.2. 2x2 matrix (FIR Parks–McClellan filtered data PRx2)

Outcome	**Impaired Autoregulation/Non-survivors (Fatal)**	**Intact Autoregulation/Survivors**
Positive test (GOS * 1)	(True positive) 12 (M-9, F-3)	(False positive) 8 (M-6, F-2)
Negative test (GOS *>1)	(False negative) 5 (M-5, F-0)	(True negative) 35 (M-27, F-8)

** GOS, Glasgow scale estimation of clinical outcome; M, male; F, female*

Sensitivity = True Positive/(True positive + False negative) = 12/17 = 70%
Specificity = True Negative/(False positive + True negative) = 35/43 = 81%

Table 5.3. The 2 × 2 matrix (moving average PRx1)

Outcome	**Impaired Autoregulation/ Non-survivors (Fatal)**	**Intact autoregulation/ Survivors**
Positive Test (GOS * 1)	(True positive) 10 (M-8, F-2)	(False positive) 13 (M-10, F-3)
Negative test (GOS *>1)	(False negative) 7 (M-5, F-2)	(True negative) 31 (M-25, F-6)

** GOS, Glasgow scale estimation of clinical outcome; M, male; F, female*

Sensitivity = True Positive/(True positive + False negative) = 10/17= 58%
Specificity = True Negative/(False positive + True negative) = 35/43= 72%

As shown in Table 5.3, patients were grouped according to PRx outcomes, where PRx1 from Czosnyka *et al*.'s moving average filtering approach included 10 patients with true positives, 31 with true negatives, 13 with false positives, and 7 with false negatives, which reflected 58% sensitivity and 72% specificity by the FIR (Parks–McClellan) filtering approach.

5.1.6 Receiver operating characteristic curve

The ROC curve was constructed from 60 patients' PRx data by using both filtering approaches, true positives (PRx associated with impaired autoregulation), and true negatives (PRx associated with intact autoregulation), where true positives and true negatives were plotted against each other for the ROC curve from Tables 5.2 and 5.3.

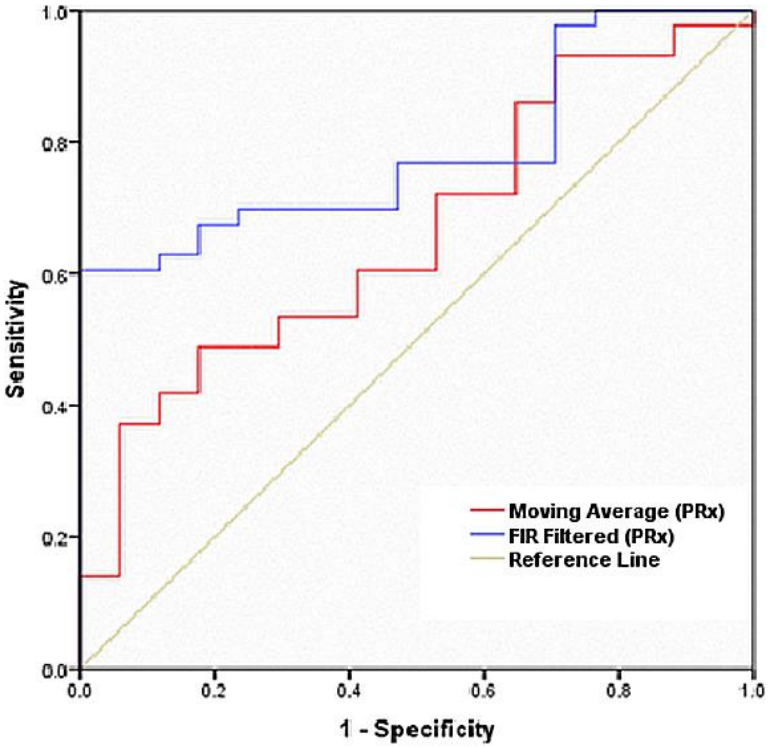

Fig. 5.2. ROC curves for both methods' PRx values, moving average filtering, and FIR (Parks–McClellan) filtering. FIR (Parks–McClellan) filtered (PRx) shows a higher diagnostic accuracy with a larger area under the curve (AUC) compared to the moving average (PRx).

For the moving average of PRx1, the ROC curve (red) had an area under the curve (AUC) of 0.661 with a sensitivity of 58%, a specificity of 72%, and a significance level of 0.054. The area under the ROC curve had a standard error of 0.075 and a 95% confidence interval of 0.515–0.807, as shown in Fig. 5.2 and Table 5.4 (ROC curve from both methods' PRx values, moving average filtering, and

FIR (Parks–McClellan) filtering). For the FIR (Parks–McClellan) filtered PRx2, the ROC curve (blue) had an area under the curve (AUC) of 0.785, with a sensitivity of 70%, a specificity of 81%, and a significance level of 0.001. The area under the ROC curve had a standard error of 0.058 and a 95% confidence interval of 0.671–0.900, as shown in Fig.5.2 and Table 5.4 (ROC curve from both methods' PRx values, moving average filtering, and FIR Parks–McClellan filtering).

Table 5.4. Results for the area under the ROC curve (AUC) obtained for the moving average and FIR (Parks–McClellan) filter criterion values and coordinates of the ROC curve (as shown).

Test Result Variable(s)	Area	Std. Error *	Asymptotic Significance. **	Asymptotic 95% Confidence Interval	
				Lower Bound	Upper Bound
Moving Average (PRx)	0.661	0.075	0.054	0.515	0.807
FIR Parks–McClellan Filtered (PRx)	0.785	0.058	0.001	0.671	0.900

** Under the nonparametric assumption. ** Null hypothesis: true area = 0.5. FIR (Parks–McClellan) filtered (PRx2) shows higher diagnostic accuracy with a higher area under the curve (AUC) compared to the moving average (PRx).*

5.1.7 Independent *t*-test

Independent *t*-tests between categorical (survivals and non-survivals based on the GOS outcome) and the continuous PRx from the moving average PRx showed a significance level (Significance (two-tailed)) of 0.040, with a 95% confidence interval of 0.01428–0.57685 and a standard error of 0.13921).

Table 5.5. Results for the independent *t*-test obtained from the moving average and FIR (Parks–McClellan) filter PRx criterion values and coordinates of the ROC curve

Test Variable (s)	t	Sig.	df	Sig. (2-tailed)	Mean Difference	Std. Error Difference	95% Confidence Interval	
							Lower	Upper

Moving average PRx	2.123	0.054	40.319	0.040	0.29557	0.13921	0.01428	0.57685
FIR (Parks–McClellan) PRx	3.743	0.000	27.370	0.001	0.45484	0.12151	0.20568	0.70401

The FIR (Parks–McClellan) filtered data PRx showed a significance level (Sig. (two-tailed)) of 0.001 with a 95% confidence interval of 0.20568–0.70401 and a standard error of 0.12151. This *t*-test indicated that FIR (Parks–McClellan) filtering had a higher significance and a lower standard error than moving average filtering, as shown in Table 5.5.

5.1.8 Discussion

In this study, the association between the CA index (PRx) associated with a patient's clinical outcomes (from the GOS scale) and the quality of the signal to estimate the CA index (PRx) was estimated. Czosnyka *et al*. described the relationship between slow changes in mean ABP and ICP, which led to the development of the relationship between CPP and CBF by using the PRx [177,178]. This index was obtained by calculating the Pearson correlation between slow-wave ABP and ICP [178–181]. With intact CA, slow increases in ABP caused vasoconstriction, which was followed by a decrease in ICP, resulting in a negative PRx. However, while the CA was impaired, a rise in luminal ABP led to passive cerebrovascular dilation and increases in the cerebral blood volume and ICP. In such cases, the correlation coefficient (PRx) between ABP and ICP was positive [182].

The short period means of ABP(t) and ICP(t) were essential for estimating the PRx [176–188]. According to prior studies, ICP signals are often polluted by a significant number of artifacts. Artifacts contaminate an average of 5% of data points in the collected ICP signals, and, in some cases, more than 20% of signals can be polluted [198]. The most common approach employed to obtain a short period means is the moving average. It has been argued that FIR (Parks–McClellan) filters for the short period means of ABP(t) and ICP(t) are higher in quality than the moving average to estimate the mean pressure [190]. Akhondi-Asl *et al*. stated that the PRx could only be evaluated when there are slow but sufficient changes in ICP and ABP waves. This shows the PRx calculation's sensitivity to slow-wave changes, and only a slight PRx variance can be seen with small slow wave changes [189]. In other words, if there are higher or lower wave changes in ABP(t) and ICP(t), the diagnostic PRx value would be different.

Hence, we used the FIR (Parks–McClellan) filters for the PRx estimation, which is an essential index for CA monitoring. In our study, we evaluated the sensitivity and specificity of the PRx, basing the quality of the signal on the clinical outcomes. The

Glasgow outcome scale (GOS) score after hospital discharge (GOSHD) was used as a clinical reference (mortality versus survival). GOS outcomes were taken as the reference for the dichotomous outcome for sensitivity, specificity, and ROC curve estimation. The patient's outcome was defined by using the following five-point scale: *1* (death), *2* (persistent vegetative state), *3* (severe disability), *4* (moderate disability), and *5* (low disability) [6].

From the ROC curve, the FIR (Parks–McClellan) filter method revealed a sensitivity of 70%, a specificity of 81%, an area under the ROC curve of 0.78, and a significance level of $p = 0.001$, with a standard error of 0.058. These results were higher than those found with the moving average method, which had a sensitivity of 58% and a specificity of 72%. The area under the ROC curve was 0.661, and the significance level was $p = 0.054$. The area under the ROC curve revealed a standard error of 0.075. An AUC closer to 1.0 is ideal for discriminative values between healthy and sick patients [193–197]. The ROC curve reflected that the FIR (Parks–McClellan) filter approach was better than the moving average method for ABP and ICP signal filtering. The *t*-test reflected that FIR (Parks–McClellan) filtering results featured a higher significance level (0.001) and a lower standard error (0.12151) than the moving average (significance level 0.040, with a standard error of 0.13921), as shown in Table 5.5.

FIR (Parks–McClellan) filtering resulted in a higher time resolution because of the filter with a 1 min time window. A single CA impairment event is approximately 5 min long and is strongly associated with postoperative cognitive dysfunction and cognition [191]. That means that CA monitoring must have a time resolution of 1 min or less, which is the duration of the output reaction of the filter to an input step function of ABP(t) or ICP(t)). Such CA monitoring would show the start of severe CA impairment with a delay of about 1 min.

5.1.9 Summary of the chapter

The association between the sensitivity of the PRx, brain-injured patient's clinical outcome, and the quality of ABP(t) and ICP(t) indicated that the FIR (Parks–McClellan) filtering approach was more sensitive for discriminating between the two clinical outcomes, namely, intact (survival) and impaired (death) cerebral autoregulation for TBI treatment decision making. ABP(t) and ICP(t) signal analysis in TBI patients is particularly essential to minimize the risk of uncertain diagnostic values (intact or impaired) of the PRx.

5.1.10 Limitations of the Study

This study was conducted on a small population of patients (60 patients). A validation study with a much larger population is still necessary. Furthermore, there is no gold standard for the cerebral autoregulation monitoring method. Another essential factor for producing more concrete results is the comparison of PRx outcomes with various filtering approaches and various alternative methods.

6. NON–INVASIVE CA MONITORING TECHNOLOGY (ULTRASONIC TIME OF FLIGHT THROUGH A HUMAN HEAD AND ATTENUATION IN THE BRAIN)

This chapter is based on data presented in the publication[3]

6.1 Comparative Study of Novel Noninvasive Cerebral Autoregulation Volumetric Reactivity Indexes Reflected by Ultrasonic Speed and Attenuation as Dynamic Measurements in the Human Brain

6.1.1 Background of the research

The mechanisms of cerebral autoregulation remain poorly understood, especially in humans. Cerebrovascular autoregulation refers to the brain's ability to maintain constant cerebral blood flow (CBF) with changes in the cerebral perfusion pressure (CPP) [198] based on cerebral metabolism independent of fluctuations in the systemic arterial blood pressure (ABP). This process is controlled by multifactor mechanisms, including myogenic, metabolic, and neurogenic metabolic mechanisms [199–201].

Cerebral autoregulation (CA) is the primary factor that influences treatment outcomes in brain trauma patients [6,175,176,202]. When CA is impaired, the outcomes for traumatic brain injury (TBI) patients are significantly impacted. Autoregulation has been described as a balancing act between vasoconstriction and vasodilation because the resistance of the cerebrovascular bed accepts slow dynamic changes in cerebral perfusion pressure. CA's impairment has the most significant influence on these outcomes, which means that it is essential to explore CA continuously over time [4,202].

Several existing methods are used to estimate CA status based on measuring fluctuations in CPP and CBF along with cerebral vascular resistance changes in CPP (or ABP) [65,203–205]. Generally, currently existing CA assessment methods are based on applying the surrogate physiological parameters that make it practically impossible to replace them with noninvasive CBF monitoring. The objective of clinically invasive methods for assessing continuous CA is to determine the pressure reactivity index (PRx) by the moving Pearson's correlation coefficient (r) between the slow waves of ABP(t) and ICP(t) over a time window of a few minutes. With intact CA, slow increases in ABP cause vasoconstriction, which is followed by a decrease in ICP, resulting in a negative PRx; however, while CA is impaired, a rise in luminal ABP can lead to passive cerebrovascular dilation and an increase in cerebral blood volume and ICP. In such cases, PRx will be positive [177,178,206]. It has been found that PRx values above a critical level associated with brain vascular deterioration can cause death [182,207]. The crucial threshold for PRx was suggested and

[3] Bajpai, B.K.; Zakelis, R.; Deimantavicius, M.; Imbrasiene, D. Comparative Study of Novel Noninvasive Cerebral Autoregulation Volumetric Reactivity Indexes Reflected by Ultrasonic Speed and Attenuation as Dynamic Measurements in the Human Brain. *Brain Sci.* **2020**, *10*, 205

recommended by various scientists (i.e., with values above 0.2 or 0.25 for PRx being associated with impaired status and those close to zero or negative values being associated with intact autoregulation) [185–188].

PRx is one of the widely used indexes for CA monitoring [182,185,206–208], as no gold standard exists. However, an important limitation of this approach is that it is invasive (i.e., ICP sensors must be inserted into brain ventricles or the parenchyma tissue).

All other existing noninvasive methods attempt to find a surrogate parameter that could replace CBF monitoring to calculate the related CA index [209]. Among several noninvasive methods, the transcranial Doppler (TCD) method for assessing CA noninvasively is primarily used. The middle cerebral artery (MCA) for blood velocity is used instead of CBF to estimate the TCD, depending on the autoregulation index (Mx) as a moving correlation coefficient between the MCA and ABP. Similarly, other methods, such as near-infrared spectroscopy (NIRS), are used to estimate the correlation coefficient between the measured local oxygen saturation and ABP. These are referred to as the cerebral oximetry (Cox or Tox) index [209, 210] and the hemoglobin volume index (HVx), which are monitored with a moving linear correlation of the blood pressure to the cerebral blood volume near-infrared spectroscopy [211]. The local dependency is a limitation of these noninvasive methods [208].

A novel noninvasive technology (Certification (CE) marked device) was developed by the Health Telematics Science Institute at Kaunas University of Technology (Kaunas, Lithuania). ICP*(t)* slow waves were replaced by IBV*(t)* slow waves to estimate the CA status which was included in the calculation of the noninvasive volumetric reactivity index VRx*(t)* as a moving correlation coefficient between the slow IBV*(t)* and ABP*(t)* waves [208]. The clinical applicability of the VRx has been proven by several clinical studies conducted by the Health Telematics Science Institute at Kaunas University of Technology (Kaunas, Lithuania), such as the noninvasive ultrasonic VRx based on time-of-flight with the invasive PRx on 61 patients with brain injuries and showed excellent coincidence with reflect autoregulation [208]. Another comparative study with 11 patients with brain injuries revealed a significant relationship associated with VRx and PRx outcomes [212], which indicated that VRx reflects autoregulation the same way as PRx. Additionally, the applicability of the noninvasive IBV estimation technique for cerebrovascular autoregulation monitoring reflected the similarity between invasive ICP and noninvasive IBV [181,213,214]; these were used to derive the reactivity indexes (PRx, VRx). In this study, we investigated novel noninvasive ultrasonic methods developed by the Health Telematics Science Institute at Kaunas University of Technology (Kaunas, Lithuania) based on real-time monitoring of the ultrasound speed and compared that with attenuation dynamics. We aimed to determine similarities in both the time-of-flight and attenuation channels to use VRx2 (attenuation-based index) as an alternative technology. This is closely similar to the time-of-flight technology related to the acoustic path, and this path crosses arterioles (small vessels) responsible for autoregulation, while attenuation shows this integrated reaction of small vessels to the changes in the blood pressure.

The clinical applicability of novel noninvasive ultrasound attenuation based VRx2 is comparable with the time-of-flight based VRx1, which is already in use for clinical studies. The attenuation ultrasound-based VRx2 is an attractive, cost-effective alternative to the time-of-flight based VRx1 and even less expensive than TCD (transcranial Doppler) and potentially easy for hardware miniaturization. A comparative study was performed by determining VRx1 and VRx2 calculations.

6.1.2 Cerebral autoregulation assessment

CA status was monitored by using a novel noninvasive ultrasonic monitor developed by the Health Telematics Science Institute at Kaunas University of Technology (Kaunas, Lithuania) for real-time monitoring of the ultrasound speed and attenuation dynamics in the human brain. The technology provides real-time information regarding IBV changes and waves in the cerebral vessels responsible for CA [181,213,214]; such changes and waves are causes of the intracranial pressure (ICP*(t)*) changes and waves [214]. The novel technology idea was based on the possibility of measuring intracranial blood volume changes and waves inside the acoustic path that crosses the human head, while applying an ultrasonic time-of-flight method, see Fig. 6.1 [215]. The speed and attenuation of ultrasound reflect the density of blood, brain tissue, and cerebrospinal fluid volumes inside an acoustic path. According to the database of the IT'IS (Information Technologies in Society) Foundation (Switzerland, 2019) [216], the values of ultrasound speed (± standard deviation) in blood, brain tissue, and cerebrospinal fluid were 1578.2 (± 11.3) m/s, 1546.3 (± 20.2) m/s, and 1505.5 (± 3.5) m/s, respectively. The Ultrasonic time-of-flight technology measures the time of short ultrasound pulses are transmitted through the human head with picosecond resolution and the attenuation of such pulses.

The method is based on the transmission of short ultrasonic pulses from one side of the head and the receiving on the other side of the ultrasonic pulses which were propagated through the external tissues, skull, and intracranial media. We are detecting the ultrasound time-of-flight variations [215,217] and ultrasound attenuation variations caused by the volume changes of intracranial media (the cerebrospinal fluid, brain parenchyma tissue, arterial and venous blood) inside the parenchymal acoustic path. The acoustic is measured as echo, and the ultrasonic signals are used for transmission through the human head.

Similarly, in order to obtain an attenuation channel surrogate (IBV), a short pulse of ultrasonic time of flight traveling through the acoustic medium of human head measuring changes in the blood volume was received at the other side of the head as shown in Fig. 6.1, where adding an additional detector of amplitude at the end of the receiver was attempted.

Both (Time of flight and attenuation) monitoring results reflect the changes of the blood and cerebrospinal fluid volume inside the acoustic path in different ways, reflected by intracranial ultrasound speed and attenuation changes caused by cardiac pulsation and respiration processes, cerebrospinal blood flow autoregulation processes, and other intracranial dynamic phenomena. However, both channels reacted to the physiology in the same way, see Figs. 6.2, 6.3, and 6.4.

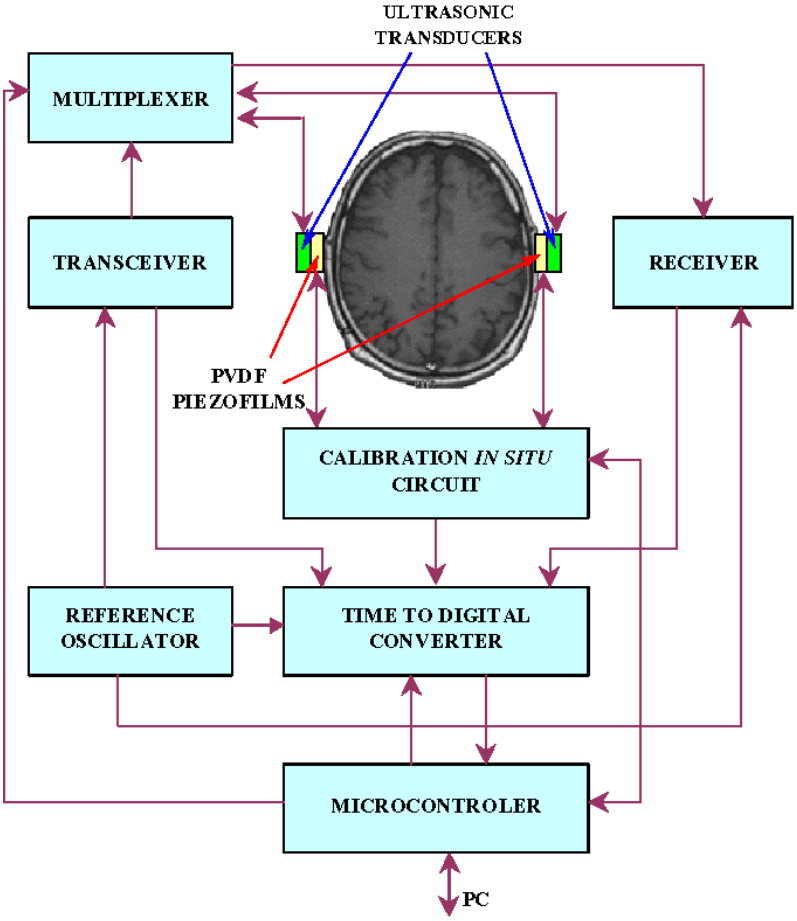

Fig. 6.1. Technological description of the ultrasonic time of flight measurement [215]

The usual invasive CA monitoring is based on ABP*(t)* and the ICP*(t)* slow-wave correlation index PRx*(t)* calculation [64,177,218–220]. In the new noninvasive technology, ICP*(t)* slow waves were replaced with IBV*(t)* slow waves, and the CA status was estimated by calculating the noninvasive VRx*(t)* as a moving correlation coefficient between the slow waves of IBV*(t)* and ABP*(t)*. Slow ABP*(t)* and IBV*(t)* B waves with a period of 0.5–2.0 minutes reflecting the vasogenic activity of cerebrovascular autoregulation and was used for VRx*(t)* calculations [181,213,214].

A head frame including a pair of ultrasonic transducers on either side of the head was positioned so that the acoustic path crossed the intracranial media, including parenchyma and brain ventricles, but avoiding large arteries and veins. IBV*(t)* changes and slow waves caused by vasodilatation and vasoconstriction mechanisms reflected the changes in the parenchymal vessels' diameter responsible for maintaining a relatively stable CBF [181,213]. The vasoconstriction of arterioles and capillary vessels was the physiological autoregulatory reaction to the increased mean arterial blood pressure (MAP). The blood volume inside the acoustic path decreased in these cases, while that monitored by the speed of ultrasound also decreased [191]. The

capability to sense the overall integrated volumetric reactions of the brain and increased temporal resolution of CA monitoring were the primary advantages of this ultrasonic method compared with other methods based on local blood volume/velocity monitoring by using near-infrared spectroscopy (NIRS) and Doppler technology applications [223–227].

The CA status of healthy participants was continuously assessed for 15 minutes by monitoring the time dependence of the two noninvasively recorded VRx*(t)* indexes, including VRx1*(t)*, which reflected ultrasound speed dynamics, and VRx2*(t)*, which reflected ultrasound attenuation dynamics. The ABP*(t)* slow-wave reference signal was taken from a noninvasive ABP*(t) Finapres Nova* monitor. Negative values of both VRx*(t)* < 0 corresponded to the intact CA status, and positive VRx*(t)* values > 0 indicated CA impairment [211,212,218–221]. Two-minute moving averages of both VRx*(t)* were used to obtain a temporal resolution of CA impairments that were at least two times higher than those obtained with NIRS or Doppler CA monitors. During cardiopulmonary bypass (CPB), continuous slow MAP*(t)* waves with a stable period of T=60 seconds were generated by periodic (60 seconds) 20-second breath-holds. This type of periodic modulation of O_2/CO_2 saturation in the cerebral blood created reference MAP*(t)* slow waves and the speed of ultrasound and ultrasound attenuation slow waves as cerebrovascular blood flow autoregulatory reactions (two informative signals for two VRx*(t)* index calculations).

6.1.3 Data analysis

The recorded data was bandpass filtered to extract the slow waves of ABP*(t)* and IBV*(t)* (of the attenuation and time-of-flight channels). The correlation coefficient was estimated between the bandpass filtered spectra of both channels' slow waves.

On the other hand, the FIR (Parks–McClellan) filter was also used to extract the slow waves of ABP*(t)* and IBV*(t)* (for the attenuation and time-of-flight channels). Moreover, the correlation coefficients were estimated between the FIR filtered spectra of both channels' slow waves.

After slow-wave correlation studies, noninvasive volumetric reactivity indexes (VRx1 and VRx2) were calculated as a moving correlation coefficient between the slow waves of IBV*(t)* and ABP*(t)* waves from the time-of-flight and attenuation channel. Slow ABP*(t)* and IBV*(t)* B waves were obtained. Two separate sets of volumetric indexes (VRx1 and VRx2) were estimated, one set from the bandpass filter and the other set from the FIR (Parks–McClellan) filter. The volumetric indexes were then compared to determine the differences in both channels' CA outcomes with different filtration approaches.

Additionally, before slow-wave filtering, hyperventilation and breath-holding tests were performed for vasoconstriction and vasodilation dynamics for a few seconds to determine whether both channels are reacted to the physiology in the same way, when the arterial blood pressure (ABP) was the same. Furthermore, pulse waves for the 10-second window were also extracted from both the time-of-flight and attenuation channels for comparison purposes.

6.1.4 Statistical analysis

Statistical analysis was performed by using the *SPSS* (*IBM Inc*., New York, USA) Version 20 software package. A linear regression analysis of VRx1 and VRx2 was performed. VRx1 and VRx2 data was averaged during each simultaneous monitoring session to produce one value per participant (43 data points). Pearson's correlation coefficient between VRx1 and VRx2 averaged data was calculated with a 3-minute time window used for each monitoring session.

6.1.5 Outcome of the analysis

Before slow-wave filtering, the pulse wave for the 10-second window was extracted from both the time-of-flight and attenuation channels, which indicated that both channels had a similar reaction to the physiology, as shown in Fig. 6.2(a) and (b). Furthermore, hyperventilation and breath-holding tests were performed for vasoconstriction and vasodilation dynamics for a few seconds by time-of-flight and attenuation ultrasonic noninvasive CA monitoring (see Figs. 6.3 and 6.4). They also reflected that both channels reacted to the physiology in the same way when ABP was the same.

The noninvasive VRx1, which reflected ultrasound speed dynamics, and VRx2, which reflected ultrasound attenuation dynamics, indexes were recorded for 43 healthy participants. The monitoring sessions were performed for 15 minutes for each participant. The correlation between the slow waves extracted from the time-of-flight and attenuation channels was as shown in Table 6.1where, the participants were grouped according to the correlation outcomes between the time-of-flight and attenuation channels, where correlation from the FIR (Parks–McClellan) filtering approach had 33 participants with a correlation of more than 0.5 (higher correlation) and ten participants with less than 0.5 (low) correlation.

Table 6.1. Correlation outcome between slow waves of TOF and attenuation channels.

Correlation outcome (r)	**Band-Pass Filtered Slow Wave**	**FIR (Parks–McClellan) Filtered Slow Wave**
>0.5	31 participants	33 participants
<0.5 to 0	12 participants	10 participants

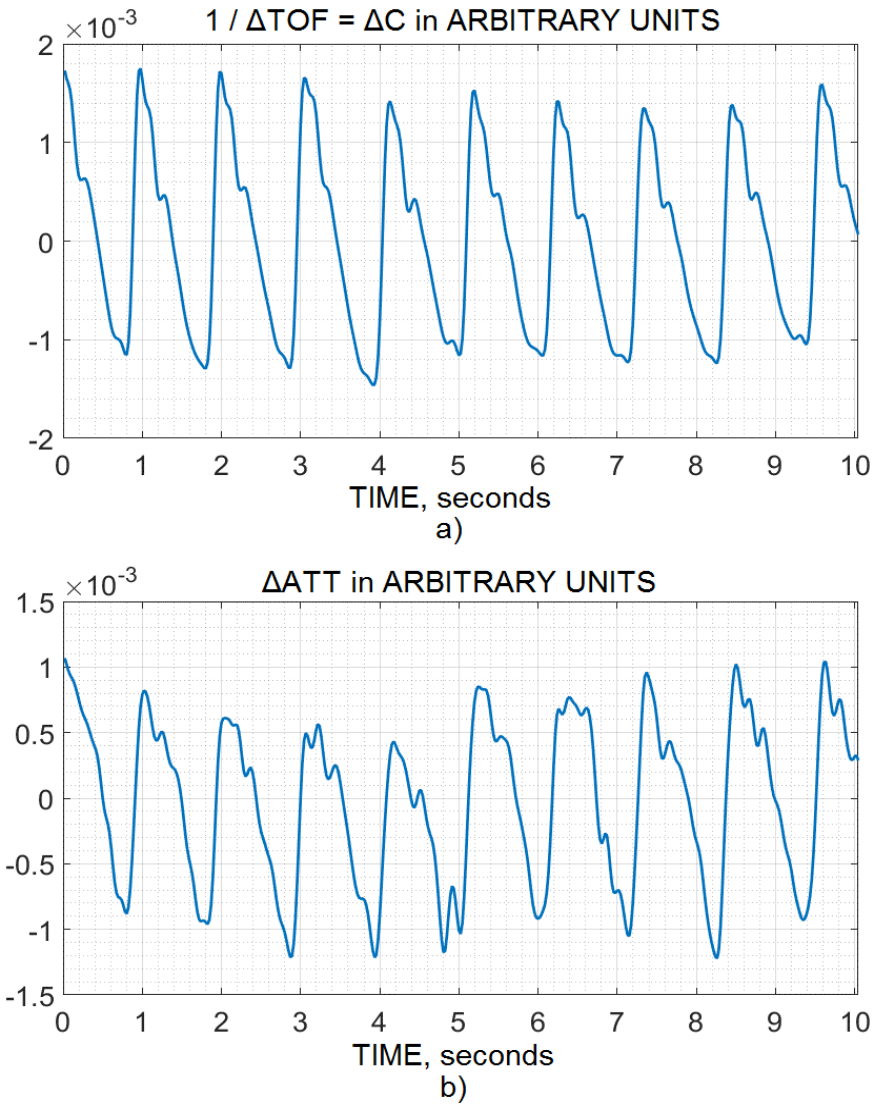

Fig. 6.2. Intracranial volumetric pulse waves (causes of ICP waves) noninvasively and simultaneously recorded by (**a**) the ultrasonic time-of-flight recording method and (**b**) the attenuation recording method inside an acoustic path which is crossing the skull and the brain

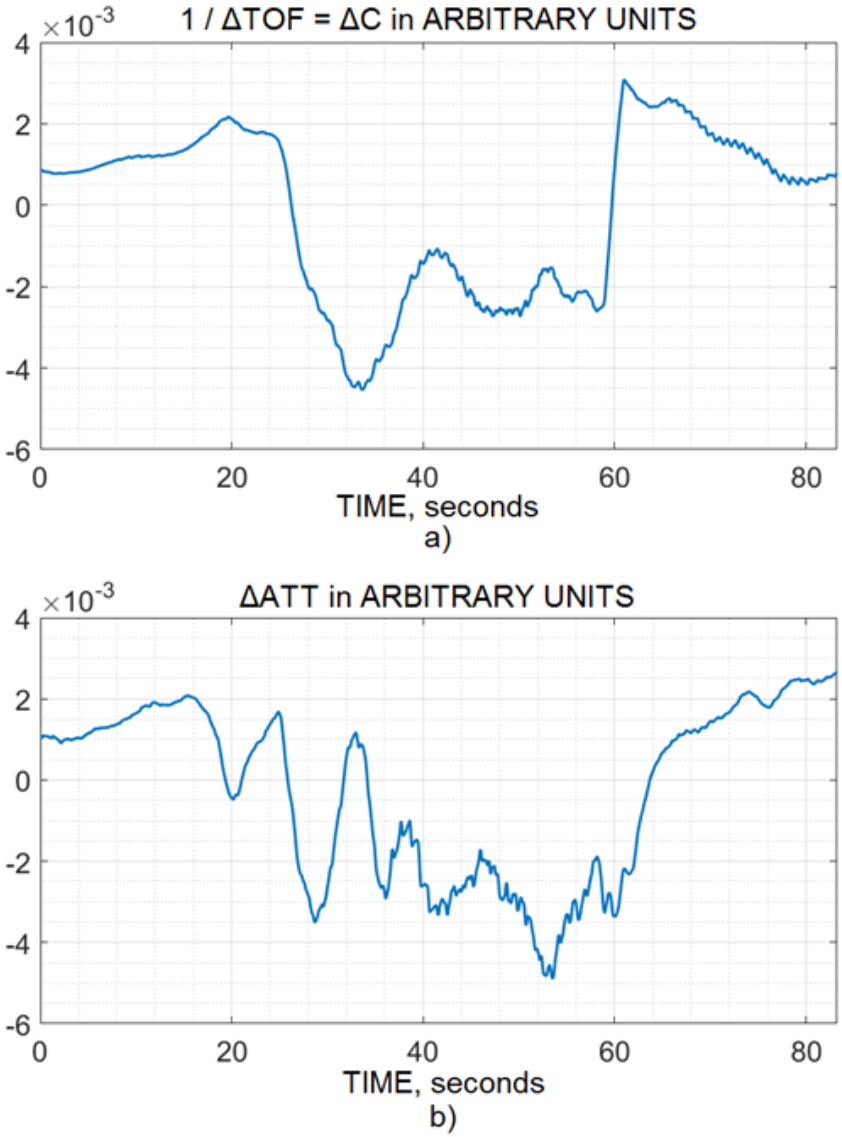

Fig. 6.3. Vasoconstriction dynamics of intracranial blood vessels caused by hyperventilation test and recorded by (**a**) the time-of-flight and (**b**) attenuation channels of the ultrasonic noninvasive CA monitor

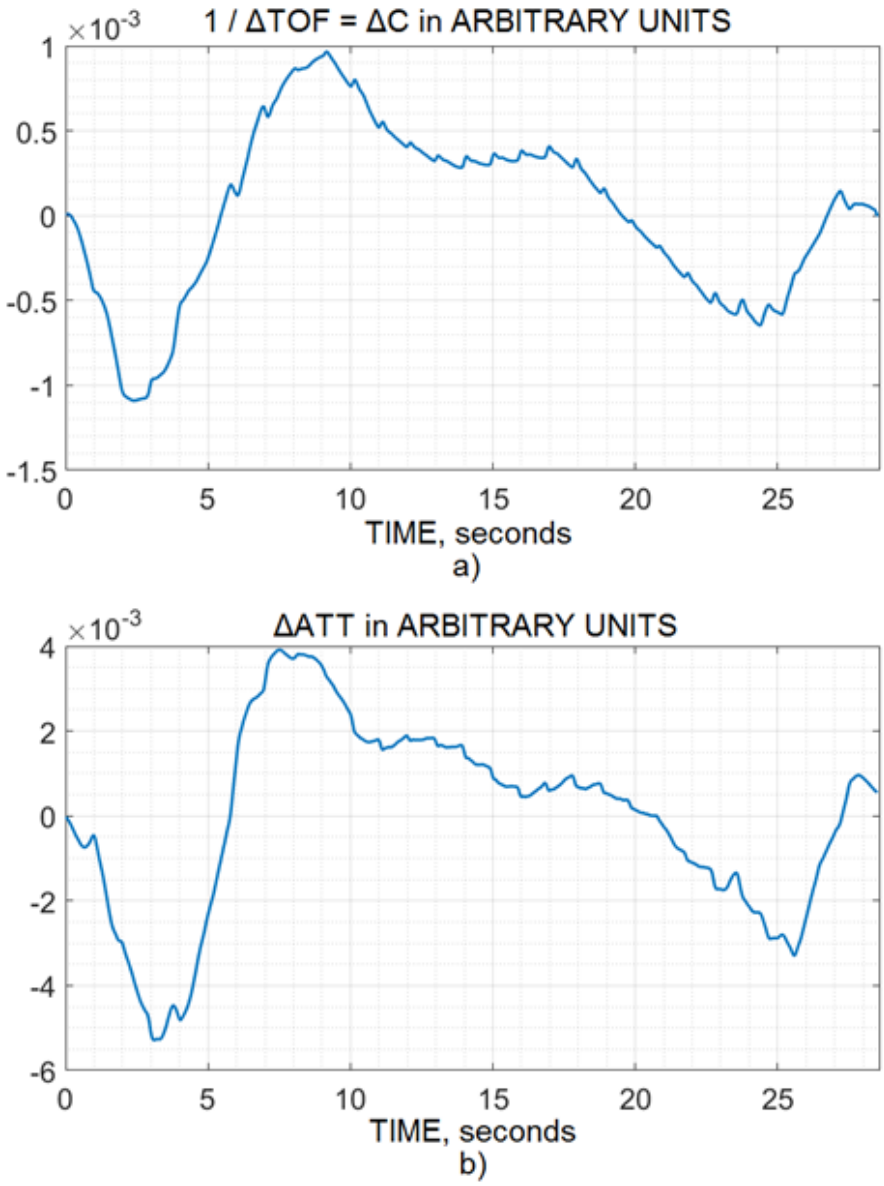

Fig. 6.4. Vasodilatation dynamics of intracranial blood vessels caused by the breath-holding test and recorded by the (a) time-of-flight and (b) attenuation channels of the ultrasonic noninvasive CA monitor

By contrast, bandpass filtering found 31 participants with a correlation of more than 0.5 (higher correlation) and 12 participants with less than 0.5 (low), which reflected a significant correlation in the ultrasound speed dynamics' (TOF) slow waves and ultrasound attenuation's slow waves. Examples of comparisons between both channels' slow waves with correlations for a three-minute window are shown in Fig. 6.5. Furthermore, examples of comparisons between VRx1 and VRx2 over 15-

minute monitoring periods are shown in Fig. 6.6. VRx1 and VRx2 parameters estimation ranges are from -1 to +1; meanwhile, the range shown in Figs. 6.6, 6.7, and 6.8 is from -1 up to 0 because the healthy volunteers were having intact autoregulation (below 0); therefore, the -1 up to 0 range was chosen for representation.

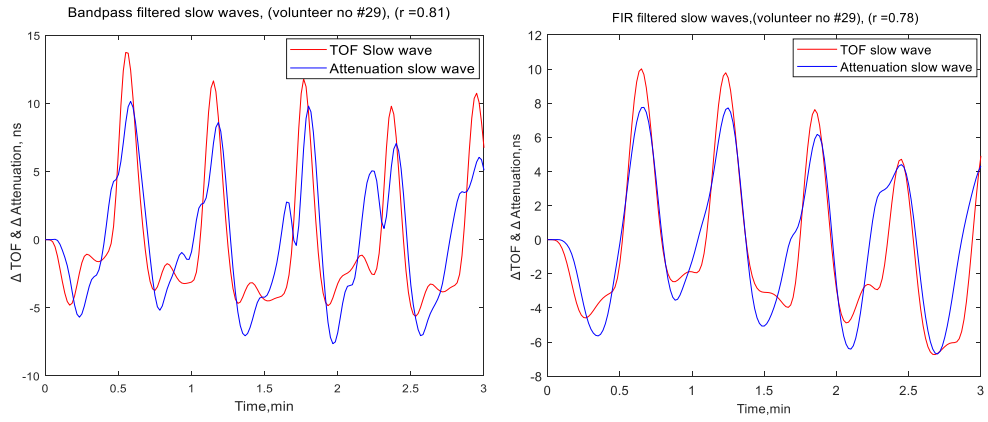

(a) (b)

Fig. 6.5. Examples of three-minute periods of slow waves extracted from time-of-flight and attenuation dynamics; comparison of participants with (a) excellent correlation by the bandpass filter and (b) excellent correlation by the FIR (Parks–McClellan) filter

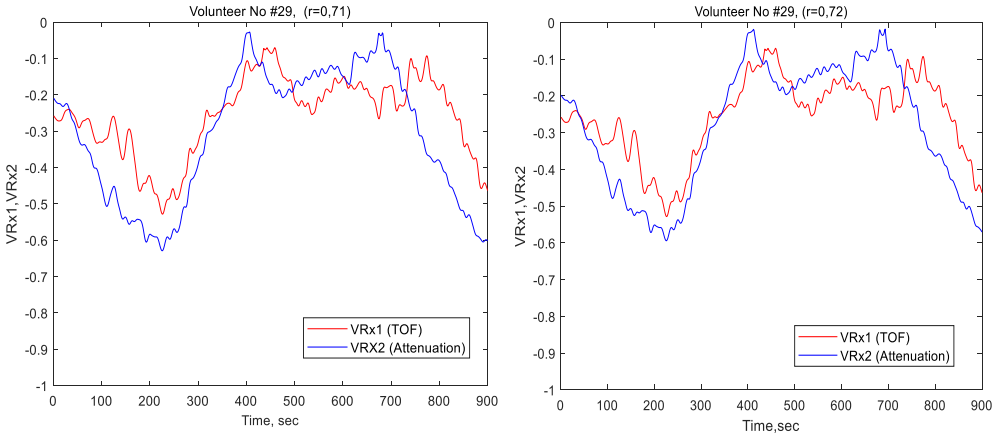

(a) (b)

Fig.6.6. Comparison window for volumetric reactivity indexes (VRx1 and VRx2) for 15-minute time with (a) an excellent correlation by the bandpass filter and (b) an excellent correlation by the FIR (Parks–McClellan) filter

Three-minute time-averaged (per participant in 43 pairs) VRx1 and VRx2 indexes were used for linear regression, where the correlation coefficient between VRx1 and VRx2 averaged 0.730, with a 95% confidence interval of 0.501–0.895, and

a statistical significance of less than 0.0001 in the studied population. Similarly, in the FIR (Parks–McClellan) filtered data, the correlation coefficient between VRx1 and VRx2 averaged 0.769, with a 95% confidence interval of 0.611–0.909 and a statistical significance of less than 0.0001 in the studied population (see Fig. 6.7a and b).

The linear regression plots between the pairs of VRx1 and VRx2 indexes were averaged per participant's monitoring sessions, as shown in Fig. 6.7a, and b. There were significant statistical similarities between both the ultrasound speed dynamics (time-of-flight), ultrasound attenuation dynamics, and their CA indexes (VRx1 and VRx2), while the FIR (Parks–McClellan) filtered approach exhibited slightly higher correlation outcomes compared to the bandpass filtration. The standard deviation of the difference between VRx1 and VRx2 was 0.1647, and the bias between VRx1 and VRx2 was −0.3444 by bandpass filtering; while in FIR (Parks–McClellan) filtered data, the standard deviation of the difference between VRx1 and VRx2 was 0.1382, and the bias between VRx1 and VRx2 was −0.3669 (see Fig. 6.7a and 6.7b).

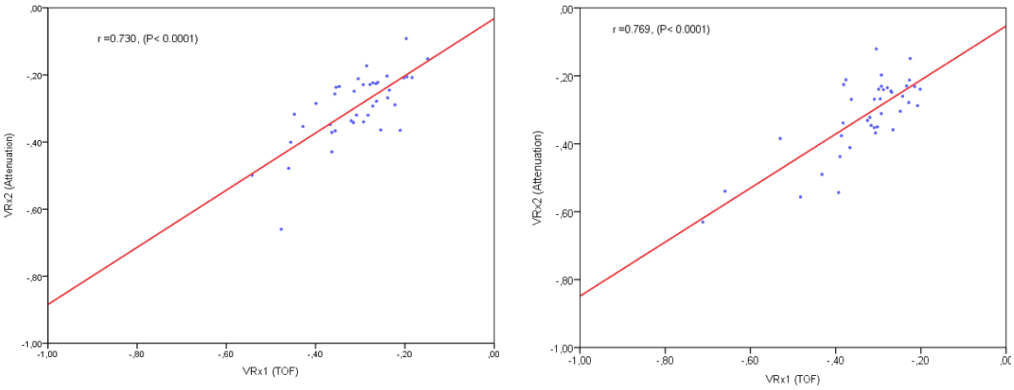

(a) (b)

Fig. 6.7. Comparison of VRx1 and VRx2 indexes by regression analysis. (a) Bandpass filtering. The correlation coefficient between VRx1 and VRx2 indexes is denoted as $r = 0.730$. The statistical significance is $p < 0.0001$. (b) FIR (Parks–McClellan) filtering. The correlation coefficient between VRx1 and VRx2 indexes is $r = 0.769$. The statistical significance is $p < 0.0001$

Bland–Altman plots between the pairs of VRx1 and VRx2 indexes averaged per participant's monitoring sessions are shown in Fig. 6.8a, and b. All these outcomes reflected a good agreement between the ultrasound speed dynamics (TOF) and the ultrasound attenuation dynamics-based indexes (VRx1, VRx2).

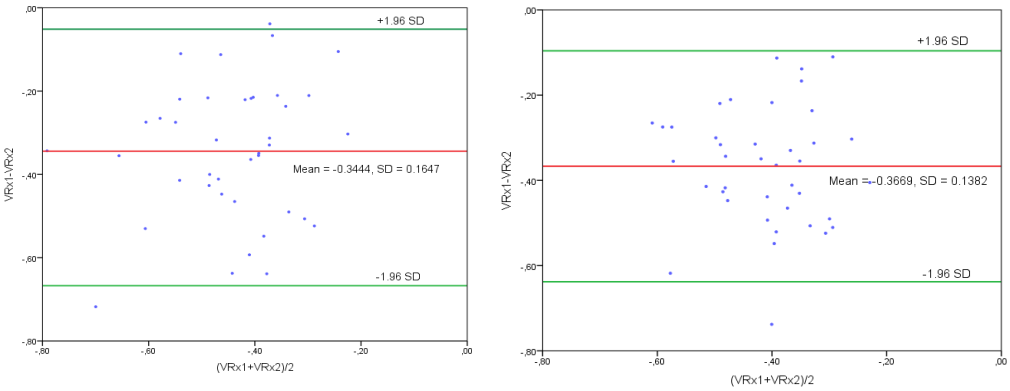

(a) (b)

Fig. 6.8. Comparison of VRx1 and VRx2 indexes by Bland–Altman plots. (**a**) Bandpass filtering. The standard deviation of the difference between the indexes is SD 0.1647. Bias is −0.3444. (**b**) FIR (Parks–McClellan) filtering. The standard deviation of the difference between the indexes is SD 0.1382. Bias is −0.03669

6.1.6 Discussion

CA status analysis was conducted for healthy participants by monitoring the time dependence of noninvasively recording the two VRx*(t)* indexes, including VRx*(t)*1, which reflected ultrasound speed dynamics, and VRx*(t)*2, which reflected ultrasound attenuation dynamics. As there was no gold standard for noninvasive CA monitoring, VRx (ultrasound speed dynamics), time-of-flight was chosen as a reference index, CE marked, and already used for clinical studies.

Changes in IBV values consist of slow respiratory and pulse waves and are associated with ICP changes [191]. Hence, the similar reaction to physiology by both the channel's (time of flight and attenuation) pulse wave, vasoconstriction, and vasodilation was evidence of similarity in both channels, Figs. 6.2–6.4 indicate that both channels (time-of-flight and attenuation) reacted to the physiology in the same way; we keep in mind the artifacts which were filtered by the bandpass and FIR (Parks–McClellan) filtration.

However, there were some differences between the channels. For example, if the surplus of oxygen provoked IBV change due to hyperventilation, there was too much oxygen in the blood, which caused vasoconstriction. Hence, the volume decreased in both channels, although the difference was small. This slight difference showed that the attenuation channel was slightly different (Fig. 6.2), which may be due to a number of factors, such as differences in transmission or differences in monitoring attenuation and time-of-flight channels because a different parameter of the dynamic media was measured. Generally, if the blood volume increased, both channels indicated an increment, and if the blood volume went down, both channels should indicate a fall.

We created a classifier; the classifier had two states: impaired (autoregulation reactivity index from 0 to 1), and intact (autoregulation reactivity index from -1 to 0).

We took an already existing classifier, (VRx1) time-of-flight, clinically tested [208,212], as a reference to create another inexpensive classifier, an attenuation-based reactivity index (VRx2). We compared both classifiers to find out whether they provided the same diagnostic information. We used linear regression and Bland–Altman methods to compare the agreement between these two methods. Linear regression showed significant correlation of 0.731, $p<0.0001$, 95% confidence interval [0.501–0.895] in the bandpass filter. FIR (Parks–McClellan) filtering had a slightly higher correlation of 0.769, $p<0.0001$, 95% confidence interval [0.611–0.909].

On the other hand, Bland–Altman's direct comparison proved that both classifiers yielded intact cerebral autoregulation values, as both curves of VRx1 and VRx2 had outcomes from −1 to 0 (see Fig. 6.8a and 6.8b), which was intact autoregulation [211,212,218–221] as we already knew that we were using healthy subjects for the study, which guaranteed an intact outcome.

The average of both VRx*(t)* values was used to achieve a temporal resolution of CA impairments' detection that was at least two times higher than that of NIRS or Doppler CA monitoring. The capability to sense the overall integrated volumetric reactions of the brain and the increased temporal resolution of CA monitoring were the primary advantages of this ultrasonic method compared with any other methods based on the local blood volume/velocity monitoring using near-infrared spectroscopy (NIRS) and Doppler applications [222–227].

Several studies have been conducted that compared invasive CA indexes, though most of them were compared against the invasive PRx. However, this study provided a comparison of two noninvasive volumetric reactivity indexes to show that the novel attenuation-based volumetric reactivity index (VRx2) could be used as an alternative to the time-of-flight based volumetric reactivity index (VRx1), where VRx1 (based on time-of-flight) is already being tested in (dynamic conditions) traumatic brain injury patients, against PRx, and it is already in use for clinical studies. Time-of-flight studies [171,175] indicated that the VRx1 (TOF channel) output signal highly correlated with invasive PRx*(t)*, which could be used for comparison with the attenuation channel's signal in healthy participant studies. However, it would be recommended in the future to test the attenuation channel directly in traumatic brain injury patients against PRx.

6.1.7 Summary of the chapter

This comparative study of the noninvasive ultrasonic volumetric reactivity indexes VRx1 (time-of-flight) and VRx2 (attenuation) monitoring was based on the ultrasonic time-of-flight and ultrasonic attenuation measurement of IBV dynamics, which showed a significant correlation. VRx2 (attenuation) could be used as a noninvasive cerebrovascular autoregulation index in the same way as VRx1 and could be used to reflect essential information related to the CA status. Compared with a bandpass filter, the FIR (Parks–McClellan) filter had slightly higher correlation outcomes between the two indexes.

6.1.8 Limitations of the study

This study was conducted on a small population of participants (only 43 participants). A validation study with a much larger population of healthy participants is necessary. Furthermore, there is no gold standard for the cerebral autoregulation monitoring method. Another essential factor in producing more concrete results is the comparison of the volumetric reactivity index (VRx1 and VRx2) outcomes with various filtering approaches and various methods. It would be recommended in the future to test the attenuation channel directly in traumatic brain injury patients against PRx.

7. CONCLUSION AND RESEARCH OUTLOOK

7.1 Discussion and Outcomes

In the case of the absence of a 'gold standard' classifier to classify the two states: impaired (autoregulation reactivity index from 0 to 1) and intact (autoregulation reactivity index from -1 to 0), the only way to test the reliability of the CA monitors is by patient treatment outcome analysis; therefore, in the case of our TBI patient CA analysis, we use the Glasgow outcome scale (GOS) score after hospital discharge (GOSHD) as the patient treatment outcome reference for the CA (the intact and impaired) state. GOS outcomes were taken as the reference for the dichotomous outcome for sensitivity, specificity, and ROC curve estimation. The patient's outcome was defined by using the following: *1* (death), *2* (persistent vegetative state), *3* (severe disability), *4* (moderate disability), and *5* (low disability). The reliability of this patient treatment outcome analysis method is higher as the reference was taken from the actual patient outcomes from GOS where it is commonly known that the inter-rater reliability of the total Glasgow coma scale is p=0.81.

On the other hand, in the case of the non-invasive classification of the CA status, we created a classifier, where we took an already existing classifier, (VRx1) time-of-flight, clinically tested [208,212], as a reference to create another inexpensive classifier, the attenuation-based reactivity index (VRx2). We compared both classifiers to find out whether they provided the same diagnostic information. The reliability of this non-invasive classifier was higher to classify the outcome into two classes (intact versus impaired) because we were using a healthy volunteer for the study, which guaranteed an intact outcome of the healthy volunteer, where VRx1 is already being tested in TBI in comparison with invasive CA monitoring.

In-depth knowledge of cerebrovascular physiology and fundamental cerebral hemodynamics is required for the current management of severe TBI. Neuromonitoring methods, for example, ABP, ICP, and IBV measurements, allow clinicians or neuro-physicians, or neuroscientists, the possibility for the examination and identification of morphological and functional defects that have a negative impact on the patient outcomes. Over a period, invasive (PRx) from FIR (Parks–McClellan) filtered ABP and ICP slow wave is modified to a better approximate to the currently used filtration methods.

Non-invasive ultrasonic attenuation dependent variables have been employed to regular patient monitoring methods (for example, VRx1 and VRx2) to offer alternate slow wave measures of cerebral autoregulation with an increased focus on the CBV signal analysis. It has enabled new derived parameters to be modified to better, more reliable and cost-effective than their invasive counterparts. The growth of the non-invasive neuro-measurements outside the neurocritical care environment has an enormous possibility for the outcome forecast in ICU management; these monitoring approaches produce a more comprehensive patient description without any extra hazard.

7.2 Main Results

This dissertation evaluated the clinical implementation of usable neurophysiological slow-wave filtering techniques and the application of the novel noninvasive neuromonitoring techniques in acute brain injury.

In Chapter 2, the core mechanisms and clinical descriptors of cerebral autoregulation and the role of slow waves were introduced and evaluated in the context of both invasive and noninvasive neuromonitoring parameters that are being used in the prediction of patient mortality following acute brain injury: Chapter 3 outlined the methodologies of the work presented in this thesis.

In Chapter 4, the impact of artifact(s) in the arterial and cerebral signal and a comparison of filters for the selection of the best filter for artifact rejection were described in several distinct patient populations. To select the best possible filtration of neurophysiological signals to avoid the false alarm in the intensive care unit, five filters were tested. Among the five filters, the FIR (Parks–McClellan) filter showed the autoregulation correctly and was most similar to the widely used moving average.

In Chapter 5, the quality of ABP and ICP indicates that the FIR (Parks–McClellan) filtering approach was more delicate for distinguishing among clinical results, intact (alive), and impaired (dead) in CA for TBI treatment decisions.

In Chapter 6, the noninvasive ultrasonic volumetric reactivity VRx1 (time-of-flight) and VRx2 (attenuation) monitoring study showed a significant correlation between VRx1 and VRx2. VRx2 (attenuation), which could be used as an alternative index in the same way as VRx1 and could also be used to estimate the noninvasive CA status. In comparison with bandpass filtering, the FIR (Parks–McClellan) filter had slightly higher correlation outcomes between both VRx1 and VRx2 indexes. While Attenuation (VRx2) based CA monitoring, ultrasonic technology is attractive as it is a cost-effective method.

7.3 Limitations to the study

Various essential limitations of all of the clinical studies submitted in this dissertation must be considered before the outcome's generalization.

- The patient data for most points estimated the same large, overlapping clinical monitoring database separated into different sets to meet the requirements of the comparison study in question.
- Reports on the clinical conditions and other nursing or clinical treatment are not regularly presented in the dataset, so it is almost not possible to attribute

detectable ICP/IBV or ABP trends as a result of TBI rather than to any other clinical manipulations that happen with the target to treat no steady patients.

- The continuous prospective data obtained from a different patient/volunteer from ICU settings, this sample size was significantly smaller to conclude the risk of mortality. A validation study on a larger population is necessary.
- There is no gold standard present for the cerebral autoregulation monitoring method, hence, there is no standard gold reference.
- To produce more concrete results, it is essential to compare invasive PRx outcomes with various filtering methods.
- The impact of a sedative on the slow arterial blood pressure waves was not analyzed, and data analysis was not considered, which may cause higher pressure reactivity index values by higher or lower sedative doses to make the patient sleep.
- Only healthy volunteer data was used for a comparative study of the noninvasive volumetric reactivity index (attenuation and time of flight).
- It would be suggestive in the future to test the attenuation channel directly in traumatic brain injury patients against PRx. However, we do not have the resources and time at the moment to invest.
- Different existing parameters that could impact neuromonitoring indexes have not been taken into account in this dissertation, for example, brain tissue oxygenation, mechanical ventilation, and microdialysis. The interaction of these parameters with the ultrasonic attenuation-based indexes and CA has not been estimated, although these relationships could provide insight into the future development of the outcome forecasting techniques.

7.4 Summary of the Research Outlook

7.4.1 Filtering of slow neurophysiological waves in CA

The presentation of the results from the filtering and estimation of the sensitivity and specificity of the slow wave in association with cerebral autoregulation introduced the concept of the signal quality estimation and enhancement in neuromonitoring and their impact as an alarm in the intensive care unit. Although not evaluated within the scope of this thesis, the comparative analysis of other invasive neuromonitoring modalities in the general intensive care, the estimators of cerebral autoregulation is of great interest to future studies of outcome prediction. Additionally, it will serve as a comparative study of various filtration techniques on a large population and data spanning over a longer period.

7.4.2 Non-Invasive ultrasonic attenuation based on autoregulation monitoring

The advancement of non-invasive approximation of the conventional invasive estimators of cerebral autoregulation (i.e., PRx and ICP) offers the potential to extend neuromonitoring inside and outside of the clinical care settings. These variables can be determined based on non-invasive ultrasonic attenuation signal evaluation. The use of ultrasonic attenuation in the clinical care environment poses no risk of infection or discomfort to patients and can swiftly depict cerebral hemodynamics in real time. If attenuation (VRx2) based measurement can be expanded to clinical patients in the future, real-time attenuation (VRx2) can detect

and track the variations or changes in the hemodynamics of brain physiology. IBV observation (and attenuation-based autoregulation index) could then be used for patient-specific care plans, instead of speculating on the research trends. Also, attenuation-based monitoring is a technology which is easy to implement and, on top of that, is cost-effective as it is even cheaper than TCD, and it could be a key market for developing nations.

7.5 Overall Conclusions

1. Among the five filters – the moving average filter, the FIR (Parks–McClellan) filter, the Kalman filter, the Butterworth low pass filter, the Chebyshev filter – the FIR (Parks–McClellan) filter showed the autoregulation correctly and was most similar to the widely used moving average. The above outcomes reflect that the FIR (Parks–McClellan) filtering approach is higher in quality than the Kalman filter, the Butterworth low pass filter, the Chebyshev filter, and slightly better than the moving average in terms of the reactivity index estimation. Therefore, the FIR (Parks–McClellan) method was selected for our autoregulation index estimation studies.
2. The relation between the sensitivity of the PRx, TBI patient's clinical outcome, and the quality of ABP and ICP shows that the FIR Parks–McClellan type filtering method (featuring a sensitivity of 70% and a specificity of 81%) was more sensitive towards autoregulation than the moving average filter (58% sensitivity and 72% specificity).
3. Two methods – VRx1 based on time-of-flight and VRx2 based on ultrasonic attenuation – were compared in the comparative study of the noninvasive ultrasonic volumetric reactivity indexes, which showed the correlation coefficient of 0.769 with a statistical significance $p<0.0001$ by the FIR (Parks–McClellan) filtering method. This reflects a significant correlation, thus VRx2 can be used as a noninvasive CA index in the same way as VRx1. Additionally, the FIR (Parks–McClellan) filter had slightly higher correlation (0.769) outcomes than the bandpass filtering method (0.730), among both indexes.
4. The attenuation based (VRx2) noninvasive CA monitoring technology is attractive because it is 3 times more cost effective than the TOF based (VRx1) CA monitoring while offering the same reliability as TOF CA monitoring.

The most important finding of this doctoral thesis is the explanation of the improving slow ABP/ICP signal quality (sensitive and specific towards CA) for better cerebrovascular autoregulation by automatic elimination of artifacts in the arterial line and by the FIR (Parks–McClellan) filtering developed under this thesis. It has been demonstrated in the process of both invasive and noninvasive subjects (patient/healthy volunteer) analysis.

REFERENCES

1. Lang, E. W., Mudaliar, Y., Sa, F. C. P., Lagopoulos, J. I. M., Dorsch, N., Yam, A., Mulvey, J. (n.d.). *A Review of Cerebral Autoregulation : Assessment and Measurements*. 161–172.
2. Council, N. E., & Policy, T. (2015). *A STRATEGY FOR AMERICAN INNOVATION A for American Innovation*. (October).
3. Antwerpen, U. Z. (2020). *Collaborative European NeuroTrauma Effectiveness Research in TBI Reporting CENTER-TBI NeuroTrauma Effectiveness Research in TBI)*. (1), 2–4.
4. Donnelly J, Budohoski KP, Smielewski P, Czosnyka M. Regulation of the cerebral circulation: bedside assessment and clinical implications. *Crit Care*. 2016;20(1):129. Published 2016 May 5. doi:10.1186/s13054-016-1293-6
5. Claassen, J. A., Meel-Van Den Abeelen, A. S., Simpson, D. M., Panerai, R. B., Alexander Caicedo Dorado, Mitsis, G. D., … Novak, V. (2015). Transfer function analysis of dynamic cerebral autoregulation: A white paper from the International Cerebral Autoregulation Research Network. *Journal of Cerebral Blood Flow and Metabolism*, *36*(4), 665–680. https://doi.org/10.1177/0271678X15626425.
6. Petkus, V., Krakauskait, S., Preikšaitis, A., Ročka, S., Chomskis, R., & Ragauskas, A. (2016). Association between the outcome of traumatic brain injury patients and cerebrovascular autoregulation, cerebral perfusion pressure, age, and injury grades. *Medicina (Lithuania)*, *52*(1), 46–53. http://doi.org/10.1016/j.medici.2016.01.004
7. Liu, X., Czosnyka, M., Donnelly, J., Cardim, D., Cabeleira, M., Hutchinson, P. J., … Brady, K. (2018). Wavelet pressure reactivity index: a validation study. *Journal of Physiology*, *596*(14), 2797–2809. https://doi.org/10.1113/JP274708
8. Lemaire, J. J., Khalil, T., Cervenansky, F., Gindre, G., Boire, J. Y., Bazin, J. E., … Chazal, J. (2002). *Slow Pressure Waves in the Cranial Enclosure*. 243–254.
9. Risberg J, Lundberg N, Ingvar DH (1969) Regional cerebral blood volume during acute transient rises of the intracranial pressure
10. Rosner MJ, Becker DP (1984) Origin and evolution of plateau waves, experimental observations and a theoretical model. J Neurosurg 60: 312–324
11. Zubaviciute, E., Rocka, S., Preiksaitis, A., Petkus, V., Ragauskas, A., Vosylius, S., … Rastenyte, D. (2017). Benefit on optimal cerebral perfusion pressure targeted treatment for traumatic brain injury patients. *Journal of Critical Care*, *41*, 49–55. http://doi.org/10.1016/j.jcrc.2017.04.029
12. Continuous recording and control of ventricular fluid pressure in neurosurgical practice. Acta Psychiat Neurol Scand1960;36(suppl 149):1–193.
13. Frederick A. Zeiler, Ari Ercole, Marek Czosnyka, Peter Smielewski, Gregory Hawryluk, Peter J.A. Hutchinson, David K. Menon, Marcel Aries, Continuous cerebrovascular reactivity monitoring in moderate/severe traumatic brain injury: a narrative review of advances in neurocritical care, British Journal of Anaesthesia, Volume 124, Issue 4, 2020, Pages 440-453, ISSN 0007-0912,

https://doi.org/10.1016/j.bja.2019.11.031.
14. Guiza F, Meyfroidt G, Piper I, et al. Cerebral perfusion pressure insults and associations with outcome in adult traumatic brain injury. J Neurotrauma 2017; 34: 2425-31
15. Adams H, Donelly J, Kolias A, et al. Characterising the temporal evolution of ICP and cerebrovascular reactivity after severe traumatic brain injury: best international abstract award. J Neurosurg 2016; 124: A1195-6.
16. Steiner LA, Czosnyka M, Piechnik SK, et al. Continuous monitoring of cerebrovascular pressure reactivity allows determination of optimal cerebral perfusion pressure in patients with traumatic brain injury. Crit Care Med 2002; 30: 733-8
17. Ursino, M. & Lodi, C. A. A simple mathematical model of the interaction between intracranial pressure and cerebral hemodynamics. *Journal of applied physiology (Bethesda, Md. : 1985)* 82, 1256–1269.
18. Czosnyka, M. *et al.* Contribution of mathematical modelling to the interpretation of bedside tests of cerebrovascular autoregulation. *Journal of neurology, neurosurgery, and psychiatry* 63, 721–73.
19. Cavus, E. *et al.* Brain tissue oxygen pressure and cerebral metabolism in an animal model of cardiac arrest and cardiopulmonary resuscitation. *Resuscitation* 71, 97–106.
20. Bowton, D. L., Bertels, N. H., Prough, D. S. & Stump, D. A. Cerebral blood flow is reduced in patients with sepsis syndrome. *Critical care medicine* 17, 399–403.
21. Darby, J. M. *et al.* Acute cerebral blood flow response to dopamine-induced hypertension after subarachnoid hemorrhage. *Journal of neurosurgery* 80, 857–864.
22. Steiner, L. A. *et al.* Responses of posttraumatic pericontusional cerebral blood flow and blood volume to an increase in cerebral perfusion pressure. *Journal of Cerebral Blood Flow & Metabolism* 23, 1371–1377.
23. Lassen, N. Cerebral blood flow and oxygen consumption in man. *Physiological reviews* 39, 183–238.
24. Paulson, O. B., Strandgaard, S. & Edvinsson, L. Cerebral autoregulation. *Cerebrovascular and brain metabolism reviews* 2, 161–92 (1990).
25. Fog, M. The relationship between the blood pressure and the tonic regulation of the pial arteries. *Journal of neurology and psychiatry* 1, 187–197.
26. Kontos, H. A. *et al.* Responses of cerebral arteries and arterioles to acute hypotension and hypertension. *The American journal of physiology* 234, H371–83.
27. Nakagawa, Y., Tsuru, M. & Yada, K. Site and mechanism for compression of the venous system during experimental intracranial hypertension. *Journal of neurosurgery* 41, 427–34.
28. Piechnik, S. K., Czosnyka, M., Richards, H. K., Whitfield, P. C. & Pickard, J. D. Cerebral venous blood outflow: a theoretical model based on laboratory simulation. *Neurosurgery* 49, 1214–22; discussion 1222–3 (2001).

29. Wilson, M. H. Monro-kellie 2.0: The dynamic vascular and venous pathophysiological components of intracranial pressure. *Journal of Cerebral Blood Flow & Metabolism* 36, 1338–1350 (2016).
30. Menon, D. K. Cerebral protection in severe brain injury: physiological determinants of outcome and their optimisation. *British medical bulletin* 55, 226–58
31. Attwell, D. *et al.* Glial and neuronal control of brain blood flow. *Nature* 468, 232–243 (2010).
32. Hall, C. N. *et al.* Capillary pericytes regulate cerebral blood flow in health and disease. *Nature* 508, 55–60 (2014).
33. Willie, C. K., Tzeng, Y.-C., Fisher, J. A. & Ainslie, P. N. Integrative regulation of human brain blood flow. *The Journal of* . . . 592, 841–59 (2014).
34. Schaller, B. Physiology of cerebral venous blood flow: From experimental data in animals to normal function in humans. *Brain Research Reviews* 46, 243–260
35. Lee, J. H. *et al.* Carbon dioxide reactivity, pressure autoregulation, and metabolic suppression reactivity after head injury: a transcranial Doppler study. *Journal of neurosurgery* 95, 222–232 (2001).
36. Fox, P. T. & Raichle, M. E. Focal physiological uncoupling of cerebral blood flow and oxidative metabolism during somatosensory stimulation in human subjects. *Proceedings of the National Academy of Sciences of the United States of America* 83, 1140–1144.
37. Zappe, A., Uludaˇg, K., Oeltermann, A., Uˇgurbil, K. & Logothetis, N. The influence of moderate hypercapnia on neural activity in the anesthetized nonhuman primate.*Cerebral Cortex* 18, 2666–2673 (2008).
38. Lieshout, J. J. van & Secher, N. H. Point:Counterpoint: Sympathetic nerve activity does/does not influence cerebral blood flow. Point: Sympathetic nerve activity does influence cerebral blood flow. *Journal of applied physiology (Bethesda, Md. : 1985)* 105, 1364–1366 (2008).
39. Ainslie, P. N. & Brassard, P. Why is the neural control of cerebral autoregulation so controversial? *F1000prime reports* 6, 14 (2014).
40. Visocchi, M., Chiappini, F., Cioni, B. & Meglio, M. Cerebral blood flow velocities and trigeminal ganglion stimulation. A transcranial Doppler study. *Stereotact Funct Neurosurg* 66, 184–192.
41. Umeyama, T. *et al.* Changes in cerebral blood flow estimated after stellate ganglion block by single photon emission computed tomography. *J Auton Nerv Syst* 50, 339–346.
42. Lingzhong, M., Hou, W., Chui, J., Han, R. & Gelb, A. W. Cardiac Output and Cerebral Blood Flow. *Anaesthesiology* 123, 1198–1208 (2015).
43. Ogoh, S. *et al.* The effect of changes in cardiac output on middle cerebral artery mean blood velocity at rest and during exercise. *The Journal of physiology* 569, 697–704.
44. Lanfranchi, P. A. & Somers, V. K. Arterial baroreflex function and cardiovascular variability: interactions and implications. *American journal of*

physiology. *Regulatory, integrative and comparative physiology* 283, R815–R826 (2002).
45. Willie, C. K. *et al*. Utility of transcranial Doppler ultrasound for the integrative assessment of cerebrovascular function. *Journal of neuroscience methods* 196, 221–37.
46. Davies, D. J. *et al*. Near-Infrared Spectroscopy in the Monitoring of Adult Traumatic Brain Injury: A Review. *Journal of Neurotrauma* 32, 933–941 (2015).
47. Vajkoczy, P. *et al*. Continuous monitoring of regional cerebral blood flow: experimental and clinical validation of a novel thermal diffusion microprobe. *Journal of neurosurgery* 93, 265–274.
48. Rajan, V., Varghese, B., Van Leeuwen, T. G. & Steenbergen, W. Review of methodological developments in laser Doppler flowmetry. *Lasers in Medical Science* 24, 269–283.
49. Rohlwink, U. K. & Figaji, A. A. Methods of monitoring brain oxygenation. *Child's Nervous System* 26, 453–464 (2010).
50. Rostami, E., Engquist, H. & Enblad, P. Imaging of Cerebral Blood Flow in Patients with Severe Traumatic Brain Injury in the Neurointensive Care. *Frontiers in Neurology*.
51. Raboel, P. H., Bartek, J., Andresen, M., Bellander, B. M. & Romner, B. Intracranial Pressure Monitoring: Invasive versus Non-Invasive Methods—A Review. *Critical Care Research and Practice* 2012, 1–14 (2012).
52. Steiner, L. a & Andrews, P. J. D. Monitoring the injured brain: ICP and CBF. *British journal of anaesthesia* 97, 26–38.
53. Lassen NA. Autoregulation of cerebral blood flow. Circ Res. 1964;15(Suppl):201–4.
54. Strandgaard S, Paulson OB. Cerebral autoregulation. Stroke. 1984;15(3):413–6.
55. Budohoski KP, Reinhard M, Aries MJH, Czosnyka Z, Smielewski P, Pickard JD, et al. Monitoring cerebral autoregulation after head injury. Which component of transcranial Doppler flow velocity is optimal? Neurocrit Care. 2012;. doi:10.1007/s12028- 011-9572-1.
56. Czosnyka M, Smielewski P, Kirkpatrick P, Menon DK, Pickard JD. Monitoring of cerebral autoregulation in head-injured patients. Stroke. 1996;27(10):1829–34.
57. Panerai RB, Kerins V, Fan L, Yeoman PM, Hope T, Evans DH. Association between dynamic cerebral autoregulation and mortality in severe head injury. Br J Neurosurg. 2004;18(5):471–9.
58. Reinhard M, Rutsch S, Lambeck J, Wihler C, Czosnyka M, Weiller C, et al. Dynamic cerebral autoregulation associates with infarct size and outcome after ischemic stroke. Acta Neurologica Scandinavica. 2011;. doi:10.1111/j.1600-0404.2011.01515.x.
59. Reinhard M. Dynamic cerebral autoregulation in acute ischemic stroke assessed from spontaneous blood pressure fluctuations. Stroke. 2005;36(8):1684–9.

60. Reinhard M, Wihler C, Roth M, Harloff A, Niesen W-D, Timmer J, et al. Cerebral autoregulation dynamics in acute ischemic stroke after rtPA thrombolysis. Cerebrovasc Dis. 2008;26(2):147–55.
61. Immink RV, van Montfrans GA, Stam J, Karemaker JM, Diamant M, van Lieshout JJ. Dynamic cerebral autoregulation in acute lacunar and middle cerebral artery territory ischemic stroke. Stroke. 2005;36(12):2595–600.
62. Reinhard M, Neunhoeffer F, Gerds TA, Niesen W-D, Buttler K-J, Timmer J, et al. Secondary decline of cerebral autoregulation is associated with worse outcome after intracerebral hemorrhage. Intensive Care Med. 2010;36(2):264–71.
63. Nakagawa K, Serrador JM, LaRose SL, Sorond FA. Dynamic cerebral autoregulation after intracerebral hemorrhage: a casecontrol study. BMC Neurol. 2011;11:108
64. Aaslid, R., Newell, D. W., Stooss, R., Sorteberg, W. & Lindegaard, K. F. Assessment of cerebral autoregulation dynamics from simultaneous arterial and venous transcranial Doppler recordings in humans. *Stroke* 22, 1148–1154 (1991).
65. Smirl, J. D., Tzeng, Y.-C., Monteleone, B. J. & Ainslie, P. N. Influence of cerebrovascular resistance on the dynamic relationship between blood pressure and cerebral blood flow in humans. *Journal of applied physiology (Bethesda, Md. : 1985)* (2014). doi:10.1152/japplphysiol.01266.2013
66. Tan, C. O. Defining the characteristic relationship between arterial pressure and cerebral flow. *J Appl Physiol* 113, 1194–1200 (2012).
67. Drummond, J. C. The lower limit of autoregulation time to revise our thinking? *Anesthesiology: The Journal of the American Society of Anesthesiologists* 86, 1431–1433
68. Lucas, S. J. E. *et al.* Influence of changes in blood pressure on cerebral perfusion and oxygenation. *Hypertension* 55, 698–705 (2010).
69. Strebel, S. *et al. Dynamic and static cerebral autoregulation during isoflurane, desflurane, and propofol anesthesia.* 83, 66–76 (1995).
70. Zhang, R., Zuckerman, J. H., Giller, C. A. & Levine, B. D. Transfer function analysis of dynamic cerebral autoregulation in humans. *American Journal of Physiology* 274, H233–41 (1998).
71. Panerai, R. B. *et al.* Assessment of dynamic cerebral autoregulation based on spontaneous fluctuations in arterial blood pressure and intracranial pressure. *Physiol Meas* 23, 59–72 (2002).
72. Tzeng, Y.-C. & Ainslie, P. N. Blood pressure regulation IX: cerebral autoregulation under blood pressure challenges. *European journal of applied physiology* 114, 545–59 (2014).
73. Panerai, R. B. Nonstationarity of dynamic cerebral autoregulation. *Medical engineering & physics* 36, 576–84 (2014).
74. Czosnyka, M., Brady, K., Reinhard, M., Smielewski, P. & Steiner, L. a. Monitoring of cerebrovascular autoregulation: facts, myths, and missing links. *Neurocritical care* 10, 373–386 (2009).

75. Czosnyka M, Czosnyka Z, Smielewski P. Pressure reactivity index: journey through the past 20 years. *Acta Neurochir (Wien)*. 2017;159(11):2063-2065. doi:10.1007/s00701-017-3310-1
76. Donnelly, J., Aries, M. J. H. & Czosnyka, M. Further understanding of cerebral autoregulation at the bedside: possible implications for future therapy. *Expert review of neurotherapeutics* 15, 169–185 (2015).
77. Czosnyka, M. *et al.* Continuous assessment of the cerebral vasomotor reactivity in head injury. *Neurosurgery* 41, 11–17; discussion 17–19 (1997).
78. Le Roux, P. *et al.* Consensus Summary Statement of the International Multidisciplinary Consensus Conference on Multimodality Monitoring in Neurocritical Care. *Neurocritical Care* 21, 1189–1209 (2014).
79. Brady, K. M. *et al.* Continuous measurement of autoregulation by spontaneous fluctuations in cerebral perfusion pressure: comparison of 3 methods. *Stroke; a journal of cerebral circulation* 39, 2531–7 (2008).
80. Aries, M. *et al.* Continuous determination of optimal cerebral perfusion pressure in traumatic brain injury*. *Critical Care Medicine* 40, 2456–2463 (2012).
81. Zweifel, C., Dias, C., Smielewski, P. & Czosnyka, M. Continuous time-domain monitoring of cerebral autoregulation in neurocritical care. *Medical engineering & physics* 36, 638–45 (2014).
82. Aaslid R, Lindegaard KF, Sorteberg W, Nornes H. Cerebral autoregulation dynamics in humans. Stroke. 1989;20(1):45–52.
83. Tiecks FPF, Lam AMA, Aaslid RR, Newell DWD. Comparison of static and dynamic cerebral autoregulation measurements. Stroke. 1995;26(6):1014–9.
84. Diehl RR, Linden D, Lu¨cke D, Berlit P. Phase relationship between cerebral blood flow velocity and blood pressure. A clinical test of autoregulation. Stroke. 1995;26(10):1801–4.
85. Reinhard M, Muller T, Guschlbauer B, Timmer J, Hetzel A. Transfer function analysis for clinical evaluation of dynamic cerebral autoregulation: a comparison between spontaneous and respiratory-induced oscillations. Physiol Meas. 2003;24(1): 27–43.
86. Reinhard M, Roth M, Muller T, Czosnyka M. Cerebral autoregulation in carotid artery occlusive disease assessed from spontaneous blood pressure fluctuations by the correlation coefficient index. Stroke. 2003;34:2138–44.
87. Imholz BP, Wieling W, van Montfrans GA, Wesseling KH. Fifteen years experience with finger arterial pressure monitoring: assessment of the technology. Cardiovasc Res. 1998;38(3):605–16.
88. Petersen NH, Ortega-Gutierrez S, Reccius A, Masurkar A, Huang A, Marshall RS. Comparison of Non-invasive and Invasive Arterial Blood Pressure Measurement for Assessment of Dynamic Cerebral Autoregulation. *Neurocrit Care*. 2014;20(1):60-68. doi:10.1007/s12028-013-9898-y.
89. Lavinio A, Schmidt EA, Haubrich C, Smielewski P, Pickard JD, Czosnyka M. Non-invasive evaluation of dynamic cerebrovascular autoregulation using Finapres plethysmograph and transcranial Doppler. Stroke. 2007;38(2):402–4.

90. Omboni S, Parati G, Frattola A, Mutti E, Di Rienzo M, Castiglioni P, et al. Spectral and sequence analysis of finger blood pressure variability. Comparison with analysis of intra-arterial recordings. Hypertension. 1993;22(1):26–33.
91. Sammons EL, Samani NJ, Smith SM, Rathbone WE, Bentley S, Potter JF, et al. Influence of non-invasive peripheral arterial blood pressure measurements on assessment of dynamic cerebral autoregulation. J Appl Physiol. 2007;103(1):369–75.
92. Iordanova, B., Li, L., Clark, R. S. B. & Manole, M. D. Alterations in Cerebral Blood Flow afer Resuscitation from Cardiac Arrest. Front. Pediatr. https://doi.org/10.3389/fped.2017.00174. (2017).
93. Pham, P., Bindra, J., Chuan, A., Jaeger, M. & Aneman, A. Are changes in cerebrovascular autoregulation following cardiac arrest associated with neurological outcome? Results of a pilot study. Resuscitation. https://doi.org/10.1016/j.resuscitation.2015.08.007 (2015).
94. Sekhon, M. S. et al. Using the relationship between brain tissue regional saturation of oxygen and mean arterial pressure to determine the optimal mean arterial pressure in patients following cardiac arrest: A pilot proof-of-concept study. Resuscitation. https://doi.org/10.1016/j.resuscitation.2016.05.019 (2016).
95. Lee, J. K. et al. A pilot study of cerebrovascular reactivity autoregulation afer pediatric cardiac arrest. Resuscitation. https://doi. org/10.1016/j.resuscitation.2014.07.006 (2014).
96. Brady, K. M. et al. Te lower limit of cerebral blood fow autoregulation is increased with elevated intracranial pressure. Anesth. Analg. 108, 1278–1283 (2009).
97. Burton, V. J. et al. A pilot cohort study of cerebral autoregulation and 2-year neurodevelopmental outcomes in neonates with hypoxicischemic encephalopathy who received therapeutic hypothermia. BMC Neurol. https://doi.org/10.1186/s12883-015-0464-4 (2015).
98. Tekes, A. et al. Apparent diffusion coefficient scalars correlate with near-Infrared spectroscopy markers of cerebrovascular autoregulation in neonates cooled for perinatal hypoxic-Ischemic injury. Am. J. Neuroradiol. https://doi.org/10.3174/ajnr.A4083 (2015).
99. Lee, J. K. et al. Optimizing Cerebral Autoregulation May Decrease Neonatal Regional Hypoxic-Ischemic Brain Injury. in. Developmental Neuroscience 39, 248–256 (2017).
100. Liu, X. et al. Cerebrovascular pressure reactivity monitoring using wavelet analysis in traumatic brain injury patients: A retrospective study. PLOS Med. 14, e1002348 (2017).
101. Sekhon, M. S. et al. Te Burden of Brain Hypoxia and Optimal Mean Arterial Pressure in Patients With Hypoxic Ischemic Brain Injury Afer Cardiac Arrest. Crit. Care Med. 1. https://doi.org/10.1097/CCM.0000000000003745 (2019).

102. Da Costa, C. S. et al. Monitoring of cerebrovascular reactivity for determination of optimal blood pressure in preterm infants. J. Pediatr. 167, 86–91 (2015).
103. Lee, J. K., Williams, M., Reyes, M. & Ahn, E. S. Cerebrovascular blood pressure autoregulation monitoring and postoperative transient ischemic attack in pediatric moyamoya vasculopathy. Paediatr. Anaesth. https://doi.org/10.1111/pan.13293 (2018).
104. Larson, A. C. et al. Cerebrovascular autoregulation afer rewarming from hypothermia in a neonatal swine model of asphyxic brain injury. J. Appl. Physiol.. https://doi.org/10.1152/japplphysiol.00238.2013 (2013).
105. Ono, M. et al. Cerebral blood fow autoregulation is preserved afer hypothermic circulatory arrest. Ann. Torac. Surg. https://doi. org/10.1016/j.athoracsur.2013.07.086 (2013).
106. Liu, X., Hu, X., Brady, K.M. *et al*. Comparison of wavelet and correlation indexes of cerebral autoregulation in a pediatric swine model of cardiac arrest. *Sci Rep* **10,** 5926 (2020)
107. Chalak, L. F. & Zhang, R. New Wavelet Neurovascular Bundle for Bedside Evaluation of Cerebral Autoregulation and Neurovascular Coupling in Newborns with Hypoxic-Ischemic Encephalopathy. Dev. Neurosci. 39, 89–96 (2017).
108. Mitra, S. et al. Pressure passivity of cerebral mitochondrial metabolism is associated with poor outcome following perinatal hypoxic ischemic brain injury. J. Cereb. Blood Flow Metab. https://doi.org/10.1177/0271678X17733639 (2019).
109. Beausoleil, T. P., Janaillac, M., Barrington, K. J., Lapointe, A. & Dehaes, M. Cerebral oxygen saturation and peripheral perfusion in the extremely premature infant with intraventricular and/or pulmonary haemorrhage early in life. Sci. Rep. https://doi.org/10.1038/ s41598-018-24836-8 (2018).
110. Panerai, R. B. Assessment of cerebral pressure autoregulation in humans–a review of measurement methods. Physiol. Meas. 19, 305–38 (1998).
111. Horiuchi, M. et al. Efect of progressive normobaric hypoxia on dynamic cerebral autoregulation. Exp. Physiol. 82, 1496–1514 (2016).
112. Budohoski, K. P. et al. Clinical relevance of cerebral autoregulation following subarachnoid haemorrhage. Nat. Rev. Neurol. 9, 152–63 (2013).
113. Simpson, D. et al. Assessing blood fow control through a bootstrap method. IEEE Trans Biomed Eng. 51, 1284–6 (2004).
114. Panerai, R. B. Transcranial Doppler for evaluation of cerebral autoregulation. Clin. Auton. Res. 19, 197–211 (2009).
115. Tzeng, Y. C. et al. Assessment of cerebral autoregulation: the quandary of quantifcation. Am. J. Physiol. Heart Circ. Physiol. 303, H658–71 (2012).
116. Ferradal, S. L. et al. Non-invasive assessment of cerebral blood fow and oxygen metabolism in neonates during hypothermic cardiopulmonary bypass: Feasibility and clinical implications. Sci. Rep. 7, (2017).
117. Guo, Z.-N. et al. Characteristics of dynamic cerebral autoregulation in cerebral small vessel disease: Difuse and sustained. Sci. Rep. 5, 15269 (2015).

118. Lee, J. K. et al. Relationships between cerebral autoregulation and markers of kidney and liver injury in neonatal encephalopathy and therapeutic hypothermia. J. Perinatol. 37, 938–942 (2017).
119. Panerai, R. B. Cerebral autoregulation: From models to clinical applications. Cardiovascular Engineering 8, 42–59 (2008).
120. Caldas, J. R., Haunton, V. J., Panerai, R. B., Hajjar, L. A. & Robinson, T. G. Cerebral autoregulation in cardiopulmonary bypass surgery: A systematic review. Interact. Cardiovasc. Torac. Surg. 26, (2018)
121. Tzeng, Y. C. & Panerai, R. B. CrossTalk proposal: dynamic cerebral autoregulation should be quantifed using spontaneous blood pressure fuctuations. J. Physiol. 596, 3–5 (2018).
122. Simpson, D. & Claassen, J. CrossTalk opposing view: dynamic cerebral autoregulation should be quantifed using induced (rather than spontaneous) blood pressure fuctuations. J. Physiol. 596, 7–9 (2018).
123. Brady, K. M. et al. Monitoring cerebral blood fow pressure autoregulation in pediatric patients during cardiac surgery. Stroke 41, 1957–1962 (2010).
124. Lang EW, et alYJNAJJ. Review of Cerebral Autoregulation: Assessment and Measurements. Australas. Anaesth. 161–172 (2005).
125. Eriksen, V. R., Hahn, G. H. & G., G. Cerebral autoregulation in the preterm newborn using near-infrared spectroscopy: a comparison of time-domain and frequency-domain analyses. J Biomed Opt 20, 37009 (2015). 23. Radolovich, D. K. et al. Pulsatile intracranial pressure and cerebral autoregulation afer traumatic brain injury. Neurocrit. Care 15, 379–386 (2011).
126. Panerai, R. B., Saeed, N. P. & Robinson, T. G. Cerebrovascular effects of the thigh cuf maneuver. Am. J. Physiol. Heart Circ. Physiol. 308, H688–96 (2015).
127. Tiecks, F. P. et al. Efects of the valsalva maneuver on cerebral circulation in healthy adults. A transcranial Doppler Study. Stroke 26, 1386–1392 (1995).
128. Reinhard, M., Müller, T., Guschlbauer, B., Timmer, J. & Hetzel, A. Transfer function analysis for clinical evaluation of dynamic cerebral autoregulation–a comparison between spontaneous and respiratory-induced oscillations. Physiol. Meas. 24, 27–43 (2003).
129. Placek, M. M. et al. Applying time-frequency analysis to assess cerebral autoregulation during hypercapnia. PLoS One 12, 7 (2017).
130. Liu, X., Czosnyka, M., Donnelly, J. *et al.* Assessment of cerebral autoregulation indexes – a modelling perspective. *Sci Rep* **10,** 9600 (2020). https://doi.org/10.1038/s41598-020-66346-6
131. Liu, X. Optimization of the assessment of cerebral autoregulation in neurocritical care unit. Apollo - University of Cambridge Repository. https://doi.org/10.17863/cam.11213 (2017).
132. Panerai, R. B., Haunton, V. J., Hanby, M. F., Salinet, A. S. M. & Robinson, T. G. Statistical criteria for estimation of the cerebral autoregulation index (ARI) at rest. Physiol. Meas. 37, 661–672 (2016).
133. Claassen, J. A., Meel-van den Abeelen, A. S., Simpson, D. M. & Panerai, R. B., international Cerebral Autoregulation Research Network (CARNet). Transfer function analysis of dynamic cerebral autoregulation: A white paper

from the International Cerebral Autoregulation Research Network. J. Cereb. Blood Flow Metab. 36, 665–80 (2016).
134. Sweeney KT, Ward TE, McLoone SF. Artifact removal in physiological signals--practices and possibilities. *IEEE Trans Inf Technol Biomed*. 2012;16(3):488-500. doi:10.1109/TITB.2012.2188536
135. McGhee BH, Bridges EJ. Monitoring arterial blood pressure: what you may not know. Crit Care Nurse. 2002 Apr;22(2):60-4, 66-70, 73 passim. PMID: 11961944.
136. Li Q, Mark RG, Clifford GD. Artificial arterial blood pressure artifact models and an evaluation of a robust blood pressure and heart rate estimator. *Biomed Eng Online*. 2009;8:13. Published 2009 Jul 8. doi:10.1186/1475-925X-8-13
137. Kim H, Lee SB, Son Y, Czosnyka M, Kim DJ: Hemodynamic instability and cardiovascular events after traumatic brain injury predict outcome after artifact removal with deep belief network analysis. J Neurosurg Anesthesiol 30:347–353, 2018
138. Edinburgh, Tom et al. "DeepClean -- self-supervised artefact rejection for intensive care waveform data using deep generative learning." *arXiv: Machine Learning* (2019):
139. Fanelli and T. Heldt, "Signal quality quantification and waveform reconstruction of arterial blood pressure recordings," *2014 36th Annual International Conference of the IEEE Engineering in Medicine and Biology Society*, Chicago, IL, 2014, pp. 2233-2236.
140. The hostile environment of the intensive care unit. *Donchin Y, Seagull FJ Curr Opin Crit Care. 2002 Aug; 8(4):316-20.*
141. Poor prognosis for existing monitors in the intensive care unit. *Tsien CL, Fackler JC Crit Care Med. 1997 Apr; 25(4):614-9*
142. Alarms in the intensive care unit: how can the number of false alarms be reduced? *Chambrin MC Crit Care. 2001 Aug; 5(4):184-8.*
143. Morphological clustering and analysis of continuous intracranial pressure. *Hu X, Xu P, Scalzo F, Vespa P, Bergsneider M IEEE Trans Biomed Eng. 2009 Mar; 56(3):696-705.*
144. Ali, W., Eshelman, L., Saeed, M., & Division, P. M. (2004). *Identifying Artifacts in Arterial Blood Pressure Using Morphogram Variability*. 697–700.
145. Feng, M., Loy, L. Y., Zhang, F., & Guan, C. (2011). *Artifact Removal for Intracranial Pressure Monitoring Signals : A Robust Solution with Signal Decomposition*. (June 2014). https://doi.org/10.1109/IEMBS.2011.6090182
146. Megjhani M, Alkhachroum A, Terilli K, et al. An active learning framework for enhancing identification of non-artifactual intracranial pressure waveforms. *Physiol Meas*. 2019;40(1):015002. Published 2019 Jan 18. doi:10.1088/1361-6579/aaf979
147. Haddad SH, Arabi YM: Critical care management of severe traumatic brain injury in adults. Scand J Trauma Resusc Emerg Med 20:12, 2012
148. Czosnyka M, Smielewski P, Kirkpatrick P, Piechnik S, LaingR, Pickard JD: Continuous monitoring of cerebrovascularpressure-reactivity in head injury.

149. Lee SB, Kim H, Kim YT, et al. Artifact removal from neurophysiological signals: impact on intracranial and arterial pressure monitoring in traumatic brain injury [published online ahead of print, 2019 May 10]. *J Neurosurg*. 2019;1-9. doi:10.3171/2019.2.JNS182260
150. Lundberg N. Continuous recording and control of ventricular fuid pressure in neurosurgical practice. Acta Psychiatrica Scandinavica Sup- plementum. 1960;36:1–193.
151. Martin G. Lundberg's B waves as a feature of normal intracranial pres- sure. Surg Neurol. 1978;9(6):347–8.
152. Droste DW, Krauss JK, Berger W, Schuler E, Brown MM. Rhythmic oscil- lations with a wavelength of 0.5–2 min in transcranial Doppler record- ings. Acta Neurologica Scandinavica. 2009;90(2):99–104.
153. Lescot T, Naccache L, Bonnet MP, Abdennour L, Coriat P, Puybasset L. The relationship of intracranial pressure Lundberg waves to electroen- cephalograph fuctuations in patients with severe head trauma. Acta Neurochir. 2005;147(2):125–9
154. Martinez-Tejada, I., Arum, A., Wilhjelm, J.E. *et al.* B waves: a systematic review of terminology, characteristics, and analysis methods. *Fluids Barriers CNS* 16, 33 (2019). https://doi.org/10.1186/s12987-019-0153-6
155. Spiegelberg A, Preuß M, Kurtcuoglu V. B-waves revisited. Interdisciplin Neurosurgery: Adv Tech Case Manage. 2016;6:13−7
156. Czosnyka M, Pickard JD. Monitoring and interpretation of intracranial pressure. J Neurol Neurosurg Psychiatry. 2004;75(6):813–21.
157. Momjian S, Czosnyka Z, Czosnyka M, Pickard JD. Link between vasogenic waves of intracranial pressure and cerebrospinal fuid outfow resistance in normal pressure hydrocephalus. Br J Neurosurg. 2004;18(1):56–61.
158. Raftopoulos C, Chaskis C, Delecluse F, Cantrainet F, Bidauti L, Brotchi J. Morphological quantitative analysis of intracranial pressure waves in normal pressure hydrocephalus. Neurol Res. 1992;14:389–96.
159. Santamarta D, González-Martínez E, Fernández J, Mostaza A. The predic- tion of shunt response in idiopathic normal-pressure hydrocephalus based on intracranial pressure monitoring and lumbar infusion. Acta Neurochir Suppl. 2016;122:267–74
160. Kasprowicz M, Bergsneider M, Czosnyka M, Hu X. Association between ICP pulse waveform morphology and ICP B waves. Acta Neurochir Suppl. 2012;114:29–34.
161. Rosiello AP, McClearly EL, Cooper PR (1989) Nonprovocative assessment of intracranial volume – pressure relationships. ICP VII. In: Ho JT, Betz AL (eds) Springer, Berlin Heidelberg New York Tokyo, pp 260–262.
162. Teasdale GM, Graham DI (1998) Craniocerebral trauma: protection and retrieval of the neuronal population after injury. Neurosurgery 43: 723–738
163. Smielewski P, Czosnika M, Kirkpatrick P, Pickard JD (1997) Evaluation of the transient hyperemic response test in head injured patients. J Neurosurg 86: 773–778

164. Steiger HJ, Aaslid R, Stoos R, Seiler RW (1994) Transcranial Doppler monitoring in head injury: relationsbetween type of injury, flow velocities, vasoreactivity, and outcome. Neurosurgery 34: 79–86
165. Czosnika M, Smielewski P, Kirkpatrick P, Menon DK, Pickard JD (1996) Monitoring of cerebral autoregulation in headinjured patients. Stroke 27: 1829–1834
166. Czosnyka M, Smielewski P, Piechnik S, Schmidt E, Al-Rawi PG, Kirkpatrick PJ, Pickard JD (1999) Hemodynamic characterization of intracranial pressure plateau waves in headinjured patients. J Neurosurg 91: 11–19.
167. Newell DW, Aaslid R, Stooss R, Reulen HJ (1993) Spontaneous fluctuations in cerebral blood flow as a cause of B waves. ICP VIII. In: Avezaat CJJ, Van Eijdhoven JHM, MaasAIR
168. Tanaka K, Nishimura S (1989) The importance of outflow resistance of the shunt system for elimination of B-waves. ICP VII. In: Ho¤ JT, Betz AL (eds) Springer, Berlin Heidelberg New York Tokyo, pp 368–373
169. Beqiri E, Czosnyka M, Lalou AD, et al. Influence of mild-moderate hypocapnia on intracranial pressure slow waves activity in TBI. *Acta Neurochir (Wien)*. 2020;162(2):345-356. doi:10.1007/s00701-019-04118-6
170. Zeiler, F.A., Cabeleira, M., Hutchinson, P.J. *et al.* Evaluation of the relationship between slow-waves of intracranial pressure, mean arterial pressure and brain tissue oxygen in TBI: a CENTER-TBI exploratory analysis. *J Clin Monit Comput* (2020).
171. Froese, L., Dian, J., Batson, C. *et al.* The impact of hypertonic saline on cerebrovascular reactivity and compensatory reserve in traumatic brain injury: an exploratory analysis. *Acta Neurochir* **162,** 2683–2693 (2020). https://doi.org/10.1007/s00701-020-04579-0
172. Weerakkody R.A. et al. (2012) Near Infrared Spectroscopy as Possible Non-invasive Monitor of Slow Vasogenic ICP Waves. In: Schuhmann M., Czosnyka M. (eds) Intracranial Pressure and Brain Monitoring XIV. Acta Neurochirurgica Supplementum, vol 114. Springer, Vienna. https://doi.org/10.1007/978-3-7091-0956-4_35
173. Popovic, N. B., Miljkovic, N., & Djordjevic, O. (2016). *Artifact cancellation using median filter, moving average filter , and fractional derivatives in biomedical signals*. (July).
174. Roozenbeek, B.; Maas, A.I.R.; Menon, D.K. Changing patterns in the epidemiology of traumatic brain injury. *Nat. Rev. Neurol.* 2013, *9*, 231–236.
175. Stein, S.C.; Georgoff, P.; Meghan, S.; Mizra, K.; Sonnad, S.S. 150 Years of Treating Severe Traumatic Brain Injury: A Systematic Review of Progress in Mortality. *J. Neurotrauma* 2010, *27*, 1343–1353.
176. Maas, A.I.R.; Menon, D.K. Traumatic brain injury: Rethinking ideas and approaches. *Lancet Neurol.* 2012, *11*, 12–13.
177. Czosnyka, M.; Smielewski, P.; Kirkpatrick, P.; Laing, R.J.; Menon, D.; Pickard, J.D. Continuous assessment of the cerebral vasomotorreactivity in head injury. *Neurosurgery* 1997, *41*, 11–17.

178. Czosnyka, M.; Smielewski, P.; Lavinio, A.; Czosnyka, Z.; Pickard, J.D. A synopsis of brain pressures: Which? when? Are they all useful? *Neurol. Res.* 2007,29, 672–679, doi:10.1179/016164107X240053.
179. Liu, X.; Maurits, N.M.; Aries, M.J.; Czosnyka, M.; Ercole, A.; Donnelly, J.; Cardim, D.; Kim, D.J.; Dias, C.; Cabeleira, M. Monitoring of Optimal Cerebral Perfusion Pressure in Traumatic Brain Injured Patients Using a Multi-Window Weighting Algorithm. *J. Neurotrauma* 2017, *34*, 3081–3088. doi:10.1089/neu.2017.5003.
180. Kasprowicz, M.; Schmidt, E.; Kim, D.J.; Haubrich, C.; Czosnyka, Z.; Smielewski, P.; Czosnyka, M. Evaluation of the cerebrovascular pressure reactivity index using non-invasive finapres arterial blood pressure. *Physiol. Meas.* 2010, *31*, 1217–1228.
181. Petkus, V.; Krakauskaite, S.; Chomskis, R.; Bartusis, L.; Ragauskas, A.; Preiksaitis, A.; Rocka, S. Novel technology of non-invasive cerebrovascular autoregulation monitoring. *Proc. Comput. Based Med. Syst.* 2014, 427–430, doi:10.1109/CBMS. 2014.40.
182. Lang, E.W.; Kasprowicz, M.; Smielewski, P.; Santos, E.; Pickard, J.; Czosnyka, M. Short pressure reactivity index versus long pressure reactivity index in the management of traumatic brain injury. *J. Neurosurg.* 2015, *122*, 588–594.
183. Ragauskas, A.; Daubaris, G.; Ragaisis, V.; Petkus, V. Implementation of non-invasive brain physiological monitoring concepts. *Med. Eng. Phys.* 2003, *25*, 667–678.
184. Ragauskas, A.; Daubaris, G.; Petkus, V.; Raisutis, R. Apparatus and Method of Non-Invasive Cerebrovascular Autoregulation Monitoring. European Patent No. 2111787 B1, 23 March 2011, U.S. Patent 20090270734, 29 October 2009.
185. Sorrentino, E.; Diedler, J.; Kasprowicz, M.; Budohoski, K.P.; Haubrich, C.; Smielewski, P.; Outtrim, J.G.; Manktelow, A.; Hutchinson, P.J.; Pickard, J.D.; et al. Critical thresholds for cerebrovascular reactivity after traumatic brain injury. *Neurocrit. Care* 2012, *16*, 258–266, doi:10.1007/s12028-011-9630-8.
186. Lavinio, A.; Ene-Iordache, B.; Nodari, I.; Girardini, A.; Cagnazzi, E.; Rasulo, F.; Smielewski, P.; Czosnyka, M.; Latronico, N. Cerebrovascular reactivity and autonomic drive following traumatic brain injury. *Acta Neurochir. Suppl.* 2008, *102*, 3–7.
187. Needham, E.; McFadyen, C.; Newcombe, V.; Synnot, A.J.; Czosnyka, M.; Menon, D. Cerebral Perfusion Pressure Targets Individualized to Pressure-Reactivity Index in Moderate to Severe Traumatic Brain Injury: A Systematic Review. *J. Neurotrauma* 2017, *34*, 963–970, doi:10.1089/neu.2016.4450.
188. Lazaridis, C.; Smielewski, P.; Steiner, L.A.; Brady, K.M.; Hutchinson, P.; Pickard, J.D.; Czosnyka, M. Optimal cerebral perfusion pressure: Are we ready for it? *Neurol. Res.* 2013, *35*, 138–148.
189. Akhondi-Asl, A.; Vonberg, F.W.; Au, C.C.; Tasker, R.C. Meaning of Intracranial Pressure-to-Blood Pressure Fisher-Transformed Pearson Correlation-Derived Optimal Cerebral Perfusion Pressure: Testing Empiric Utility in a Mechanistic Model. *Crit. Care Med.* 2018, 46, e1160–e1166, doi:10.1097/CCM.0000000000003434.

190. Ellis, T.; McNames, J.; Goldstein, B. Optimal filter design to compute the mean of cardiovascular pressure signals. *IEEE Trans. Biomed. Eng.* 2008, *55*, 1399–1407, doi:10.1109/TBME.2007.906491.
191. Kumpaitiene, B.; Svagzdiene, M.; Sirvinskas, E.; Adomaitiene, V.; Petkus, V.; Zakelis, R.; Krakauskaite, S.; Chomskis, R.; Ragauskas, A.; Benetis, R. Cerebrovascular autoregulation impairments during cardiac surgery with cardiopulmonary bypasses are related to postoperative cognitive deterioration: Prospective observational study. *Minerva Anestesiol.* 2019, *85*, 594–603.
192. Filip, S.-I. A Robust and Scalable Implementation of the Parks-McClellan Algorithm for Designing FIR Filters. ACM Transactions on Mathematical Software 2016, *43*, 1–24, doi:10.1145/2904902.
193. Florkowski, C.M. Sensitivity, specificity, receiver-operating characteristic (ROC) curves and likelihood ratios: Communicating the performance of diagnostic tests. The Clinical Biochemist. *Reviews* 2008, *29* (Suppl. 1), S83–S87.
194. Vetter, T.R.; Schober, P.; Mascha, E.J. Diagnostic testing and decision-making: Beauty is not just in the eye of the beholder. *Anesth. Analg.* 2018, *127*, 1085–1091, doi:10.1213/ANE.0000000000003698.
195. Šimundić, A.-M. Measures of Diagnostic Accuracy: Basic Definiti. Measures of Diagnostic Accuracy: Basic Definitions. *EJIFCC* 2009, *19*, 203–211. Available online: http://www.ncbi.nlm.nih.gov/pubmed/27683318ons (03.10.2019).
196. Kumar, R.; Indrayan, A. (2011). Receiver operating characteristic (ROC) curve for medical researchers. *Indian Pediatrics* 2011, *48*, 277–287. Available online: http://www.ncbi.nlm.nih.gov/pubmed/21532099 (05.10.2019).
197. Zou, K.H.; O'Malley, A.J.; Mauri, L. Receiver-Operating Characteristic Analysis for Evaluating Diagnostic Tests and Predictive Models. *Circulation* 2007, *115*, 654–657, doi:10.1161/CIRCULATIONAHA.105.594929.
198. Salinet, A.S.; Panerai, R.B.; Robinson, T.G. The longitudinal evolution of cerebral blood flow regulation after acute ischaemic stroke. *Cerebrovasc. Dis. Extra* 2014, *4*, 186–197.
199. Aries, M.J.H.; Czosnyka, M.; Budohoski, K.P.; Kolias, A.G.; Radolovich, D.K.; Lavinio, A.; Pickard, J.D.; Smielewski, P. Continuous monitoring of cerebrovascular reactivity using pulse waveform of intracranial pressure. *Neurocrit. Care* 2012, *17*, 67–76.
200. Panerai, R.B. Assessment of cerebral pressure autoregulation in humans--a review of measurement methods. *Physiol. Meas.* 1998, *19*, 305–338.
201. Peterson, E.C.; Wang, Z.; Britz, G. Regulation of cerebral blood flow. *Int. J. Vasc. Med.* 2011, 2011, 823525, 1–8.
202. Silverman, A.; Petersen, N.H. *Physiology, Cerebral Autoregulation*; StatPearls Publishing: Treasure Island, FL, USA, 2020; Available online: https://www.ncbi.nlm.nih.gov/books/NBK553183/ (accessed on 5 February 2020).
203. Klein, S.P.; Depreitere, B.; Meyfroidt, G. How I monitor cerebral autoregulation. *Crit. Care* 2019, *23*, 160.
204. Moerman, A.; de Hert, S. Why and how to assess cerebral autoregulation? *Best Pract. Res. Clin. Anaesthesiol.* 2019, *33*, 211–220.

205. Eames, P.J.; Blake, M.J.; Dawson, S.L.; Panerai, R.B.; Potter, J.F. Dynamic cerebral autoregulation and beat to beat blood pressure control are impaired in acute ischaemic stroke. *J. Neurol. Neurosurg. Psychiatry* 2002, *72*, 467–73.
206. Kasprowicz, M.; Schmidt, E.; Kim, D.J.; Haubrich, C.; Czosnyka, Z.; Smielewski, P.; Czosnyka, M. Evaluation of the cerebrovascular pressure reactivity index using noninvasive finapres arterial blood pressure. *Physiol. Meas.* 2010, *31*, 1217–1228.
207. Ragauskas, A.; Daubaris, G.; Petkus, V.; Raisutis, R. Apparatus and Method of Noninvasive Cerebrovascular Autoregulation Monitoring. European Patent No. 2111787 B1, 23.03.2011, U.S. Patent 20090270734, 29 October 2009.
208. Petkus, V.; Preiksaitis, A.; Krakauskaite, S.; Bartusis, L.; Chomskis, R.; Hamarat, Y.; Ragauskas, A. Non - invasive cerebrovascular autoregulation assessment using the volumetric reactivity index: Prospective study. *Neurocrit. Care* 2019, *30*, 42–50.
209. Zweifel, C.; Castellani, G.; Czosnyka, M.; Carrera E.; Brady KM.;Kirkpatrick PJ.; Pickard JD.; Smielewski P.Continuous assessment of cerebral autoregulation with near-infrared spectroscopy in adults after subarachnoid hemorrhage. *Stroke* 2010, *41*, 1963–1968.
210. Rivera-Lara, L.; Geocadin, R.; Zorrilla-Vaca, A.; Healy, R.; Radzik, B.R.; Palmisano, C.; Mirski, M.; Ziai, W.C.; Hogue, C. Validation of near-infrared spectroscopy for monitoring cerebral autoregulation in comatose patients. *Neurocrit. Care* 2017, *27*, 362–369.
211. Blaine E.; Kibler KK.; Brady KM.; Joshi B.; Brown, C.; Hogue, C.W.;. Continuous cerebrovascular reactivity monitoring and autoregulation monitoring identify similar lower limits of autoregulation in patients undergoing cardiopulmonary bypass. *HHS Public Access* 2017, *35*, 344–354.
212. Petkus, V.; Preiksaitis, A.; Krakauskaite, S.; Chomskis, R.; Rocka, S.; Kalasauskiene, A. Novel method and device for fully noninvasive cerebrovascular autoregulation monitoring. *Electron. Electr. Eng.* 2014, *20*, 24–29.
213. Ragauskas, A.; Daubaris, G.; Ragaisis, V.; Petkus, V. Implementation of noninvasive brain physiological monitoring concepts. *Med. Eng. Phys.* 2003, *25*, 667–678.
214. Petkus, V.; Ragauskas, A.; Jurkonis, R. Investigation of intracranial media ultrasonic monitoring model. *Ultrasonics* 2002, *40*, 829–833.
215. Ragauskas, A., Daubaris, G., Petkus, V., & Chomskis, R. (2002). Ultrasonic non-invasive intracranial wave monitor.
216. Schmidt, B.; Reinhard, M.; Lezaic, V.; McLeod, D.D.; Weinhold, M.; Mattes, H.; Klingelhöfer, J. Autoregulation monitoring and outcome prediction in neurocritical care patients: Does one index fit all? *J. Clin. Monit. Comput.* 2016, *30*, 367–375.
217. UAB VITTAMED (LT). Apparatus and method of non-invasive cerebrovascular utoregulation monitoring: Arminas RAGAUSKAS, Vytautas PETKUS, Daubaris; Gediminas, Raisutis; Renaidas, et al. IPC: A61B 8/06

August 16, 2011. United States Patent and trademark Office [viewed on 2020-11-20]. Access via the Internet: https://patents.google.com/patent/US7998075
218. Bruggemans, E.F. Cognitive dysfunction after cardiac surgery: Pathophysiological mechanisms and preventive strategies. *Neth. Heart J.* 2013, *21*, 70–73.
219. Zweifel, C.; Lavinio, A.; Steiner, L.A.; Radolovich, D.; Smielewski, P.; Timofeev, I.; et al. Continuous monitoring of cerebrovascular pressure reactivity in patients with head injury. *Neurosurg. Focus* 2008, *25*, E2.
220. Czosnyka, M.; Czosnyka, Z.; Momjian, S.; Pickard, J.D. Cerebrospinal fluid dynamics. *Physiol. Meas.* 2004, *25*, R51–R76.
221. Spiegelberg, A.; Preuß, M.; Kurtcuoglu, V. B-waves revisited. *Interdiscip. Neurosurg.* 2016, *6*, 13–17.
222. Hori, D.; Hogue, C.W., Jr.; Shah, A.; Brown, C.; Neufeld, K.J.; Conte, J.V.; et al. Cerebral autoregulation monitoring with ultrasound-tagged near-infrared spectroscopy in cardiac surgery patients. *Anesth. Analg.* 2015, *121*, 1187–1193.
223. Ono, M.; Joshi, B.; Brady, K.; Easley, R.B.; Zheng, Y.; Brown, C.; Baumgartner, W.; Hogue, C.W. Risks for impaired cerebral autoregulation during cardiopulmonary bypass and postoperative stroke. *Br. J. Anaesth.* 2012, *109*, 391–398.
224. Brady, K.; Joshi, B.; Zweifel, C.; Smielewski, P.; Czosnyka, M.; Easley, R.B.; Hogue CW.Real-time continuous monitoring of cerebral blood flow autoregulation using near-infrared spectroscopy in patients undergoing cardiopulmonary bypass. *Stroke* 2010, *41*, 1951–1956.
225. Fantini, S.; Sassaroli, A.; Tgavalekos, K.T.; Kornbluth, J. Cerebral blood flow and autoregulation: Current measurement techniques and prospects for noninvasive optical methods. *Neurophotonics* 2016, *3*, 031411.
226. Horsfield, M.A.; Jara, J.L.; Saeed, N.P.; Panerai, R.B.; Robinson, T.G. Regional differences in dynamic cerebral autoregulation in the healthy brain assessed by magnetic resonance imaging. *PLoS ONE* 2013, *8*, e62588.
227. Larsen, F.S.; Olsen, K.S.; Hansen, B.A.; Paulson, O.B.; Knudsen, G.M. Transcranial Doppler is valid for determination of the lower limit of cerebral blood flow autoregulation. *Stroke* 1994, *25*, 1985–1988.

LIST OF PUBLICATIONS

1. **Bajpai BK**, Preiksaitis A, Vosylius S, Rocka S. Association between the Cerebral Autoregulation Index (Pressure Reactivity), Patient's Clinical Outcome, and Quality of ABP(t) and ICP(t) Signals for CA Monitoring. ***Medicina***. 2020; 56(3):143. Published **2020 Mar 20**. **(IF 1.467), (Q3).**
2. **Bajpai BK**, Zakelis R, Deimantavicius M, Imbrasiene D. Comparative Study of Novel Noninvasive Cerebral Autoregulation Volumetric Reactivity Indexes Reflected by Ultrasonic Speed and Attenuation as Dynamic Measurements in the Human Brain. ***Brain Sci*. 2020; 10**(4):205. Published **2020 Apr 1**. **(IF 2.786), (Q2).**

UDK 616.831-005(043.3)

SL344. 2021-*-*, * leidyb. apsk. l. Tiražas * egz.
Išleido Kauno technologijos universitetas, K. Donelaičio g. 73, 44249 Kaunas
Spausdino leidyklos „Technologija" spaustuvė, Studentų g. 54, 51424 Kaunas